Mathematical models of Ebola virus disease with socio-economic dynamics

by

Sylvie Diane Djiomba Njankou

Dissertation presented for the degree of Doctor of Philosophy in Mathematics in the Faculty of Science at Stellenbosch University

Supervisor: Prof. Farai Nyabadza

April 2019

Declaration

By submitting this dissertation electronically, I declare that the entirety of the work contained therein is my own, original work, that I am the sole author thereof (save to the extent explicitly otherwise stated), that reproduction and publication thereof by Stellenbosch University will not infringe any third party rights and that I have not previously in its entirety or in part submitted it for obtaining any qualification.

Date: April 2019 . . . . . .

Abstract

West Africa hosted the deadliest Ebola virus disease epidemic from 2013 to 2016 and one of the common characteristics of the affected countries is their status of being developing countries. Poor economic and social living conditions is a reality in these countries and they have deeply affected the fight against Ebola virus disease. In this work, we focus on the potential impact of socio-economic factors on Ebola virus disease dynamics. First, we use a compartmental model to study the dynamics of Ebola virus disease when there is a limited number of beds for patients. We use a non linear hospitalisation rate and formulate the rate at which the time dependent number of available beds evolves. The results suggest that a timely supply of sufficient beds to Ebola treatment units, limits the spread of the disease by keeping the infectious in one place, during their infectious period. Second, we formulate a mathematical model of Ebola virus disease that considers human behaviour through an exponential non linear incidence rate. Suitable Lyapunov functions are built and the proofs of the global stability of equilibria are presented. The results advocate for an immediate and efficacious behaviour change, as a control measure to rapidly control an Ebola virus disease epidemic. Third, we build a mathematical model of Ebola virus disease dynamics, that describes the introduction of a new strain of Ebola virus, through continuous or impulsive immigration of infectives. The results suggest controlled movements of people between countries that have had Ebola outbreaks. Finally, we develop a model of Ebola virus disease that considers two patches with different economic statuses represented by the respective gross-national incomes of these patches. We assume that susceptible, exposed and recovered individuals from the poorer patch move to the rich patch. The results indicate a decrease of the number of infected individuals in the rich patch when movements of populations are limited through the improvement of the economy in the poor patch. We conclude that the improvement of the economy of poorer countries may be critical in avoiding potential outbreaks of Ebola virus disease. The results in this thesis point to the need to consider socio-economic factors in Ebola virus disease epidemic models.

Keywords: Ebola virus disease, limited resources, human behaviour, migration, economy, model fitting.

Opsomming

Wes-Afrika het die dodelikste epidemie van die Ebola-virus siekte vanaf 2013 tot 2016 gehad en een van die algemene kenmerke van die geaffekteerde lande is hul status as ontwikkelende lande. Swak ekonomiese en sosiale lewensomstandighede is in hierdie lande 'n werklikheid en het die stryd teen Ebola-virus siektes erg beïnvloed. In hierdie tesis het ons gekies om te fokus op die moontlike impak van sosio-ekonomiese faktore op die dinamika van die Ebola-virus siekte. Eerstens gebruik ons 'n kompartementele model om die dinamika van Ebola-virus siekte te bestudeer wanneer daar 'n beperkte aantal beddens vir pasiënte is. Ons gebruik 'n nie-lineêre hospitalisasie koers en formuleer die koers waarteen die tyd afhanklike aantal beskikbare beddens ontwikkel. Die resultate dui daarop dat 'n tydige voorsiening van voldoende beddens vir Ebola-behandelingseenhede die verspreiding van die siekte beperk deur die aansteeklikes op een plek te hou gedurende hul aansteeklike tydperk. Tweedens formuleer ons 'n wiskundige model van Ebola-virus siekte wat menslike gedrag oorweeg deur 'n eksponensiële nie-lineêre voorkomsskoers. Geskikte Lyapunov funksies word gebou en die bewyse van die globale stabiliteit van ewewig word aangebied. Resultate argumenteer vir 'n onmiddellike en doeltreffende gedragsverandering as 'n beheermaatreël om 'n Ebola-virus siekte-epidemie vinnig te beheer. Derdens bou ons 'n wiskundige model van Ebola-virus sindinamika, wat die bekendstelling van 'n nuwe stam Ebola-virus beskryf, deur middel van deurlopende of impulsiewe immigrasie van infektiewe. Resultate dui op beheerde bewegings van mense tussen lande wat Ebola-uitbrake gehad het. Ten slotte, ons ontwikkel 'n model van Ebola-virus siekte wat twee gebiede met verskillende ekonomiese statusse beskou, verteenwoordig deur die onderskeie bruto nasionale inkomste van hierdie gebiede. Ons aanvaar dat vatbare, blootgestelde en verhaalde individue van die armer gebied na die ryk gebied beweeg. Resultate dui 'n afname aan in die aantal besmette individue in die ryk gebied wanneer bewegings van bevolkings beperk word deur die verbetering van die ekonomie in die arm gebied. Ons kom tot die gevolgtrekking dat die verbetering van die ekonomie van armer lande krities kan wees om potensiële uitbrake van Ebola-virus siektes te vermy. Die resultate in hierdie proefskrif dui op die nood-

saaklikheid om sosio-ekonomiese faktore in Ebola-virus siekte epidemiese modelle te oorweeg.

Acknowledgements

I first thank God for giving me life and the opportunity to study up to this level.
I thank my supervisor, Professor Farai Nyabadza for his guidance and countless advices that built this work from the beginning to the end.
I am grateful to my parents, Njankou Francois and Mfaleu Frida, whose love and support have always been my main strength. Particular thanks to my blessed and lovely daughter Diolvie for growing stronger despite my absence.
I am grateful to Stellenbosch University for providing the resources that allowed me to complete this thesis.
This research project has benefited from the intellectual and material contribution of the Organization for Women in Science for the Developing World (OWSD) and the Swedish International Development Cooperation Agency (SIDA).

Dedications

To my lovely daughter Nganso Ngoma Eveline Diolvie

Contents

List of Figures

List of Tables

Chapter 1

Introduction

1.1 Ebola virus disease

The first Ebola virus disease (EVD) outbreak started in 1976 in the Democratic Republic of Congo (DRC) also called Zaire at that time [3]. The name Ebola is a name of the river in Kikwit close to where the first EVD cases were noticed. Since then, there has been over 20 EVD outbreaks and all occurring in Africa [4]. There are five different strains of Ebola virus namely Zaire Ebola virus strain, Sudan Ebola virus strain, Bundigbuyo Ebola virus strain, Taï forest Ebola virus strain and Reston Ebola virus strain. The Zaire Ebola virus strain is responsible of the most recent and deadliest outbreak of 2013 – 2016 [5], with over 28 700 cases and 11 000 deaths. The large death toll of this outbreak raised suspicions on an eventual mutation of the virus. Indeed, Ebola virus glycoprotein with increased infectivity dominated the 2013 – 2016 EVD epidemic [6]. The high infectivity of the Zaire Ebola virus strain facilitated the disease transmission, thus increasing the number of cases. During this outbreak, the chances of recovering were very low due to the absence of treatment or vaccine and poor living conditions of those who were affected. Guinea, Liberia and Sierra Leone were the most affected countries in the 2013 – 2016 EVD outbreak and are classified as low income countries [2]. The majority in these countries live in poor conditions, which may have increased their chances of dying from EVD during the outbreak [7]. This study seeks to investigate the role of social and economic factors of these countries in the increased number of cases and deaths due to EVD.

1.2 Geographical distribution of countries affected by EVD

The natural habitation of Ebola virus reservoirs helps to geographically locate countries that can be potentially affected by EVD. Fruit bats and chimpanzees are

known reservoirs of Ebola virus [8, 9, 10]. They contaminate other animals like gorillas, monkeys, forest antelopes and porcupines that are killed and served, to be eaten by humans, as "bush meat", which can lead to the spread of Ebola virus into humans [10].

Fruit bats and chimpanzees populations are mostly found in equatorial and tropical forests of Africa [10]. In fact, the first cases of EVD were identified in DRC and thereafter EVD was detected in neighbouring countries, but with different strains of the virus [3, 7, 10]. DRC is a country which is geographically located at the center of the African continent and which is a member state of the Southern African Development Community. In 1976, the Sudan ebolavirus strain was detected in South Sudan formerly part of Sudan and caused 151 deaths in humans. The Sudan ebolavirus strain was also responsible for other outbreaks in Sudan in 1997, 2004 and in Uganda in 2000, 2012 [3, 7]. The Zaire ebolavirus species was responsible for the EVD outbreaks in DRC and the outbreaks in other countries like the Republic of Congo, Gabon, Guinea, Liberia and Sierra Leone [3, 7]. The Bundibugyo ebolavirus strain affected Uganda in 2007 and the DRC in 2011. Central Africa is a natural reservoir of Ebola virus. It is a region occupied by large tropical rain forests, very suitable habitat for fruit bats and chimpanzees. Tropical rainforests like Taï forest in Ivory Coast, Western Congo swamp forest in Congo and Minkebe forest in Gabon (see map in Figure 1.1), habor animals that are potential hosts of Ebolavirus [7].

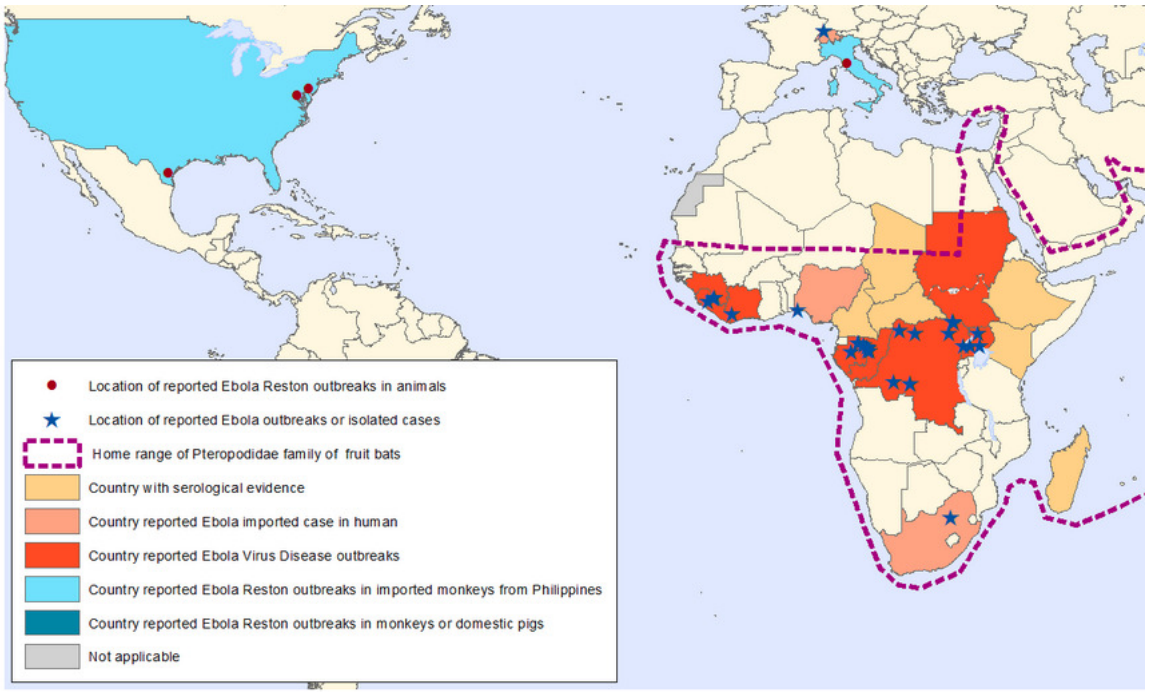

Figure 1.1: Map of the past and present Ebola distribution in Africa, with a more global distribution of fruit bats [1].

West Africa was surprisingly affected by the deadliest EVD in 2013 – 2016. The Taï forest ebolavirus strain was first discovered in Ivory Coast in 1994 but never caused any human deaths [3, 7]. The recent EVD epidemic in West Africa caused by the Zaire ebolavirus strain may have been a result of migration of animals and humans since this strain is common in Central and Southern Africa. The index case of EVD epidemic of 2013 – 2016 was located in Gueckedou, a southern forested district of Guinea which neighbours other districts in Liberia and Sierra Leone [7, 11]. The index case was located in a small village bordering Sierra Leone and Liberia called Nzerekore [7]. Nzerekore is situated near major roads networks, leading to Liberia and Sierra Leone [12, 13]. At the southern boundary of Guinea, are located the districts of Gueckedou and Macenta. These districts are connected to Lofa in Liberia and Kailahlun in Sierra Leone [12]. Within and cross-border human mobility is a common characteristic in West Africa as a result of war, population growth and poverty [14, 15]. In Liberia, between 30% – 40% of citizens reside outside their country of birth and over 54% of the internally displaced are 14 years old [16, 17]. Thus, human mobility between west African countries facilitated the geographic spread of EVD in West Africa and certainly contributed to enlarge the geographic spread of the disease. It is worth noting that migration was the main cause of few EVD cases in America and Europe [16, 17].

1.3 Economic situation of countries affected by EVD: pre and post EVD outbreak situations

The Gross Domestic Product (GDP) is a measure of the strength of a country's economy [18]. It provides a good approximation of expenditures, output and input of a country. It does not account for general well being like safety, life expectancy and population literacy which are considered in the Human Development Index (HDI) [18]. Agriculture and mining were the main sources of income in Zaire in 1975 and the GDP of Zaire in 1976 was 3% [19]. However, the fall in copper prices, decline of agriculture, unplanned investment activity, lack of consistency in budget management and uncontrolled external borrowing lead to slow economic growth in the country [20]. By the time the first EVD outbreak occurred in Zaire, the country's infrastructure and economy could not cope with the much needed control measures. In 1995, another EVD outbreak hit the country, killing 245 people among the 317 infected [3], representing a case fatality ratio of 77%. About 40 years later, the deadliest EVD epidemic ever, hit West Africa, whose countries are classified as low income countries.

Guinea's economy is driven by agriculture, construction and mining [21]. However, political and institutional challenges, keep the country in persistent poverty, with a GDP of 3% at the time of the outbreak in 2013. It is clear that EVD outbreak of $2013-2016$ started in an economically disadvantaged country which contributed to the rapid spread of the disease. It is also worth noting that the epidemic slowed down economic growth in Guinea, causing the GDP growth to drop from 4.5% to 2.4% [22].

Liberia's economy is mainly driven by iron, rubber, construction and service sectors [21]; having been growing steadily before EVD outbreak also reported a drop of its GDP growth [21]. The largest economic effects of EVD crisis were those resulting from changes in behaviour of the affected populations.

Sierra Leone economy, driven predominantly by the mining sector, alongside agriculture and services sectors, experienced a drop in GDP from the projected growth rate of 12.1% to 9.1% in 2014 as a result of the $2013-2016$ EVD outbreak. After EVD outbreak, the annual loss in GDP was estimated to 2.2 billion \$ (U.S. dollar) in the affected countries, which contributed to slowing of the affected economies [23]. Currently, Liberia's economy is progressively returning to normalcy while Guinea's economy has stagnated and Sierra Leone is in recession [24]. The improvements in the health care facilities weakened by EVD outbreak could also accelerate economic growth in these countries.

1.4 Health care systems of countries affected by EVD

A health care system consists of all the organisations, institutions, resources and people whose primary purpose is to improve health including efforts to influence determinants of health and health improvement activities [25]. It is a combination of state and non-state actors' actions. Health care systems thus need staff, funds, information, supplies, transport, communication and direction to function [25, 26]. The monitoring and evaluation strategy of the World Health Organisation (WHO) is structured around the WHO framework that describes health care systems in six essential components: service delivery, health workforce, health information systems, access to essential medicines, financing and governance [25]. Most of the healthcare systems of Africa are characterized as having inadequate infrastructure, under-staffed and under-resourced [26]. Prior to EVD outbreak, most African countries affected didn't meet the average of one hospital for 100,000 inhabitants. Guinea and Liberia, for example, had 0.4 each. The problem of access to hospitals, also due to an unbalanced distribution and poor transport infrastructure, worsened the situation during the outbreak. Further, the lack of qualified hospital personnel also slowed EVD control efforts. Health care staff standards of the WHO are one doctor per 10,000 inhabitants, one nurse per 300 inhabitants and one midwife per 300 women of reproductive age. Overall doctor to population ratio in Africa in 2013 was 2.6 per 10,000 with 1 in Guinea, 0.2 in Sierra Leone and 0.1 in Liberia. Besides the insufficient number of healthcare workers in hospitals, the health care systems of the affected areas within the respective countries were under staffed during EVD epidemic. For example, in Guinea, Conakry had 75% of the health workers while EVD epicentre in the country (Coyah, Dubreka, Forecariah and Kindia prefectures) only had 22% of them [26]. These low rates are in part the consequences of dual job holding or poorly paid doctors. In fact, many doctors in the public sector also work privately and some, attracted by higher salaries, move to cities.

During the 2013 – 2016 EVD epidemic, the community health volunteers were trained and their role was to trace EVD patients' contacts, actively find new cases and safely bury EVD deceased [27]. Community health practitioners, commonly named traditional healers, despite some of their practices previously contributing to EVD spread, provided essential services closer to communities under good supervision and adequate funding [27]. Limited funding during this EVD outbreak was responsible for the death of 513 health care workers [23]. According to the WHO, countries should devote at least 9% of public spending to health care. In 2011, these rates were 19.1%, 12.3% and 6% in Liberia, Sierra Leone and Guinea respectively; in addition to private sector funding [26]. However, low salaries have

driven personnel from public to better paying private hospitals and clinics, leading to near collapse of public health facilities. Private health care facilities offer services which are expensive for most people who end up going to traditional practitioners [26]. Traditional healers combine traditional religion, culture and health, which are important aspects of life in Africa. In the case of EVD outbreak, some traditional healers attributed the origin of the disease to spiritual causes, denying then the scientific methods used to stop the disease spread. This raises the issue of culture in health care on the continent where the lack of overall approach integrating the cultural dimensions of the people for the promotion of health is observed. In Africa, culture and healthcare are interrelated. It was evident in this outbreak that changes in human behaviour were important in stopping the spread of EVD [28].

1.5 Cultural practices of countries affected by EVD and their effects on the implementation of control measures

Interpersonal relationships are the foundation and theme of human life. Psychologists believe that human relationships influence behaviours and development [29]. For example, human behaviour determines the magnitude of infectious diseases. The local culture (language, tradition, religion, rites, food, clothing, etc) should be studied in case its practices are drivers of the spread of the epidemic [30]. Teams in charge of the implementation of control measures, consisting of both local and foreign individuals, require a cultural competence to modify existing behaviour and health care system [30]. Cultural competence is a set of congruent behaviours, attitudes and policies that come together in a system or among professionals to enable that system or group of professionals to work effectively in cross-cultural situations [30]. Behaviour change was a determining factor in the fight against EVD epidemic in West Africa [31].

After 2 to 21 days of exposure to Ebola virus, exposed individuals can present one of the following symptoms: fever, diarrhoea, bleeding, vomiting or haemorrhage [8, 32]. Almost all EVD symptoms include body fluids through which the disease can be transmitted to a susceptible individual when there is body contact [33]. A change in behaviour limiting contact with fluids can slow down or even stop the epidemic [31]. It is possible that the case fatality rate of the $2013-2016$ EVD outbreak could have been reduced if control measure were adopted into the local context [28]. Behaviour change was needed in the affected communities because of unsafe burials, exposed individuals not presenting early at health care facilities but rather to traditional healers and home based care of EVD infected individuals [34]. In Sierra Leone for example, people are concerned about the strict respect of mortu-

ary rites and funeral practices. They believe that practising mortuary rights enables the spirit of the death to reach the village of the deads and eternally live with the ancestors. Otherwise, the angry spirit will send illnesses to the family and the spirit of the deceased will return to torment the family as well. So, whether a person dies from EVD or not, the rites should be respected. During a burial in Mende-speaking region of Sierra Leone, a widow smears her head with mud formed by the deceased husband bathing water after washing his body [34]. Bodies are washed and touched by the elders of the community as well. In this community, many EVD deceased were unsafely buried and this practice contributed to disease transmission [34]. To adapt to such cultural behaviour, health authorities trained a specific staff in charge of burials of EVD victims. They consulted and included families in the burial process of their relatives, financially compensated those families and assisted them in organising funerals.

Further, rumours emerged that medical teams were collaborating with powerful locals to snatch the ill for use in cannibalistic rituals or to harvest organs or that EVD was caused by witchcraft [34]. EVD infected individuals were hid in homes so that even police had to intervene to stop some families from removing their sick relatives from EVD treatment centers. Authorities drafted a cultural behaviour change communication on EVD to communicate the correct behaviour change. Some of the EVD patients who were kept at home because of a limited number of beds in the local EVD treatment center were attended to mostly by women who didn't have any medical training and this contributed to EVD spread. Healthcare workers then intervened in these houses to give necessary indications and material. Some people believed that EVD was a punishment from God for the corruption in the population, which led people to consult traditional healers. To bring about behavioural change in some areas of Sierra Leone or Guinea, traditional healers and some secret societies had to be involved in EVD control. Behaviours changes influenced the dynamics of the $2013-2016$ EVD epidemic in West Africa.

1.6 Motivation

1.6.1 Problem statement

Ebola virus is very virulent, killing individuals after a short period of becoming ill. It has a mean case fatality rate of 50% [3], meaning half of the people who get infected die of the disease. EVD has no vaccine and reliable treatment apart from giving the patient enough fluids and blood. It can only be prevented by quarantining the cases. During the $2013-2016$ outbreak in West Africa, social and be-

havioural characteristics of the population in this region were responsible for high number of EVD cases. For example, washing and touching of the deceased and bush-meat consumption, which are common practices in West Africa [7]. Further, the economic conditions also helped the spread of EVD and slowed down its eradication. This being a limited resource setting region, there were insufficient number of EVD treatment centers in West Africa at the early stage of the epidemic, which contributed to high rates of EVD transmission [35]. Meltzer *et al.* [36] admitted that the effects of hospital-based interventions depend on treatment center capacity and admission rate. Following the $2013-2016$ outbreak, various scenarios of EVD were investigated in mathematical models. The following scenarios were analysed: the uncertainty around EVD reproduction number [37, 38, 39, 40, 41]; the importance of asymptomatic immunity against EVD and symptomless EVD infection [9, 42, 43] and the impact of interventions like case isolation, contact tracing with quarantine, safe burials, pharmaceutical interventions and vaccination [32, 36, 44, 45]. To our knowledge, there is scarce literature about the effect of socio-economic conditions on the spread of EVD. Using the West African countries as a case study, we investigate the effects of social and economic conditions on the spread of EVD. Further, using mathematical modelling we study the link between EVD dynamics and socio-economic conditions. Countries affected by EVD in $2013-2016$ were economically weak with poor health care systems, which limited their ability to combat EVD. Socio-economic factors of these countries such as the lack of health care personnel, limited financial resources and inappropriate human behaviour fuelled the disease spread. To our knowledge, there is scarce literature about the effect of socio-economic conditions on the spread of EVD. Using the West African countries as a case study, we investigate the effects of social and economic conditions on the spread of EVD. Further, using mathematical modelling we study the link between EVD dynamics and socio-economic conditions.

1.6.2 Justification of the study

During the $2013-2016$ EVD outbreak, the three most affected countries had similar characteristics, for example, lack of medicine, ambulance facilities and trained personnel, which affected their response to stopping the EVD epidemic [46]. Further, intermittent Water Supply, Sanitation and Hygiene (WASH) services in rural and urban areas exacerbated poor hygiene practices [27]. In 2013, the Gross Domestic Product (GDP) of Guinea was only 3%, with a HDI ranking of 178 out of 187 and had poor infrastructure, services, and persistent poverty [21]. Access to water in rural areas was low and national sanitation coverage was 18.9% only [27]. In Liberia and Sierra Leone, civil war had weakened the health sector and physi-

cal infrastructure. However, their economy, which is based on mining, agriculture, services and construction was stronger than the Guinean economy (GDP 7.7% and 7.2%, respectively). National water supply rates for Liberia and Sierra Leone were 65% and 60%, respectively, whereas sanitation coverage were 16.8% and 13%, respectively [21]. West Africa is composed of several ethnic groups which define cultural behaviours within communities. It is common in this region to visit traditional healers or to physically assist relatives when they are sick. Some West African tribes require that the relatives of a deceased wash his corpse before burial [7].

These conditions were ripe for increased infection due to EVD in the region. Previous studies about the EVD epidemic of 2013 – 2016 studied the economic impact of the outbreak and ways through which these economies can be revived [27, 46]. Kaitleen e*t al.* [7] focused on the factors that might have led to the emergence of EVD in West Africa, but did not do a mathematical model of these elements and their impact on EVD dynamics. To the best of our knowledge, mathematical modelling of infectious disease, adjusting for socio-economic factors has already been done for diseases like dengue and cholera [47, 48, 49], but not for EVD. Camacho *et al.* [50] from their study on the potential for large outbreaks of EVD in Zaire, suggested that the decline of the first EVD outbreak was the result of changes in host behaviour.

We ask, can similar conclusions be made using the 2013 – 2016 EVD outbreak data? We study the impact of limited resources, human behaviour, human migration and economy on EVD dynamics in order to find an answer to such question.

1.7 Objectives

The main objective of this research was to develop mathematical models which describe and advise on the dynamics of EVD, taking into consideration socio-economic conditions of the West African countries affected by the 2013 – 2016 EVD outbreak. Its specific objectives are:

1. To develop a mathematical model of EVD that considers limited hospital beds,
2. To develop a mathematical model of EVD that takes into account human behaviour,
3. To develop a mathematical model of EVD that considers Ebola virus strain mutation and immigration of infectives,

4. To develop a mathematical model of EVD with economic migration of populations,

5. To fit these models to observed data when possible,

6. To evaluate the impact of these socio-economic conditions on EVD evolution and make suggestions that may influence policy direction in the management of EVD epidemics.

The software Matlab is used for all the numerical simulations that helped to attain these objectives.

1.8 Outline of the thesis

Socio-economic factors of countries affected by EVD in $2013-2016$ such as limited resources, human behaviour, migration of populations and weak economy, drive the present work and constitute the main ideas of four chapters which follow the literature review contained in Chapter 2. We review in the literature, mathematical models for limited resources, human behaviour and populations' migration so as to have an overview of the previous work done and improve our modelling.

Chapter 3 looks at the potential impact of limited hospital beds on EVD dynamics. A mathematical model of EVD with a compartment for the hospitalised individuals is built to take into account the number of beds allocated to ETUs. The mathematical analysis of the model is done including a sensitivity analysis of the model to its parameters using the Latin hypercube sampling scheme. The bifurcation analysis of the model and the model fitting are done. The long term dynamics of the infected population is assessed through numerical simulations.

Chapter 4 looks at a qualitative analysis of an EVD model where a non linear exponential incidence rate is used to represent the effect of human behaviour on EVD dynamics. The mathematical analysis of the model is done. The sensitivity analysis is done with the Latin hypercube sampling scheme and the model fitting is also done.

Chapter 5 looks at the potential influence of strain mutation and human migration on EVD dynamics. This model considers the introduction of a new strain of Ebola virus through continuous or impulsive immigration of infectives. We consider a continuous and an impulsive type of immigration of infectives and the model analysis in each case is done. The numerical simulations that ascertain the long term dynamics of the infected population is done.

Chapter 6 looks at the potential influence of a one way economic migration on EVD dynamics. The mathematical analysis of the model as well as the sensitivity analysis are done. Numerical simulations that assess the long term dynamics of the infected population are done. This chapter also analyses a two way migration model and presents some simulations of the model.

Chapter 7 contains the discussion and concluding remarks.

1.9 Publications

The following papers present the results obtained in the different chapters of this thesis:

- SD Djiomba Njankou and F Nyabadza. "Modelling the potential impact of limited hospital beds on Ebola virus disease dynamics", *Mathematical Methods in the Applied Sciences*, 1–17, 2018.

  This **published** paper is extracted from Chapter 3 and its results were presented at the International Conference on Mathematical Methods and Models in Biosciences hosted in Kruger Park, South Africa on the 25-30 June 2017.

- SD Djiomba Njankou and F Nyabadza. "A qualitative analysis of a simple Ebola model with a non linear incidence rate", extracted from Chapter 4 and **in review** in the journal Bulletin of Mathematical Biology.

- SD Djiomba Njankou and F Nyabadza. "Modelling the potential influence of human migration and strain mutation on Ebola virus disease dynamics", extracted from Chapter 5 and **in review** in the journal Theoretical Population Biology.

- SD Djiomba Njankou and F Nyabadza. "Modelling the potential influence of a one way economic migration and return on Ebola virus disease dynamics", extracted from Chapter 6 and **in review** in the Journal of Biological Systems.

Chapter 2

Literature Review

2.1 Mathematical models with limited resources

Mathematical modelling is an important interdisciplinary activity involving biology, epidemiology, ecology [51]. Diseases' dynamics are some of the various aspects of the disciplines studied using mathematical modelling. In case of emergence of an outbreak, health care resources are needed for the implementation of control measures and the effect of limited resources on the dynamics of the outbreak can be assessed through mathematical modelling. In disease modelling, mathematical models with limited resources do not only focus on the effects of limited resources on disease dynamics, but also predict the amount of resources required for disease eradication.

Models in mathematics can consider health care resources in general or focus on laboratory materials and hospital beds. For example, Zhou and Fan [52] described the dynamics of a SIR (Susceptible-Infected-Recovered) model with limited medical resources. They used an saturation type function $\frac{\beta S I}{1+k I}$ to represent the incidence rate of an infectious disease, where k represents the inhibition effects caused by infected individuals. Besides the issue of limited medical resources, the efficiency of supplied materials is also raised by the authors and a half-saturation function is used to measure the efficiency of the medical resources available. Their study revealed the existence of a backward bifurcation and Hopf bifurcation with varying amount of medical resources and their supply efficiency. The authors concluded that, if an infectious disease has a high case fatality rate with limited treatment and prevention resources, people will adopt a protective behaviour to avoid new infections.

As an application of the model in [52], Abdelrazec *et al.* [53] chose hospital beds as a particular type of medical resource and dengue fever as an example of the

infectious disease. They then modelled the spread and control of dengue fever with limited hospital beds. To describe the impact of the limited resources on the transmission and dynamics of dengue, they formulated a vector-host model. They considered a non linear recovery rate, denoted $\mu(I)$. The recovery rate in this case incorporates the bed-population ratio b and is formulated as

$$\mu(I) = \mu_0 + (\mu_1 - \mu_0)\left(\frac{b}{b+I}\right),$$

with μ_0 and μ_1 as the minimum and the maximum recovery rates. They found the existence of oscillatory dynamics and backward bifurcation. They concluded that besides the reproduction number, other parameters like the bed-population ratio dramatically affect the disease evolution. They recommended the public health authorities to consider the results of their study in future allocations of hospital beds.

In the case of EVD, several authors also looked at the disease dynamics with limited resources with both deterministic and stochastic models. For deterministic models, Nouvellet *et al.* [54] used a $SEIR$ (Susceptible-Exposed-Infectious-Recovered) model with delays between key epidemiological events to evaluate the role of rapid diagnostics in managing Ebola. The delays considered in the model are due to limited laboratory capacity and local transport infrastructure, whose availability would have helped to avoid nosocomial EVD transmission and to allow more available hospital beds. The authors concluded that the use of appropriate test combined with early allocation of the cited resources would have reduced the scale of the epidemic by over a third in Sierra Leone.

Similar conclusion were made by Lewnard *et al.* [55] who focused on pharmaceutical interventions as a control measure to stop EVD. They studied the speed at which non-pharmaceutical interventions were implemented in order to curb the $2013-2016$ EVD epidemic with data from Montserrado county. The authors developed a transmission model of EVD to evaluate the effectiveness of expanding EVD treatment units, improving case ascertainment and allocating protective kits. They suggested in November 2014 that allocating 4, 800 additional EVD treatment beds and increasing case ascertainment five fold could have avoided 77, 312 EVD cases by December 15, 2014. But, despite basic epidemiological truth on the need of more health care resources, predictions of mathematical models are sometimes different from the reality. In fact, Paul Drain [56] pointed at the over projection made in [55] and emphasized the need to fund prevention and control of diseases, other than EVD [56]. The need for an optimal control of EVD is thus raised.

Optimal control of EVD, where minimizing the number of EVD cases is the aim, was done in several research works, see for instance [44, 57, 58]. The aspect of

limited resources not raised in these works, was considered by Hansen and Day [59] who extended the existing optimal control of epidemics to optimal control with limited resources. In fact, in addition to the usual minimization process of the objective functional, which includes the cost and size of an outbreak, the assumption of limited public resources is considered. The aspect of limited resources is reflected in the constraint on the number of people who can be isolated or vaccinated in the model. The authors concluded that optimal isolation policy is not unique when resources are limited and it gives much freedom to policy makers to choose how to isolate individuals with less infrastructure. They concluded that a vaccination policy would be effective and suggested to employ vaccination from the beginning of the epidemic, for as long as possible. The authors acknowledged that time-optimal control of the basic SIR (Susceptible-Infected-Recovered) model is still not fully understood.

Besides the limited health resources during EVD outbreak of $2013-2016$, human behaviour also contributed to EVD spread and some mathematical models that integrate human behaviour already exist in the literature [60, 61, 62, 63, 64].

2.2 Mathematical models with human behaviour

Stopping a disease outbreak in general relies on the technical implementation of control strategies like vaccination, treatment or educational campaigns. One of the objectives targeted by these controls is a change in human behaviour which will stop the disease spread. Even in the case where treatment is available, health workers expect their patients to behave in a prescribed way, by taking their pills at the right time for example. During the EVD outbreak of $2013-2016$, security personnel were often present in Ebola Treatment Units (ETUs) to make sure that the prescriptions were respected by patients [65]. So, human behaviour is at the core of any disease eradication and from different domains, it has been monitored and used for disease control [60].

Psychology and anthropology are not the only domains interested by human behaviour. Mathematical modelling as well has focused on the effects of human behaviour on various diseases evolution, see for instance [60, 61, 62, 63, 64, 66, 67, 68, 69, 70, 71, 72, 73, 74, 75, 76, 77, 78, 79]. However, the quantification of human behaviour remains a challenge that leads to difficulties in building and analysing mathematical models with human behaviour [61]. This idea is shared by Funk *et al.* [62] who listed nine challenges faced in incorporating the dynamics of human behaviour in infectious diseases models. These challenges that help to transit

from theoretical models to relevant models for policy makers are: setting the baseline and determining the effect of departing from it, assessing how and to what extend behaviour should be modelled explicitly, determining the minimal level of detail required to model differences in behaviour, quantify changes in reporting behaviour, predict the response to interventions and health campaigns, identify the role of movement and travel, developing models that can be verified against data from digital sources, informing real-time data collection and engaging in dialogue across disciplines [62]. Funk *et al.* [62] proposed the use of Bluetooth, wireless sensor networks and web based social networks to collect data that will help modellers. Besides the issue of quantification of human behaviour, the origin and type of information leading to a behavioural change was also raised by the authors.

Funk *et al.* [62] reviewed mathematical models with self-initiated behaviour and reaction to information from the outside world. They made a distinction between information from the neighbourhood described as local and information from the TV, WHO described as global. They stated that local information lead to belief based mathematical models where the change in human behaviour is motivated by cultural, religious or even word of mouth information [63, 64]. But, individuals are most likely to change their contact patterns when mortality or the perception of risk is high [66]. Prevalence based models thus represent behaviour change influenced by a high disease mortality or infectivity [67, 68, 69]. For example, Del Valle *et al.* [75] formulated a model to investigate the effects of behavioural changes in a smallpox attack. They assumed that individuals within a community change their behaviour and move from normal active group to less active group, reducing their average number of contacts, in response to a high prevalence of smallpox in their community. The compartments of their model are vaccinated, susceptible, quarantined, exposed, infectious, isolated, recovered and deceased. The per-capita transfer rate between compartments are given by the function

$$\phi_i = \frac{a_i(I_n + I_l)}{1 + b_i(I_n + I_l)} \frac{1}{day}$$

with $i = S, E, I$ and $n =$ normally active, $l =$ less active, a_i and b_i are positive constants that modulate the rate of change. Behavioural change was assumed to vary ϕ_i values and the transmission rate of smallpox [75]. The authors showed that the spread of smallpox is sensitive to how rapidly people reduce their contact activities and found that even mild behavioural change can have a dramatic impact on slowing an epidemic [75].

Behavioural change can affect the disease status of an individual, the infection, the recovery rate or the contact network structure relevant to the disease spread and

this approach is used by several authors when modelling [61]. For example, Bauch *et al.* [70] used a SIR model to represent vaccination , through a game theoretic approach with imitation dynamics, where a proportion of children are vaccinated at birth by parents who base their decision on disease prevalence and perceived vaccines risks. In this case, parents adapt vaccinator or non vaccinator strategy with a payoff $f_r = -r_v$, r_v being the perceived probability of significant morbidity from the vaccine [70]. Their model predicted that oscillations in vaccine uptake are more likely in populations where individuals imitate others more readily or where vaccinating behaviour is more sensitive to changes in disease prevalence [70]. Children vaccination as a result of parent behaviour change, is also considered to be dependent on the mortality and vaccination risks in [71], where susceptible children can become infectious if they are not vaccinated or lose their vaccine immunity and may later on recover. In [71], Bauch and Earn incorporated p as the proportion of vaccinated individuals to the usual SIR model and the new recruitment rate into the susceptible class was $\mu(1-p)$. They also computed the reproduction number and used it to find infection probability. Game theoretical analysis of the model lead to the conclusion that increases in perceived vaccine risk will tend to induce larger decline in vaccine uptake for pathogens that cause more secondary infection [71].

Unlike children vaccination that is initiated by parents, voluntary vaccination is a self initiated vaccination that can also be used for modelling purposes in some cases. For example, social contact networks and disease eradicability under voluntary vaccination were represented by a $SEIR$ model in [72]. Perisic and Bauch, [72] formulated a vaccine preventable infectious disease model, assuming that a newly-infected person remains in the latent stage for a duration of time drawn from a gamma probability density function (PDF). Another gamma PDF with a different value for the mean is used to represent the time duration of the infectious period. Game theory and networks are used to show that when infection is transmitted only through close contacts in the network, an outbreak can be easily contained using only voluntary vaccination [72].

Parameters are modified in some models to represent the effect of behavioural change. Probabilities were also used by Eames [73] who incorporated them to the force of infection of a disease and to the recovery rate of the infected individuals. The author used a SIR/V (Susceptible-Infected-Recovered or Vaccinated) model to represent social influence within a network of parents and the transmission of infection through a network of children. The author assumed that the epidemic is updated at every time step δ and each susceptible offspring becomes infected with

probability $(1 - \exp(-\beta is))$, with β as transmission rate, i as infected and s as the separation distance between two parents locations; each infected individual recovering with probability δ [73]. The author assumed that the probability of forming a link between two parents is 0.1 if s is below a certain threshold and zero otherwise. Children are also linked by the same rule when they have linked parents. Opinion clustering was measured within parental network by calculating the probability $A = c^2 + (1 - c)^2$ that two connected parents have the same vaccination opinion, where c is the fraction of parents who are in favour of vaccination. The author concluded that the effects of opinion clustering among parents is stronger when there is more overlap between their networks and those of their children and the risk of an outbreak is caused by many contacts between the two networks [73].

The age of an individual may influence the type of behaviour an individual is expected to develop in a given situation. Previously cited models mostly focused on the type of relationship between individuals (children and parents), ignoring the type of behaviour presented by each class of persons. But, some authors considered this important aspect in their modelling process. For example, Tanaka *et al.* [74] examined the effects of within-generation transmission of traits by including a culturally transmitted behaviour that affects disease spread in a population. Their model divides individuals as susceptibles or infected, whose behaviour can be risky or careful, which represent the two cultural types considered in this case. The contact rate of individuals was set as θ_1 for individuals of the same cultural type and θ_2 for those of different cultural types. The probability that disease is transmitted from an infected in state j to a susceptible in state i was b_{ij} and the disease transmission coefficients were finally $\theta_1 b_{ii}$ and $\theta_2 b_{ij}$ with i, j in $\{$ careful, risky $\}$. So, by varying these coefficients, the number of infected varied and their effect on the disease dynamics could be estimated. The authors found that behaviours increasing the risk of infection can also evolve when they are inherently favoured or when there is sufficient clustering of contacts between like behaviours. They indicated that the model was not appropriate for diseases of urban areas [74].

The type of a behaviour depends on the information received whose validity can be influenced by the number of transmission of this information from the source to the final destination. Funk *et al.* [76] considered this aspect when investigating the impact of the spread of awareness on epidemic outbreaks. They assumed that people aware of a disease in their proximity can change their behaviour towards a reduced susceptibility. First, they associated to each individual a level of awareness i, to indicate the number of passages the information had undergone before arriving at the given individual. They assumed that information transmission decreases

the quality of the concerned information [76]. These assumptions were thus incorporated into a SIR model where the impact of individuals actions were captured in the disease transmission. The disease transmission was made dependent of the quality of information available to a given susceptible individual and the susceptibility of individuals in stage i, decreased with i as $(1-p^i)$, with $i = 1, 2, \ldots N$ and N is the total population size. They formulated the probability generating function of awareness as $g(\rho, S_i(t)) = \sum \left(\frac{S_i(t)}{S(t)}\right) \rho^i$. So, awareness of the disease in this case led to a reduced susceptibility of individuals [76]. This principle was then used by the authors together with mean field analysis to draw the conclusion that the impact of locally spreading awareness is amplified if the social network over which individuals communicate overlaps [76].

Information transmission and epidemic outbreaks were also studied by Kiss *et al.* [77]. They considered the case of sexually transmitted infections, where in general the whole population is aware of the risk. Responsive individuals can decide either to protect themselves or seek treatment and non-responsive ones do not react to information. The usual $SIRS$ model was extended into a model made of susceptibles non-responsive S_{nr}, susceptibles responsive S_r, infected non-responsive I_{nr}, infected responsive I_r and treated T [77]. Non-responsive individuals were assumed to move to responsive class as a result of information disseminated via direct contact between individuals, given by $f = \frac{X(S_r + I_r + T)}{N}$ and population wide dissemination of the disease related information, given by $g = \frac{(I_{nr} + I_r)^n}{k + (I_{nr} + I_r)^n}$ where $n \geqslant 1$ and $k > 0$. The authors assumed that the value of information decays with time and used it together with f and g in the model formulation to represent the effect of awareness on sexually transmissible infections (STIs). They showed that infection can be eradicated if the dissemination of information is fast enough [77]. Modification of the contact structure was also used to investigate the effect of behaviour change on disease dynamics [67, 68].

In the case of EVD, a stochastic model representing the impact of behaviour change on the spread of EVD with a linear force of infection was done in [80]. In order to reach similar objective, which is to assess the impact of behaviour change on EVD dynamics, we have used a deterministic model with a non linear incidence rate in this work.

Human migration is an example of behavioural response, which might be motivated by poor economic conditions or war and can also be incorporated to mathematical models.

2.3 Mathematical models of population migration and geographic spread of infectious diseases

Geographic localisation can be used to differentiate several groups of people and interactions between individuals can occur within each group or between different groups when people move to a different location. Some individuals within a given group might have contracted an infectious disease and their interactions with healthy people can lead to the transmission of the disease. Migration of infectives can then cause the geographic spread of a disease and several mathematical models describing this phenomenon have been built, see for instance [81, 82, 83, 84, 85, 86]. Modelling the spatial heterogeneity of a population is a complex task that can be done by structuring the population into households, sub-populations, patches, cities or even countries for modelling purpose. Social, behavioural or even labour mobility which are more deterministic have shed the light on such models [86]. Sattenspiel and Dietz [86] formulated a mover-stayer meta-population model, that incorporates heterogeneity in individuals' migration rates for disease spread with population mobility. This model has been used as a template for future models of large population migration and disease dynamics in disease prevalence regions. The authors partitioned the population into subgroups made of large numbers of individuals who are homogeneous in their mobility patterns. They considered a multi-city model in which the total number of permanent residents in a city i is

$$N_i = \sum_{j,j\neq i} N_{ij} + N_{ii}$$

where N_{ii} is the number of residents of city i present in the city, N_{ij} is the number of individuals from city i visiting city j. The transmission term describing the disease spread after infectious contacts in this case is

$$\sum_{j=1}^{n}\sum_{k=i}^{n} K_k\, \beta ijk\, \frac{I_{jk}\, S_{ik}}{N_k^*}$$

where K_k is the average number of contacts per person made in region k, βijk is the proportion of contacts in region k between individuals from regions i and j, I_{jk} is the number of infectives in region k who are permanent residents of region j, S_{ik} is the number of susceptibles present in city k who are permanent resident of city i, N_k^* is the number of people actually present in region k [86].

Similar patterns were used by Wang and Zao [87] to model an epidemic in a patchy environment. Using a SI model with mass action incidence rate, they modelled disease transmission as a result of population dispersal between n patches and assumed that susceptible and infected individuals have similar dispersal rates in

each patch. They established two threshold parameters to draw conclusions on the disease persistence or extinction: the reproduction number R_0 and the stability modulus $S(J)$ which is the largest eigenvalue of a matrix J. They used the next generation matrix method to compute the reproduction number $\left(R_0 = \rho(\mathcal{F}\mathcal{V}^{-1})\right)$ and it was proven that the reproduction number is equivalent to the stability modulus $S(J)$ of the matrix $J = \mathcal{F} - \mathcal{V}$ where $S(J) = \rho(J)$ [87]. The authors showed that

$$S(J) > 0 \Leftrightarrow R_0 > 1 \quad \text{and} \quad S(J) < 0 \Leftrightarrow R_0 < 1,$$

so that the disease free equilibrium is globally asymptotically stable when $S(J) < 0$. They concluded that if the reproduction number is large for one patch, then the population dispersal can increase the disease spread and can limit the disease transmission for appropriate reproduction number and high population dispersal rate [87].

The next generation matrix method was also used to find the reproduction number of a multi-city model by Arino and Van Den Driesche [88]. They developed a multi-city epidemic model for a population travelling between n cities and used a SIS (Susceptible-Infected-Susceptible) model to describe the disease dynamics in each city. They determined the reproduction number as $R_0^i = \dfrac{K_i\,\beta_{iii}}{d+\gamma}$ when the city i is isolated from others, where K_i is the number of contacts between individuals living in city i, β_{iii} is the probability of infectious contacts in city i, d is the death rate and γ is the recovery rate of infectives [88].

As an application to the use of the reproduction number as a threshold parameter in a meta-population model, Njangara and Nyabadza [89] formulated a meta-population model for cholera transmission dynamics between communities linked by migration. A SIR pattern was used by the authors to model the spread of cholera between two communities linked by population migration and the model considered the pathogen shedding into the aquatic reservoir. The shedding rate was assumed to be high in communities with poor facilities and low in communities with improved facilities. The authors computed the specific reproduction number for each community when it is isolated and when it is connected to the other one. From the stability analysis of equilibrium points, they concluded that, first in isolated communities, a big outbreak followed by a small episode of infection characterises the endemic cholera. Second, when the communities are connected, the persistence of the infection is influenced by the movement of individuals. The authors admitted that besides migration, temperature and rainfall are vital contributors causing synchrony in meta-population driven epidemics.

Chance plays a major role in the spread of an infection in small groups, requiring in this case the use of stochastic models [81]. Small households are used to structure the geographic spread of populations in stochastic models. For example, a continuous time Markov chain was used by Arigoni and Pugliese [83] in a SIS stochastic model to model the spread of epidemics among a population partitioned into M sites, each containing N individuals. The authors analysed the limit behaviour of the system as M and N increases and concluded that the infected population converges to a Dirac measure. Becker and Dietz [84] also used a stochastic model to study the effect of household distribution on transmission and control of highly infectious diseases. They defined a household as any group of individuals having frequent contacts with each other. They denoted the household distribution as h_{ns} for a household of size $n(n \leq N)$ containing s susceptible individuals. In a randomly selected household, the means μ_H, μ_s and the variances σ_H^2, σ_s^2, respectively of the number of members and susceptibles, were needed for summary statistics of a household distribution. The proportion of households of size n was denoted by $h_{n+} = \sum_{s=0}^{n} h_{ns}$ and the proportion of households with s susceptibles members was denoted by $h_{+s} = \sum_{n=s}^{N} h_{ns}$. Assuming that the disease is transmitted from person to person, they introduced g_{ns} as the proportion of individuals living in households with n members of whom s are susceptible with $g_{ns} = \frac{n\,h_{ns}}{\mu_H}$. The authors used two main criteria to classify the infectives and compute different reproduction numbers: the disease transmission between individuals and between households. First, a newly infected individual is said of type s if there are still s susceptibles in the considered household after his/her infection and the basic reproduction number R_0 is computed. Second, an infected household is said to be of type i if there are i eventual infected cases in the considered household, including the introductory case and the reproduction number R_{H0} is computed as well. The authors used R_0 and R_{H0} to derive the levels of immunity needed for the prevention of epidemics and to evaluate various vaccination strategies. They found that random vaccination of individuals is more efficient for households of the same size whereas immunizing all members of a household is preferable for large households of different sizes.

Whether we use a stochastic or a deterministic approach when modelling, migration of individuals between different patches connects these patches. Migration influences and responds to the prevalence of a disease, to the cost of migration and to health regulation in endemic settings [85]. According to Mesnard *et al.* [85], individuals' choices to migrate, modelled in discrete time is given by the following conditions: For healthy (H) and sick (S) individuals, migration will occur when the utility to migrate $\left(U_M^i(H), U_M^i(S)\right)$ is greater than the utility not to migrate

$\left(U_N^i(H), U_N^i(S)\right)$. Here $i = 1,2$ represents in this case two cities, of which city 1 is poor and unhealthier than city 2. The authors found that migration can lower disease incidence in low prevalence cities and they suggested to policy makers to encourage migration away from highly infected areas in some cases.

Migration in West Africa was seen as a challenge to stopping EVD because experts believed that it contributed to the disease spread in the region [90]. This motivated the work done by Goufo and Maritz in [91] who used a $SIRD$ (Susceptible-Infected-Recovered-Deceased) model and a mover-stayer model to model the dynamics of human migration and EVD outbreak. They developed a multi-country model, where each of the four patches represents a country in West Africa based on the research done in [86, 92]. They assumed that the number of residents in each country is variable, but the total population in the four countries considered is constant. From the numerical simulations performed on a sample of 1000 individuals, they concluded that very few infected visitors in a given country can infect or transmit EVD to the entire population.

Within the borders of Guinea, the spatio-temporal dynamics of EVD epidemic and implications for vaccination and disease elimination was studied by Ajelli *et al.* [93]. Unlike Goufo and Maritz [91] who considered migration of infectives, they assumed that EVD infected individuals in Guinea were unlikely to travel when they have active symptoms, unless they were seeking hospitals. The authors thus chose a stochastic computing agent based model to reproduce the geographical incidence of EVD in Guinea as was done for Liberia in [94]. They concluded that computational modelling approach is useful to characterize the role of interventions in Guinea and could be used for Liberia and Sierra Leone. They also identified contact tracing and early availability of beds in ETUs as key drivers of the different patterns of spread observed in Guinea. The negligence of asymptomatic infection and acquired immunity, which can accelerate the elimination of EVD, was recognized as a limitation of the model.

A stochastic model for the spatial spread of EVD was also used by Kiskowski and Chowell [11]. The authors modelled household and community transmission of EVD by employing a stochastic individual-level model. They used a network to locate infectious individuals and implemented the spatial spread of the epidemic on the network with a household-community structure. They assumed that control measures or behaviour change could explain sub-exponential growth of EVD. They showed that varying a community mixing size C for a fixed household of size H, would lead to different rates in epidemic growth. They modelled epidemic control with delay by decreasing the reproductive numbers based on external

or internal clock. They used simulations to characterise patterns of the early growth phase and long-term disease dynamics of the epidemic. Defining the term endemic as infectious wave in steady equilibrium with a fixed size and speed, they concluded that greater epidemic control and limited community mixing decrease the size of an infectious wave.

These models cited did not consider the cause of population migration. We have incorporated in this work the social or economic conditions within a country affected by EVD that force people to migrate.

All the mathematical models cited in this chapter will constitute the framework of this thesis, that intends to associate social and economic factors to EVD dynamics. Precisely, the first model we build deals with the potential impact of limited hospital beds on the dynamics of EVD.

2.4 Health, economy, poverty and mathematical models

"Poverty is a pervasive risk factor underlying poor health" [95]. In fact, people living in poverty are more susceptible to diseases and health issues such as obesity, human immunodeficiency virus (HIV), heart failure, cancer ...[95]. In mathematical modelling, health and poverty can be linked through classes or compartments [47, 96, 97]. They can also be linked through parameters such as the per capita income [98, 99]. Bhunu *et al.* [47] used a $SEIR$ (Susceptible-Exposed-Infected-Recovered) model to assess the effects of poverty in tuberculosis transmission dynamics. Two main groups constituted their model: individuals living in poverty noted p and those not living in poverty noted r. Their respective forces of infection were $\lambda_p = \frac{P_{pp}C_p\beta_pI_p}{N_p} + \frac{P_{pr}C_p\beta_rI_r}{N_r}$ and $\lambda_r = \frac{P_{rr}C_r\beta_rI_r}{N_r} + \frac{P_{rp}C_r\beta_pI_p}{N_p}$ where group $j(j = r, p)$ members make C_j contacts per unit time, with $\beta_i(i = r, p)$ as the probability of being infected. A fraction of the contacts made by a member of group i is p_{ij} [47]. They considered $C_p = b_1C_r$ with $b_1 > 1$ to represent the fact that poor live in overcrowded condition. Assuming heterogeneous interaction, the authors concluded that homogeneous mixing of the rich and the poor will improve the eradication whereas heterogeneous mixing, will make it worse. However, they encouraged the rich to contribute to tuberculosis eradication within the poor communities [47]. Rich and poor communities groups have been used by Mushayabasa *et al.* [96] to evaluate the impact of poverty on yaws eradication. The authors in this case used a unique force of infection, but considered that susceptible children from poor families acquire yaws at an increased rate. The reproduction number was

used in this case to assess the impact of birth rate in poor families on the dynamics of yaws and the authors concluded that more needs to be done in addressing issues such as high fertility rate and poverty in order to eradicate yaws [96]. More socio-economic classes have been used to analyse infectious diseases models. Collins *et al.* [48] analysed a waterborne disease SIR model with n socioeconomic classes (SEC), $n \geq 1$. They only considered indirect transmission of pathogen and assumed that SEC 1 was the poorest, followed by SEC 2 until SEC n considered as the richest class. The authors first determine the effects of a 2-SEC model on cholera transmission dynamics and extended their results to an n-SEC model. They concluded that a model without SEC may underestimate the reproduction number of the system and lead to a failure in the disease control [48].

According to Ngonghala *et al.* [100], economic growth models and infectious diseases models are highly dependent and this dependence can be represented through the use of parameters. The interdependence between disease prevalence and income is also analysed by Bonds *et al.* [101]. The authors assumed in [101] that the natural death rate $\mu(M)$, the recovery rate $\gamma(M)$ and the transmission rate $\beta(M)$ of a disease vary with economic wealth. They represented these parameters as a function of income M as

$$\mu(M) = \frac{\varrho}{h(M)} + \bar{\mu},\ \gamma(M) = \tau h(M),\ \beta(M) = \frac{\bar{\beta}\phi}{M+\phi}$$

where h is a metric of nutrition and is determined by income M, $\bar{\mu}$ is is the minimum death rate for a completely nourished individual, ϱ and τ are exogenous parameters, $\bar{\beta}$ is the maximum transmission rate, ϕ is the amount of income necessary to reduce the transmission rate by half. The authors used a classic saturation function to model nutrition as a function of income using the expression $h(M) = \dfrac{\bar{h}M}{M+k}$ where $\bar{h}$ is the maximum level of nutrition attainable with unlimited income. Income is also represented as a function of disease prevalence in [101] by $M(I) = \delta\pi_s$, where I is the number of infected individuals, δ is an exogenous parameter that determines the rate at which individuals produce income per unit time healthy and π_s is the time spent susceptible which can be represented by a Markov chain. The authors concluded that the effect of income on disease prevalence and vice versa are important. They also found that the feedbacks between income and disease have the potential to generate divergent trajectories of health and economic development that are dependent on the initial conditions [101]. As an application of the feedback between income and disease, Pluciński *et al.* [102] analysed a SIS model using Gillespie algorithm to analyse the system and concluded from their model that clusters of poverty and disease result from feedbacks between health and economic conditions at the individual level and feedback between individual-

and population-level health conditions.

Infectious diseases and economy are also studied in statistics. A n-SEC model with data was used in statistical modelling to study the role of socio-economic status in longitudinal trends of cholera in Matlab [49]. Phuong Do *et al.* [103] used probability density functions to investigate the relationship between neighbourhood poverty and mortality risk.

Methods and hypothesis used in the cited mathematical models helped to link economy and EVD in a mathematical model in this research.

Chapter 3

Modelling the potential impact of limited hospital beds on Ebola virus disease dynamics

3.1 Introduction

The 2013 – 2016 Ebola virus disease (EVD) was declared to be over, despite the resurgence of isolated cases [104, 105]. The success was due to the combination of efforts at national and international levels. Controlling an EVD outbreak relies on applying several packages of interventions, that include case management, surveillance and contact tracing, a good laboratory service, safe burials and social mobilisation [106]. In the three West African nations most affected by the epidemic, the disease incidence was observed to be correlated with several factors among which was the availability of beds for patients, as the incidence diminished shortly after an increase in the number of beds [107]. The introduction of thousands of treatment beds for the infected in Sierra Leone, averted a significant number of EVD cases [35]. It is however unclear how much hospital beds can contribute to the decline of an epidemic.

Mathematical modelling has been used to evaluate interventions implemented against EVD. Interventions aiming at stopping the 2013 – 2015 EVD epidemic were incorporated into mathematical models, see [35, 36, 39, 44, 57, 108]. A comparative review of mathematical models for EVD was done in [108]. Caitlin *et al.* [32] used a $SEIHFR$ (Susceptible-Exposed-Infectious-Hospitalized-Funeral-Removed) compartmental model to describe the evolution of an Ebola epidemic, as well as the efficacy of several interventions. Using existing data from Liberia and Sierra Leone until December 2014, to parameterize the mathematical model, they found that

an improved infection control and an increased contact tracing had a substantial impact on the number of EVD cases. They also concluded that pharmaceutical interventions have a smaller effect on the disease trajectory.

In most of the highly affected communities, the pre-existing health facilities were either far or limited and in some cases totally non existent [65, 109]. Any suspected case of EVD was admitted into a Community Care Center (CCC) and triage was the first process during which their status was defined. After the triage stage, suspected individuals were either released, sent to a quarantine area for more observations or admitted into an ETU (Ebola Treatment Unit) when they were confirmed Ebola seropositive. But admission into an ETU did not only depend on health personnel but also on the number of available beds. The provision of sufficient beds for an Ebola CCC determined patients' admission and treatment [65]. Recovery of EVD patients remains an international concern, since there is still no treatment against the disease. So, recovery from EVD largely depends on other factors like behavioural change or the availability of physicians, nurses, Ebola treatment centers and hospital beds [53].

The effects of limited hospital beds on the evolution of a disease have been studied, with an application to the control of dengue fever, see [53, 110]. In the case of EVD, Kucharski and Camacho [35] used a stochastic mathematical model to measure the impact of control measures in Sierra Leone at community level, with the introduction of isolation beds. However, thousands of beds were necessary at the national level to hospitalise the very large number of EVD patients [111]. In such a case, a deterministic mathematical model can be used. So, unlike in [35], we use a deterministic model to study the dynamics of EVD with limited hospital admission capacity with the number of newly available beds being time dependent. In order to estimate resource availability to the public, health planners use hospital bed-population ratio, i.e the number of hospital beds available for $10,000$ population [53]. From 2005 to 2012, the number of beds available per every $10,000$ people in Guinea was 3, before the emergence of EVD in the country [112]. This value was very low compared to the number of beds in low income countries which lies between 21 and 165, set by the World Health Organisation (WHO) during the same period [112]. So, the number of beds allocated to EVD patients was largely insufficient to accommodate the unexpected increase in the number of cases.

Beds allocation to any hospital depends on the offer and demand. In the case of Ebola Treatment Units (ETUs), we assume that the demand is a function of the bed carrying capacity, b_{max}, and one would like to have b_{max} as large as possible to ensure prompt hospitalisation ($b_{max} \geq 1$). Here, b_{max} is assumed to be the product of

the number of ETUs times the number of beds each ETU can contain. During the last EVD outbreak, beds were progressively added to ETUs until the carrying capacity was reached. Therefore, we assume that the growth in the number of beds is logistic in nature. We thus use a logistic growth equation to describe the dynamics of the number of new beds allocated to ETUs. The rate of change in the number of available beds is thus formulated as

$$\frac{d\,b(t)}{dt} = \pi\left(1 - \frac{b(t)}{b_{max}}\right) b(t),\ \forall\, t \geq 0,$$

where π is the addition rate of beds (growth rate).

We also innovatively introduce a per capita dynamic hospitalisation rate $\gamma\big(b(t), I(t)\big)$ to capture the impact of limited hospital beds represented by the time dependent number of newly available beds $b(t)$. $I(t)$ represents the number of infected individuals, $\gamma\big(b(t), I(t)\big)$ is assumed to be an increasing function of $b(t)$ and a decreasing function of the number of infected individuals. We set μ_1 and μ_0 to be the maximum and minimum per capita hospitalisation rate respectively due to sufficient and insufficient resources, see for instance [53]. It is important to note that a function similar to $\gamma\big(b(t), I(t)\big)$ was suggested in [110]. Unlike in [110], where b is constant, in this work, b is dynamic. This allows us to account for variability in the number of beds. The hospitalisation function is thus given by

$$\gamma\big(b(t), I(t)\big) = \mu_0 + (\mu_1 - \mu_0)\,\frac{b(t)}{\Big(b(t) + I(t)\Big)}.$$

We thus aim to model the potential impact of limited hospital beds on the dynamics of EVD. This work is presented as follow: Section 3.2 is dedicated to the model formulation and Section 3.3 for the model properties and analysis. Section 3.4 describes the steady states analysis, Section 3.5 describes the numerical simulation, Section 3.6 describes the model fitting and the conclusion is given in Section 3.7.

3.2 Model formulation

To evaluate the effects of limited hospital capacity on EVD dynamics, we formulate a deterministic model of five distinct compartments of susceptibles (S), infected (I), hospitalized (H), recovered (R) and deceased (D). Susceptible individuals are recruited at a rate Λ. After exposure to Ebola virus, susceptibles become infected and can transmit the disease. At the contact rate c with susceptibles, an infectious individual can transmit the disease with a probability β. Thus $c\,\beta$ is the effective transmission rate of the disease. When access to Ebola treatment units or hospitals is guaranteed, infected individuals can either be hospitalized at a per capita rate

$\gamma\big(b(t), I(t)\big)$ or die from the disease at a rate δ_1, or in some rare cases recover at a rate α. In this case we assume that infected individuals get hospitalised without delay. Hospitalized EVD patients can recover at a rate ω or die at a rate δ_2 because of the disease. Hospitalized individuals are assumed to be infectious, but with a lower infectivity than individuals in class I because of the controlled environment in which they are isolated. So we consider $0 < \eta_1 < 1$. The natural death rate is assumed for each class μ and dead bodies are buried at a rate ρ. Dead bodies of EVD deceased are highly infectious and this high infectivity is represented by a factor $\eta_2 > 1$. The force of infection is given by

$$\lambda(t) = c\,\beta\left(I(t) + \eta_1 H(t) + \eta_2 D(t)\right)$$

where $N = S(t) + I(t) + H(t) + R(t) + D(t),\ \forall\, t \geq 0$. The flow between different compartments of the model is represented by Figure 3.1 and the system of ordinary differential equations (3.2.1) – (3.2.6). We assume that at $t = 0$,

$$S(0) > 0, \quad I(0) \geqslant 0, \quad H(0) \geqslant 0, \quad R(0) \geqslant 0, \quad D(0) \geqslant 0 \quad \text{and} \quad b(0) > 0.$$

$$\dot{S}(t) = \Lambda - (\lambda + \mu)\, S(t), \tag{3.2.1}$$

$$\dot{I}(t) = \lambda\, S(t) - \gamma\big(b(t), I(t)\big)\, I(t) - Q_1\, I(t), \tag{3.2.2}$$

$$\dot{H}(t) = \gamma\big(b(t), I(t)\big)\, I(t) - Q_2\, H(t), \tag{3.2.3}$$

$$\dot{R}(t) = \alpha\, I(t) + \omega\, H(t) - \mu\, R(t), \tag{3.2.4}$$

$$\dot{D}(t) = \delta_1\, I(t) + \delta_2\, H(t) - \rho\, D(t), \tag{3.2.5}$$

$$\dot{b}(t) = \pi\left(1 - \frac{b(t)}{b_{max}}\right) b(t), \tag{3.2.6}$$

where $Q_1 = \mu + \alpha + \delta_1$ and $Q_2 = \delta_2 + \omega + \mu$.

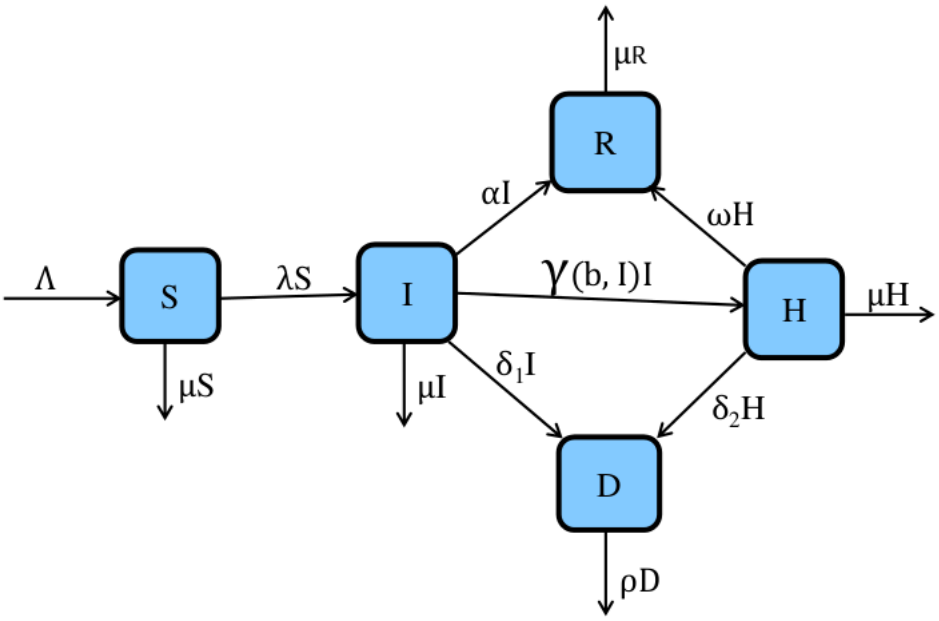

Figure 3.1: Flow chart diagram representing population dynamics with beds dependent hospitalization rate.

Since the recovered individuals do not contribute to EVD transmission, $R(t)$ dynamics may be decoupled from other variables in the closed system and we obtain

$$\dot{S}(t) = \Lambda - (\lambda(t) + \mu)\, S(t), \tag{3.2.7}$$

$$\dot{I}(t) = \lambda(t)\, S(t) - \gamma\big(b(t), I(t)\big)\, I(t) - Q_1\, I(t), \tag{3.2.8}$$

$$\dot{H}(t) = \gamma\big(b(t), I(t)\big)\, I(t) - Q_2\, H(t), \tag{3.2.9}$$

$$\dot{D}(t) = \delta_1\, I(t) + \delta_2\, H(t) - \rho\, D(t), \tag{3.2.10}$$

$$\dot{b}(t) = \pi \left(1 - \frac{b(t)}{b_{max}}\right) b(t). \tag{3.2.11}$$

We set $M(t) = S(t) + I(t) + H(t)$.

3.3 Model properties and analysis

Theorem 3.3.1. *Picard's existence theorem is sufficient to conclude the existence and uniqueness of solutions of system (3.2.7)-(3.2.11), for given initial conditions.*

$$\Omega = \left\{ \Big(S(t), I(t), H(t), D(t), b(t)\Big) \in \mathbb{R}^5 : M(t) \leq \frac{\Lambda}{\mu},\ D(t) \leq \frac{\Lambda(\delta_1 + \delta_2)}{\mu\rho} \ \text{ and } \ b(t) \leq b_{max} \right\}$$

which is attracting and positively invariant with respect to the flow of system (3.2.7)-(3.2.11).

Proof. In fact, the right hand side of system (3.2.7)-(3.2.11) is made of Lipschitz continuous functions, which is a necessary and sufficient condition in Picard's existence Theorem [113] for the solutions to exist and the system (3.2.7)-(3.2.11) has positive and bounded solutions in the region.

Given that $M(t) = S(t) + I(t) + H(t)$, adding equations (3.2.7)-(3.2.9) yields

$$\frac{\mathrm{d}M}{\mathrm{d}t} \leq \Lambda - \mu\, M. \tag{3.3.1}$$

Using Gronwall inequality [114] and integrating (3.3.1) we obtain the following solution

$$M(t) \leqslant \left(M(0) - \frac{\Lambda}{\mu}\right) \exp\Big(-\mu\, t\Big) + \frac{\Lambda}{\mu}, \quad \forall\ t \geqslant 0.$$

If $M(0) \leqslant \dfrac{\Lambda}{\mu}$, then the upper bound of $M(t)$ is $\dfrac{\Lambda}{\mu}$ when $t \to \infty$. If $M(0) \geq \dfrac{\Lambda}{\mu}$, then $M(t)$ decreases to $\dfrac{\Lambda}{\mu}$ when $t \to \infty$ and enters Ω or approaches Ω asymptotically. Similarly, since $I(t) < M(t)$ and $H(t) < M(t)$, from equation (3.2.10) we have

$$\dot{D}(t) \leq \frac{\Lambda(\delta_1 + \delta_2)}{\mu} - \rho\, D(t), \tag{3.3.2}$$

whose solution is

$$D(t) = \frac{1}{\rho}\left(\frac{\Lambda(\delta_1 + \delta_2)}{\mu} - \rho\left(\frac{\Lambda(\delta_1 + \delta_2)}{\mu\rho} - D(0)\right)\exp\Big(-\rho\, t\Big)\right)$$

and

$$\lim_{t\to\infty} D(t) = \begin{cases} \dfrac{\Lambda(\delta_1 + \delta_2)}{\mu\rho} & \text{if} \quad D(0) \geq \dfrac{\Lambda(\delta_1 + \delta_2)}{\mu\rho}, \\[2ex] \dfrac{\Lambda(\delta_1 + \delta_2)}{\mu\rho} & \text{if} \quad D(0) < \dfrac{\Lambda(\delta_1 + \delta_2)}{\mu\rho}. \end{cases} \tag{3.3.3}$$

So, from equations (3.3.2) and (3.3.3) we obtain $D(t) \leq \dfrac{\Lambda\,(\delta_1 + \delta_2)}{\mu\rho}$.
The solution of equation (3.2.11) is the standard solution to a logistic differential equation given by

$$b(t) = b_{max}\, \frac{K\,\pi\, \exp\Big(\pi\, t\Big)}{\Big(b_{max} + K\,\pi\, \exp\Big(\pi\, t\Big)\Big)}$$

where $K = \dfrac{b(0)\, b_{max}}{\pi\left(b_{max} - b(0)\right)}$.

So, $b(t) \leq b_{max}$, since $\dfrac{K\,\pi\, \exp\Big(\pi\, t\Big)}{\Big(b_{max} + K\,\pi\, \exp\Big(\pi\, t\Big)\Big)} \leq 1$ and we can conclude that Ω is positively invariant and attracts all solutions of the system (3.2.7)-(3.2.11). □

Theorem 3.3.2. *Solutions of system* (3.2.7)-(3.2.11) *exist and are positive for any given positive initial conditions.*

Proof. From equation (3.2.7) we have

$$\frac{\mathrm{d}\,S(t)}{\mathrm{d}t} \geqslant -\left(\lambda(t)+\mu\right)S(t), \quad \forall\, t \geqslant 0. \tag{3.3.4}$$

Solving for $S(t)$ in (3.3.4) and using Gronwall inequality yields

$$S(t) \geq S(0)\, \exp\Big(-\Big(\int_0^t \lambda(\tau)\, d\tau + \mu\, t\Big)\Big) > 0.$$

Similarly, from equation (3.2.8) we have

$$\frac{\mathrm{d}\,I(t)}{\mathrm{d}t} \geqslant -\,Q_1\,I(t) - \gamma\big(b(t), I(t)\big)\; I(t)$$

which implies

$$I(t) \geq I(0)\, \exp\Big(-\,Q_1\,t - \int_0^t \gamma\big(b(t), I(t)\big)(u)\, du\Big) \geq 0.$$

Similarly, from equation (3.2.9) we can write

$$\frac{\mathrm{d}\,H(t)}{\mathrm{d}t} \geqslant -Q_2\,H(t)$$

so that

$$H(t) \geqslant H(0)\exp\Big(-\,Q_2\,t\Big) \geq 0.$$

Equation (3.2.10) yields

$$D(t) \geqslant D(0)\exp\Big(-\,\rho\,t\Big) \geq 0.$$

The solution of the differential equation (3.2.11) is

$$b(t) = b_{max}\,\frac{K\,\pi\,\exp\Big(\pi\,t\Big)}{\Big(b_{max} + K\,\pi\,\exp\Big(\pi\,t\Big)\Big)} > 0.$$

So $S(t)$, $I(t)$, $H(t)$, $D(t)$ and $b(t)$ are all non-negative for non-negative initial conditions. □

3.4 Steady states analysis

At equilibrium, equation (3.2.11) $\left(\frac{db}{dt} = 0 \right)$ yields $b = 0$ or $b = b_{max}$. The case $b = 0$ leads to either a disease free equilibrium (DFE) E_1^0 in the total absence of infected individuals or an endemic equilibrium (EE) E_1^* when $I > 0$. The DFE is given by $E_1^0 = (S^0, 0, 0, 0, 0)$ where $S^0 = \frac{\Lambda}{\mu}$, $I = H = b = D = 0$ and the endemic equilibrium E_1^* is explicitly given in Subsection 3.4.3.1. We set $I = H = b = D = 0$ and solve equation (3.2.7) for S to get S^0.

The case $b = b_{max}$ leads to either a DFE $E_2^0 = \left(S^0, 0, 0, 0, b_{max}\right)$ with the maximum number of beds or an endemic steady state E_2^* also discussed in Subsection 3.4.3.1.

At equilibrium, equation (3.2.11) is equivalent to $\frac{db}{dt} = 0$, which gives $b = 0$ or $b = b_{max}$ when solved for b. Equation (3.2.7) is equivalent to $\frac{dS}{dt} = 0$, which gives $S = S^0$ when solved for S.

3.4.1 The reproduction number

The next generation matrix method is used to compute the reproduction number, see [115]. The reproduction number in this case is the spectral radius of the product of the new infections matrix $\mathcal{F}$ and the inverse of the transfer matrix $\mathcal{V}$.

$$R_h = \rho(\mathcal{F}\mathcal{V}^{-1}).$$

The matrix F is obtained by differentiating the new infection term λS with respect to the infected compartment state variables which are I, H, D. The matrix V is obtained by differentiating (with respect to I, H, D) the opposite of the right hand side of the differential equations (3.2.8)-(3.2.10) without the new infection term. Note that we can either use E_1^0 or E_2^0 to compute the reproduction number and obtain in both cases the same result since the beds compartment $b(t)$ is not an infected individuals compartment and then is not used in the calculation of the reproduction number. From model (3.2.7)-(3.2.11) we have

$$\mathcal{F} = \begin{bmatrix} S^0\beta c & S^0\beta c\,\eta_1 & S^0\beta c\,\eta_2 \\ 0 & 0 & 0 \\ 0 & 0 & 0 \end{bmatrix} \quad \text{and} \quad \mathcal{V} = \begin{bmatrix} Q_1 + \mu_1 & 0 & 0 \\ -\mu_1 & Q_2 & 0 \\ -\delta_1 & -\delta_2 & \rho \end{bmatrix}.$$

The reproduction number, denoted by R_h, is given by the spectral radius of $\mathcal{F}\mathcal{V}^{-1}$ so that

$$R_h = S^0\beta\, c\left(\frac{1}{Q_1+\mu_1}+\frac{1}{\rho\,(Q_1+\mu_1)}\left[\delta_1\eta_2+\frac{\mu_1\,(\delta_2\eta_2+\rho\,\eta_1)}{Q_2}\right]\right).$$

$R_h = R_I + R_H + R_D$ where $R_I = \dfrac{S^0\beta\, c}{Q_1+\mu_1}, R_H = \dfrac{S^0\beta\, c\,\mu_1\,\eta_1}{(Q_1+\mu_1)\,Q_2}$,
$R_D = \dfrac{S^0\beta\, c\,\eta_2}{\rho\,(Q_1+\mu_1)}\left(\delta_1+\dfrac{\mu_1\,\delta_2}{Q_2}\right)$.

We note that R_I, R_H and R_D respectively give the contribution of the infected, hospitalised and deceased to EVD transmission.

From the formulation of the reproduction number R_h, we have

$$\frac{\mu}{\Lambda\beta c}=\frac{1}{R_h}\left(\frac{1}{Q_1+\mu_1}+\frac{1}{\rho\,(Q_1+\mu_1)}\left[\delta_1\eta_2+\frac{\mu_1\,(\delta_2\eta_2+\rho\,\eta_1)}{Q_2}\right]\right). \tag{3.4.1}$$

3.4.2 Stability of E_1^0 and E_2^0

Theorem 3.4.1. *E_1^0 is locally unstable and E_2^0 is locally stable whenever $R_h < 1$.*

Proof. The Jacobian matrix J_{dfe} of the linearised system (3.2.7)-(3.2.11) at the DFE is given by

$$J_{dfe}=\begin{bmatrix} -\mu & -S^0\beta c & -S^0\beta c\,\eta_1 & -S^0\beta c\,\eta_2 & 0\\ 0 & S^0\beta c-Q_1-\mu_1 & S^0\beta c\,\eta_1 & S^0\beta c\,\eta_2 & 0\\ 0 & \mu_1 & -Q_2 & 0 & 0\\ 0 & \delta_1 & \delta_2 & -\rho & 0\\ 0 & 0 & 0 & 0 & \pi\left(1-\dfrac{2b}{b_{max}}\right)\end{bmatrix}.$$

The eigenvalues of J_{dfe} are $-\mu$, $\pi\left(1-\dfrac{2b}{b_{max}}\right)$ together with the eigenvalues of the reduced matrix Γ given by

$$\Gamma=\begin{bmatrix} S^0\beta c-Q_1-\mu_1 & S^0\beta c\,\eta_1 & S^0\beta c\,\eta_2\\ \mu_1 & -Q_2 & 0\\ \delta_1 & \delta_2 & -\rho\end{bmatrix}.$$

Let x be an eigenvalue of the matrix Γ. The characteristic polynomial $Q(x)$ of Γ is given by

$$Q(x) = -x^3+\nu_1x^2+\nu_2x+\nu_3 \tag{3.4.2}$$

where

$$\nu_1 = (Q_1 + \mu_1)\left(R_a - 1\right) - (\rho + Q_1),$$
$$\nu_2 = \rho\,(Q_1 + \mu_1)\left(R_b - 1\right) + Q_2\,(Q_1 + \mu_1)\left(R_c - 1\right),$$
$$\nu_3 = \rho\,(Q_1 + \mu_1)\left(R_h - 1\right),$$

with $R_a = \dfrac{S^0 \beta\, c}{Q_1 + \mu_1} < R_h$, $R_b = \dfrac{S^0 \beta\, c\,(\rho + \delta_1\,\eta_2)}{\rho\,(Q_1 + \mu_1)} < R_h$ and $R_c = \dfrac{S^0 \beta\, c\,(Q_2 + \eta_1\,\mu_1)}{Q_2\,(Q_1 + \mu_1)} < R_h$.

So, when $R_h < 1$, all the coefficients of the polynomial (3.4.2) are negative. According to Descartes' law of signs (stated in Appendix A), if there is no sign change in the coefficients of a polynomial, then the polynomial admits zero positive root. When $R_h < 1$, all the coefficients of the polynomial (3.4.2) are negative and thus the polynomial admits no positive root. Hence, matrix Γ has only negative eigenvalues when $R_h < 1$. Moreover,

$$\pi\left(1 - \frac{2b}{b_{max}}\right) = \begin{cases} \pi & \text{if} \quad b = 0, \\ -\pi & \text{if} \quad b = b_{max}. \end{cases}$$

Hence, all the eigenvalues of the Jacobian matrix J_{dfe} are negative if $b = b_{max}$ leading to the local stability of E_2^0. If $b = 0$, one of the eigenvalues π is positive, thus the corresponding DFE E_1^0 is unstable. So, having hospital beds for EVD control is better than not having them, since a positive number of beds guarantees at least a locally stable DFE. □

3.4.3 The endemic equilibria E_1^* and E_2^*

We now look at the two endemic equilibria corresponding to the cases when $b = 0$ and $b = b_{max}$.

3.4.3.1 The endemic equilibrium E_1^*

When $b = 0$, the endemic equilibrium for the EVD model in terms of I^* is given by $E_1^* = \left(S^*, I^*, H^*, D^*, 0\right)$ where $S^* = \dfrac{1}{R_h^0}$, $I^* = \dfrac{\mu\,(R_h^0 - 1)}{R_h^0}$, $H^* = \dfrac{\mu_0\, I^*}{Q_2}$,

$D^* = \frac{(Q_2\,\delta_2 + \mu_0\,\delta_2)\,I^*}{\rho\,Q_2}$ with $R_h^0 = S^0\beta\,c\left(\frac{(\rho+\eta_2\,\delta_1)\,Q_2 + (\rho\,\eta_1+\eta_2\,\delta_2)\,\mu_0}{\rho\,Q_2\,(Q_1+\mu_0)}\right)$.
At equilibrium $\left(\dot{S}(t) = 0, \dot{I}(t) = 0, \dot{H}(t) = 0, \dot{D}(t) = 0\right)$, we solve equation (3.2.9) for H to obtain H^*. Then we set $H = H^*$ in equation (3.2.10) and solve for D to get D^*. We set $D = D^*$ in equation (3.2.7) and solve for S to get S^* and finally we set $S = S^*$ in equation (3.2.8) and solve for I to obtain I^*. We replace the obtained value of I^* in (3.2.7) and simplify to obtain the final results.

At the endemic equilibrium,

$$
\begin{aligned}
(3.2.9) &\iff \dot{H}(t) = 0 \Longrightarrow H = H^*,\\
(3.2.10) &\iff \dot{D}(t) = 0 \Longrightarrow D = D^*,\\
(3.2.7) &\iff \dot{S}(t) = 0 \Longrightarrow S = S^*,\\
(3.2.8) &\iff \dot{I}(t) = 0 \Longrightarrow I = I^*.
\end{aligned}
$$

$I^* > 0$ when $R_h^0 > 1$. In this case, the existence of E_1^* is driven by R_h^0 which is considered as the reproduction number at minimum hospitalisation rate μ_0. In the absence of beds for hospitalisation of EVD patients, the existence of endemic equilibrium points depends on the reproduction number at minimum hospitalisation rate. This is reasonable since admission into ETU is minimal or even stopped when there are no new beds supplied to ETU.

Theorem 3.4.2. *The endemic equilibrium E_1^* is globally asymptotically stable for $R_h > 1$.*

The global stability of the endemic equilibrium, stated by Theorem 3.4.2, is proven using LaSalle's invariance principle, following [116, 117, 118, 119, 120].

Proof. We first set the Lyapunov function as

$$
\begin{aligned}
L = &\left(S - S^* - S^*\ln(\frac{S}{S^*})\right) + A\left(I - I^* - I^*\ln(\frac{I}{I^*})\right) + B\left(H - H^* - H^*\ln(\frac{H}{H^*})\right)\\
&+ G\left(D - D^* - D^*\ln(\frac{D}{D^*})\right),
\end{aligned}
$$

where A, B and G are positive constants to be determined. At the endemic point $E^* = (S^*, I^*, H^*, D^*)$, we have $L(E^*) = 0$. Besides, the partial derivatives of L with respect to each state variable are

$$\frac{\partial L}{\partial S} = \left(1 - \frac{S^*}{S}\right), \frac{\partial L}{\partial I} = A\left(1 - \frac{I^*}{I}\right), \frac{\partial L}{\partial H} = B\left(1 - \frac{H^*}{H}\right), \frac{\partial L}{\partial D} = G\left(1 - \frac{D^*}{D}\right).$$

So the endemic state E^* is a critical point of L and the second derivative is

$$\frac{\partial^2 L}{\partial S^2} = \left(\frac{S^*}{S^2}\right), \frac{\partial^2 L}{\partial I^2} = A\left(\frac{I^*}{I^2}\right), \frac{\partial^2 L}{\partial H^2} = B\left(\frac{H^*}{H^2}\right), \frac{\partial^2 L}{\partial D^2} = G\left(\frac{D^*}{D^2}\right).$$

The second derivative of L being positive at any point of Ω, the Lyapunov function L is concave up and the unique endemic equilibrium point is a minimum of F. Let us prove that $\dot{L} \leq 0$. The derivative of L with respect to time t, denoted $\dot{L}$ is

$$\dot{L} = \left(1 - \frac{S^*}{S}\right)\dot{S} + A\left(1 - \frac{I^*}{I}\right)\dot{I} + B\left(1 - \frac{H^*}{H}\right)\dot{H} + G\left(1 - \frac{D^*}{D}\right)\dot{D}.$$

First we take into account the following inequality

$$\gamma(b(t), I(t)) \geq \mu_0 \quad \text{for all} \quad t \geq 0 \tag{3.4.3}$$

and particularly $\gamma(b(t), I(t)) = \mu_0$ in this case since we consider $b = 0$ at equilibrium. Considering inequality (3.4.3) and the system of equations (3.2.7)-(3.2.11), we obtain

$$\begin{aligned}\dot{L} \leq & \left(1 - \frac{S^*}{S}\right)\left(\Lambda - \left(c\,\beta(I + \eta_1 H + \eta_2 D) + \mu\right) S\right) \\ & + A\left(1 - \frac{I^*}{I}\right)\left(\beta\, c\,(I + \eta_1 H + \eta_2 D)\, S - Q_{1,0}\, I\right) \\ & + B\left(1 - \frac{H^*}{H}\right)(\mu_0 I - Q_2 H) + G\left(1 - \frac{D^*}{D}\right)(\delta_1 I + \delta_2 H - \rho D).\end{aligned} \tag{3.4.4}$$

At equilibrium, the system of equations (3.2.7)-(3.2.11) yields

$$\begin{aligned}\Lambda = \left(c\,\beta(I^* + \eta_1 H^* + \eta_2 D^*) + \mu\right) S^*, \quad Q_{1,0} = \mu_0 + \frac{c\,\beta(I^* + \eta_1 H^* + \eta_2 D^*)\, S^*}{I^*}, \\ Q_2 = \mu_0 \frac{I^*}{H^*}, \quad \rho = \frac{1}{D^*}(\delta_1 I^* + \delta_2 H^*), \quad H^* = g_1 I^*, \quad D^* = g_2 I^*\end{aligned} \tag{3.4.5}$$

with

$$g_1 = \frac{\mu_0}{Q_2} \quad \text{and} \quad g_2 = \frac{(\delta_1 Q_2 + \mu_0 \delta_2)}{\rho\, Q_2}.$$

We set

$$x = \frac{S}{S^*},\ y = \frac{I}{I^*},\ z = \frac{H}{H^*},\ u = \frac{D}{D^*}.$$

Replacing expressions from the system (3.4.5) into inequality (3.4.4) yields

$$\dot{L} \leq -\mu \frac{(S - S^*)^2}{S} + c\,\beta\, I^* F(x, y, z, u)$$

where

$$\begin{aligned} F(x,y,z,u) = &\left(1 - \frac{1}{x}\right) S^* \Big((1 - x\,y) + g_1\,\eta_1\,(1 - x\,z) + g_2\,\eta_2\,(1 - u\,x) \Big) \\ &+ A \left(1 - \frac{1}{y}\right) S^* \Big(y\,(x-1) + \eta_1\,g_1\,(x\,z - y) + g_2\,\eta_2\,(u\,x - y) \Big) \\ &+ \frac{G}{\beta\,c} \left(1 - \frac{1}{u}\right) \Big(\delta_1\,(y - u) + \delta_2\,g_1\,(z - u) \Big) \\ &+ \frac{B\,\mu_0}{\beta\,c} \left(1 - \frac{1}{z}\right) (y - z). \end{aligned} \tag{3.4.6}$$

Expanding the expression of $F(x, y, z, u)$ from system (3.4.6) and grouping the coefficients of the same variable give

$$\begin{aligned} F = &\frac{B\,\mu_0}{\beta\,c} + \frac{G\,\delta_1}{\beta\,c} + \frac{G\,g_1\,\delta_2}{\beta\,c} + S^*\,(A+1) + S^*(A+1)\,\eta_1\,g_1 + S^*(A+1)\,\eta_2\,g_2 \\ &+ y \left(\frac{B\,\mu_0}{\beta\,c} + \frac{G\,\delta_1}{\beta\,c} + S^*\,(1 - A) - \eta_1\,g_1\,A\,S^* - \eta_2\,g_2\,A\,S^* \right) + \frac{y}{z} \left(- \frac{B\,\mu_0}{\beta\,c} \right) \\ &+ z \left(\eta_1\,g_1\,S^* - \frac{B\,\mu_0}{\beta\,c} + \frac{G\,g_1\,\delta_2}{\beta\,c} \right) + u \left(- \frac{G\,\delta_1}{\beta\,c} - \frac{G\,g_1\,\delta_2}{\beta\,c} + \eta_2\,g_2\,S^* \right) \\ &+ \frac{y}{u} \left(- \frac{G\,\delta_1}{\beta\,c} \right) + \frac{z}{u} \left(- \frac{G\,g_1\,\delta_2}{\beta\,c} \right) + \frac{1}{x} \left(- S^* - \eta_1\,g_1\,S^* - \eta_2\,g_2\,S^* \right) - x\,A\,S^* \\ &+ x\,y \left(- S^* + A\,S^* \right) + u\,x \left(- \eta_2\,g_2\,S^* + \eta_2\,A\,g_2\,S^* \right) + \frac{u\,x}{y} \left(- A\,S^*\,g_2\,\eta_2 \right) \\ &+ \frac{z\,x}{y} \left(- \eta_1\,g_1\,S^*\,A \right) + x\,z \left(- \eta_1\,g_1\,S^* + A\,g_1\,\eta_1\,S^* \right). \end{aligned} \tag{3.4.7}$$

The point is to prove that $\dot{L} \leq 0$. Having already the term $-\mu \dfrac{(S - S^*)^2}{S} \leq 0$ from the expression of $\dot{L}$, it remains to prove that $F \leq 0$. From the expression of F in (3.4.7), we will first set the terms containing variables and with non negative coefficients to zero in order to get rid of the positive and non constant part of F. The coefficients of $y, z, u, x\,y$ and $u\,x$ are thus set to zero and solved for A, B and G. We obtain

$$A = 1,\ B = \frac{\beta\,c}{\mu_0} \left[\eta_1\,g_1 + \frac{\delta_2\,g_1}{\beta\,c} \left(\frac{\eta_2\,g_2}{\delta_1 + g_1\,\delta_2} \right) \right] S^* \quad \text{and} \quad G = \beta\,c\,\frac{\eta_2\,g_2}{(\delta_1 + g_1\,\delta_2)} S^*.$$

Then

$$F(x,y,z,u) = \frac{B\,\mu_0}{\beta\,c}\left(3-\frac{1}{x}-\frac{z\,x}{y}-\frac{y}{z}\right)+\frac{G\,\delta_1}{\beta\,c}\left(3-\frac{1}{x}-\frac{y}{u}-\frac{x\,u}{y}\right) + \frac{G\,\delta_2\,g_1}{\beta\,c}\left(1+\frac{zx}{y}-\frac{x\,u}{y}-\frac{z}{u}\right)+\left(2-x-\frac{1}{x}\right)S^*. \quad (3.4.8)$$

Apply the arithmetic mean-geometric mean inequality [117]

$$a_1+a_2+\ldots+a_n \geq n\,\sqrt[n]{a_1\,a_2\,\ldots\,a_n} \quad \text{for} \quad i=1,2\ldots,n \quad \text{and} \quad n>0.$$

We set for example, $p_1=\dfrac{1}{x}, p_2=\dfrac{zx}{y}, p_3=\dfrac{y}{z}$. Then,

$$p_1+p_2+p_3 \geq 3\sqrt[3]{p_1p_2p_3}$$

according to the arithmetic mean-geometric mean inequality.

$$p_1p_2p_3=1 \quad \text{and} \quad p_1+p_2+p_3 \geq 3.$$

So,

$$3-(p_1+p_2+p_3) \leq 0$$

which means

$$\frac{B\,\mu_0}{\beta\,c}\left(3-\left(\frac{1}{x}+\frac{z\,x}{y}+\frac{y}{z}\right)\right) \leq 0.$$

Similarly, we prove that other terms composing $F(x,y,z,u)$ in (3.4.8) are negative.

F is then negative and will be equal to zero if $x=y=z=u=1$. So L is positive definite at the endemic equilibrium and $\dot{L} \leq 0$ with equality in the set

$$\mathcal{C} = \left\{(S,I,H,D) : S=S^*, I=I^*, H=H^*, D=D^*\right\}.$$

The singleton $E_1^* = \left(S^*, I^*, H^*, D^*, 0\right)$ is the unique endemic equilibrium point considered in this case. So any solution which intersects $\mathbb{R}^5_+$ limits to the endemic equilibrium E_1^*. By LaSalle's invariance principle [116], E_1^* is globally asymptotically stable on Ω. □

3.4.3.2 The endemic equilibrium E_2^*

We note $E_2^* = \left(S^*, I^*, H^*, D^*, b_{max}\right)$ with

$$S^* = \frac{\rho\, Q_2 \left(b_{max}\left(Q_1+\mu_1\right) + I^*\left(Q_1+\mu_0\right)\right)}{\xi_0}, H^* = I^* \frac{\left(b_{max}\,\mu_1 + I^*\,\mu_0\right)}{\left(b_{max}+I^*\right) Q_2},$$

$$D^* = \frac{\left(Q_2\,\delta_1\left(b_{max}+I^*\right) + \delta_2\left(b_{max}\,\mu_1 + I^*\,\mu_0\right)\right) I^*}{\rho\, Q_2\left(b_{max}+I^*\right)}, \tag{3.4.9}$$

where

$$\xi_0 = \beta\, c\left(Q_2\left(b_{max}+I^*\right)\left(\rho+\eta_2\,\delta_1\right) + \left(b_{max}\,\mu_1 + I^*\,\mu_0\right)\left(\rho\,\eta_1 + \delta_2\,\eta_2\right)\right).$$

At equilibrium $\left(\dot{S}(t)=0, \dot{I}(t)=0, \dot{H}(t)=0, \dot{D}(t)=0\right)$, we solve equation (3.2.9) for H to obtain H^*. Then we set $H = H^*$ in equation (3.2.10) and solve for D to get D^*. We set $D = D^*$ in equation (3.2.8) and solve for S to get S^* and I^* is obtained by substituting the state variables $(S = S^*, D = D^*)$ in equation (3.2.7) at equilibrium. We obtain the following polynomial:

$$a_0(I^*)^3 + a_1(I^*)^2 + a_2 I^* + a_3 = 0 \tag{3.4.10}$$

with

$$a_0 = \rho\, Q_2\left(Q_1+\mu_0\right)^2 R_h^0,$$

$$a_1 = \rho\, Q_2\left(Q_1+\mu_0\right)\left(b_{max}\left(Q_1+\mu_1\right)\left(R_h^0+R_h\right) + \mu\left(1-R_h^0\right)\right),$$

$$= \rho\, Q_2\left(Q_1+\mu_0\right)\left(\mu\left(1+R_h^0\left(b_{max}-1\right)\right) + b_{max}\left(\mu_1+\delta+\alpha\right)\left(R_h^0+R_h\right)\right),$$

$$a_2 = \rho\, Q_2\, b_{max}\left(\mu\left(\left(Q_1+\mu_1\right)\left(1-R_h\right) + \left(Q_1+\mu_0\right)\left(1-R_h^0\right)\right)\right.$$

$$\left. + b_{max}\left(Q_1+\mu_1\right)^2 R_h\right),$$

$$a_3 = \mu\,\rho\, Q_2\, b_{max}^2\left(Q_1+\mu_1\right)\left(1-R_h\right).$$

Descartes' law of signs is used to determine the possible number of positive roots of the polynomial (3.4.10) that are summarised in Table 3.1.

	$a_0 > 0$			
	$a_1 > 0$			
	$a_2 > 0$		$a_2 < 0$	
	$a_3 > 0$ $(R_h < 1)$	$a_3 < 0$ $(R_h > 1)$	$a_3 > 0$ $(R_h < 1)$	$a_3 < 0$ $(R_h > 1)$
I^*	0	1	2	1

Table 3.1: Number of possible endemic fixed points.

Since $b_{max} \geq 1$, the coefficient a_1 will always be positive and the possibility of having 3 positive roots for polynomial (3.4.10) is completely discarded. Conditions of existence of endemic fixed points of system (3.2.7)-(3.2.11) are summarized in Theorem 3.4.3.

Theorem 3.4.3.

- *If all the coefficients of the polynomial* (3.4.10) *are positive, then system* (3.2.7)-(3.2.11) *has no endemic steady state.*
- *If* $R_h > 1$ *then the system* (3.2.7)-(3.2.11) *has a unique endemic equilibrium point.*
- *If* $R_h < 1$ *then the system* (3.2.7)-(3.2.11) *has two endemic equilibrium points.*

Although polynomial (3.4.10) is of order 3, it admits at most two positive roots. So, multiple endemic equilibria exist and these equilibrium points are locally stable. The local stability of E_2^* is proven using a theorem based on the center manifold theory [121]. In this case, the threshold value of the reproduction number, R_h^c, below which the DFE is globally stable is a critical point of the polynomial (3.4.10). Besides, the discriminant Δ of the polynomial (3.4.10) is equal to zero at this point. We have

$$\Delta = \xi_1 a_3^2 + \xi_2 a_3 + \xi_3$$

and

$$\xi_1 a_3^2 + \xi_2 a_3 + \xi_3 = 0 \tag{3.4.11}$$

with $\xi_1 = -27 a_0^2$, $\xi_2 = 18 a_0 a_1 a_2 - 4 a_1^3$ and $\xi_3 = a_1^2 a_2^2 - 4 a_0 a_2^3$.
Finding the positive roots (a_3) of the polynomial in (3.4.11) and setting

$$R_h^c = 1 - \left(\frac{a_3}{\mu \rho Q_2 b_{max}^2 (Q_1 + \mu_1)} \right)$$

will give the analytical expression of a threshold value for the reproduction number. If polynomial in (3.4.11) has two positive roots ($\Delta > 0$), then the largest should be considered.

The following theorem is stated and proved:

Theorem 3.4.4. *E_2^0 is locally asymptotically stable when $\mathcal{A} > 0$ and there exists a positive unstable endemic equilibrium E_2^* for $R_h^c < R_h < 1$. E_2^0 is globally asymptotically stable when $R_h < R_h^c < 1$ and $\mathcal{A} > 0$. When $\mathcal{A} < 0$, E_2^0 becomes unstable and a negative unstable endemic equilibrium E_2^* becomes positive and locally asymptotically stable for $R_h > 1$. $\mathcal{A} = 2\,\rho\,Q_2\left(\dfrac{\mu\left(Q_2\,(\rho+\eta_2\,\delta_2)-Q_1\,(\rho\,\eta_1+\delta_2\,\eta_2)\right)(\mu_1-\mu_0)-\xi_5}{\mu\,b_{max}\,\xi_4}\right)$.*

Proof. We set $\phi = \beta\,c$ as our bifurcation parameter, so that for

$$R_h = 1, \qquad \phi = \phi^* = \frac{\rho\,(Q_1+\mu_1)\;Q_2}{S^0(\rho\,\eta_1+\delta_2\,\eta_2)\,\mu_1+(\delta_1\,\eta_2+\rho\,)\,Q_2}.$$

In order to linearise system (3.2.7)-(3.2.11), we set

$$S = x_1, I = x_2, H = x_3, D = x_4, b = x_5$$

and

$$\dot{S} = f_1, \dot{I} = f_2, \dot{H} = f_3, \dot{D} = f_4, \dot{b} = f_5.$$

The Jacobian matrix $\mathcal{J}$ of the linearised system (3.2.7)-(3.2.11) at the DFE E_2^0 and for $\phi = \phi^*$ is given by

$$\mathcal{J} = \begin{bmatrix} -\mu & -S^0\phi & -S^0\phi\,\eta_1 & -S^0\phi\,\eta_2 & 0 \\ 0 & -Q_1-\mu_1+S^0\phi & S^0\phi\,\eta_1 & S^0\phi\,\eta_2 & 0 \\ 0 & \mu_1 & -Q_2 & 0 & 0 \\ 0 & \delta_1 & \delta_2 & -\rho & 0 \\ 0 & 0 & 0 & 0 & -\pi \end{bmatrix}.$$

Zero is a simple eigenvalue of $\mathcal{J}$. The left eigenvector of $\mathcal{J}$, $V = (v_1, v_2, v_3, v_4, v_5)$ and the right eigenvector $W = (w_1, w_2, w_3, w_4, w_5)'$, both associated to the eigenvalue zero are solutions of the system

$$\begin{cases} \mathcal{J}W = [0,0,0,0,0]', \\ V\mathcal{J} = [0,0,0,0,0]', \\ VW = 1 \end{cases} \tag{3.4.12}$$

and we obtain after some tedious algebraic manipulations

$$\begin{aligned} w_1 &= -\frac{(Q_1+\mu_1)}{\mu}, & v_1 &= 0,\\ w_2 &= 1, & v_2 &= \frac{(\rho\,\eta_1+\delta_2\,\eta_2)\,\mu_1+(\delta_1\,\eta_2+\rho\,)\,Q_2}{\xi_4},\\ w_3 &= \frac{\mu_1}{Q_2}, & v_3 &= \frac{\rho\,Q_2\,(\rho\,\eta_1+\delta_2\,\eta_2)\,(Q_1+\mu_1)}{\xi_4},\\ w_4 &= \frac{\delta_1\,Q_2+\mu_1\,\delta_2}{\rho\,Q_2}, & v_4 &= \frac{\eta_2\,\rho\,Q_2^2\,(Q_1+\mu_1)}{\xi_4},\\ w_5 &= 0, & v_5 &= 0, \end{aligned}$$

where

$$\begin{aligned} \xi_4 =&\rho\,(\rho\,\eta_1+\delta_2\,\eta_2)\,\mu_1\,(Q_1+\mu_1)\\ &+\eta_2\,Q_2\,(\rho+Q_1+\mu_1)\,(\mu_1+Q_2)+Q_2\,\rho^2\,(Q_2+\eta_1\,\mu_1). \end{aligned}$$

Besides, we notice that for $j=2,3,4$, $E_2^0(j)=0$ and $W(j)>0$ with $W(j)=w_j$. So Remark 4 in [121] is verified. Two constants $\mathcal{A}$ and $\mathcal{B}$ are defined in [121] as

$$\mathcal{A}=\sum_{k,i,j=1}^{n} v_k w_i w_j \frac{\partial^2 f_k}{\partial x_i \partial x_j}(E_2^0,\phi^*),$$

$$\mathcal{B}=\sum_{k,i=1}^{n} v_k w_i \frac{\partial^2 f_k}{\partial x_i \partial \phi}(E_2^0,\phi^*).$$

We compute these constants and find

$$\mathcal{A}=2\,\rho\,Q_2\left(\frac{\mu\left(Q_2\,(\rho+\eta_2\,\delta_2)-Q_1\,(\rho\,\eta_1+\delta_2\,\eta_2)\right)(\mu_1-\mu_0)-\xi_5}{\mu\,b_{max}\,\xi_4}\right)$$

and

$$\mathcal{B}=\frac{1}{\xi_4}\Big((\rho\,\eta_1+\delta_2\,\eta_2)\,\mu_1+(\delta_1\,\eta_2+\rho\,)\,Q_2\Big)^2,$$

with $\xi_5=b_{max}\,(Q_1+\mu_1)^2\Big((\rho\,\eta_1+\delta_2\,\eta_2)\,\mu_1+(\delta_1\,\eta_2+\rho\,)\,Q_2\Big)$.

The direction of the bifurcation is determined by the signs of $\mathcal{A}$ and $\mathcal{B}$. Obviously $\mathcal{B}>0$ and the sign of $\mathcal{A}$ determines the following:

$$\begin{cases} \text{if} \quad \mathcal{A}>0 \quad \text{then the bifurcation is backward,}\\ \text{or}\\ \text{if} \quad \mathcal{A}<0 \quad \text{then the bifurcation is forward.} \end{cases}$$

□

3.5 Numerical simulations

3.5.1 Sensitivity analysis

Variability in the model predictions is introduced by uncertainty in the parameter values [122]. Sensitivity analysis is performed to assess this variability in the model predictions. Latin Hypercube Sampling/Partial Rank Correlation Coefficient (LHS/PRCC) sensitivity analysis is used to explore the entire parameter space of a model with a minimum number of computer simulations [123].

To implement the LHS, we list our parameters and determine those which are uncertain or those which are not. In this work, we consider all the parameters to be uncertain. We hypothetically provide the range in which the parameters' values fall. The simulations are run 1000 times in order to have a large sample size which will make the results more precise. To implement the LHS sampling scheme, we specify a probability density (pdf) function for each unknown parameter. In this case, we chose by default a uniform distribution for the variables since the pdf of each parameter is often unknown. In general, it is after observation of the plot of available data that a probability density function is chosen. Each parameter is independently sampled and monotonicity plots are done to choose the most sensitive and monotonic parameter. The PRCC value for a specific parameter is a Pearson correlation coefficient for the residuals from two regression models. A rank transformation is applied to ranks of the data for the PRCC values. The first regression model represents the ranked parameters in terms of other ranked parameters, and the second regression represents the ranked outcome in terms of the other ranked parameter values [122]. The parameters whose PRCC values are greater than 0.5 or less than -0.5 are the most important [124].

As an application of the LHS/PRCC sensitivity analysis theory, we look at the relationship between the reproduction number R_h and the parameters composing it. Parameters value used for the sensitivity analysis are found in [32, 125].

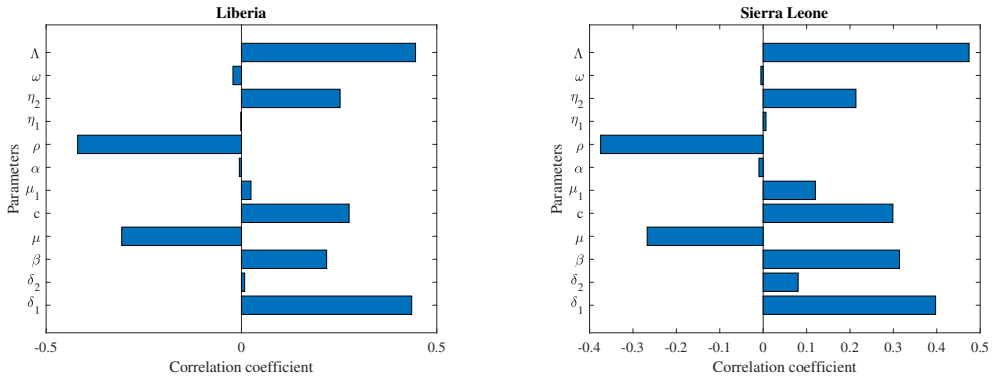

(a) (b)

Figure 3.2: Sensitivity plot of the reproduction number. The parameter values are the same as in Figure 3.5 and 3.6.

From Figure 3.2, the most important parameters with a positive correlation to the reproduction number are $\beta, c, \eta_2, \delta_1$ and δ_2. The product $c\beta$ is the effective transmission rate, which by definition drives the infection in the total population. δ_1 and δ_2 contribute to increase the number of infectious deceased, who are η_2 times more infectious than the infected that are alive. The parameter ρ has a negative correlation with R_h since burials limit EVD transmission. Also, ω and α have a negative correlation to R_h. In fact, recovered individuals are assumed not to transmit EVD, leading to a reduction of R_h.

3.5.2 Bifurcation analysis

A bifurcation is a change of the topological structure of a system as its parameters pass through a critical value [126]. $R_h = 1$ is a critical point since the system behaviour changes as R_h passes the value 1. Theorem 3.4.4 gives the conditions for the existence of a backward or a forward bifurcation for our model. Figures 3.3 and 3.4 illustrate different bifurcations and show the effect of increased parameter values on the disease endemicity.

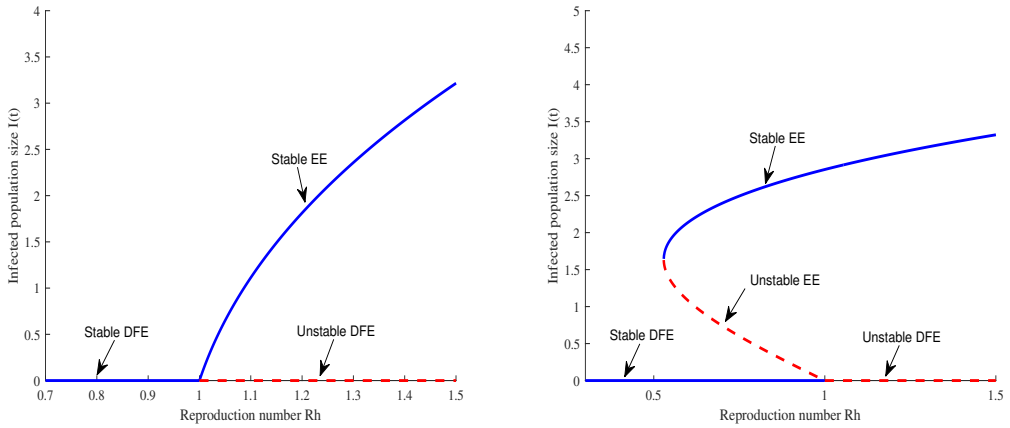

(a) (b)

Figure 3.3: Forward bifurcation in (a) for $b_{max} = 10.8$ and backward bifurcation in (b) for $b_{max} = 1.8$. Other parameters' value used are $\beta = 0.569$, $c = 15.5$, $\mu = 194$, $\alpha = 0.177$, $\delta_1 = 0.309$, $\delta_2 = 0.251$, $\rho = 0.457$, $\omega = 0.256$, $\eta_1 = 0.341$, $\eta_2 = 3.78$, $\mu_0 = 0.087$, $\mu_1 = 0.172$, $\Lambda = 1866$.

A change in the qualitative behaviour of the system of equations (3.2.7)-(3.2.11) is observed when $R_h = 1$. In fact, it has been proven that sub-critical endemic equilibrium exists for values of the reproduction number less than one, which is unusual since the endemic steady state in general, exists when the values of the reproduction number are above one. So, the coexistence of the DFE and the EE when $R_h < 1$ makes it difficult to clear the disease from the human population. In this case, there is no secondary transmission within the human population, but EVD remains persistent. This describes the backward bifurcation, depicted by Figure 3.3(b) and extensively discussed in [127, 128].

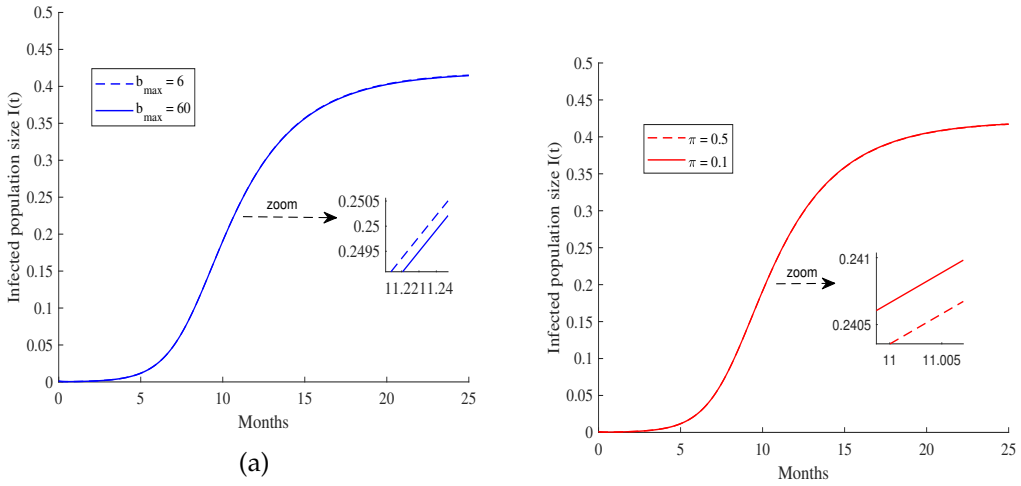

Figure 3.4: Effects of increased bed capacity in (a) and increased growth rate in (b) on the number of infected individuals. The parameter values are $b_{max} = 1.2$, $\beta = 0.19$, $c = 40$, $\mu = 8.08$, $\alpha = 0.235$, $\delta_1 = 0.357$, $\delta_2 = 0.076$, $\rho = 0.468$, $\omega = 0.14$, $\eta_1 = 0.235$, $\eta_2 = 2.64$, $\mu_0 = 0.256$, $\mu_1 = 0.383$, $\Lambda = 8.08$, $\pi = 0.304$.

Figure 3.3(a) is obtained from Figure 3.3(b) by increasing the value of b_{max}. These figures show how additional beds in ETU changes a backward bifurcation into a forward bifurcation, making easier the control of EVD. Figures 3.4(a) and 3.4(b) show a decrease of the number of infected individuals when more beds are allocated to ETU, confirming the utility of hospitalisation during an EVD epidemic. It is important however to note that the decrease is very minimal, showing that stopping an outbreak of EVD only with hospitalisation as control measure will be a very daunting task. It is therefore necessary to incorporate other controls like educational campaigns, active case finding or vaccination to rapidly control EVD.

3.6 Model fitting

Data from the two most affected countries in terms of number of deaths due to Ebola, are used in the fitting process. Liberia accounted for 42.5% and Sierra Leone accounted for 34.9% of the deaths of EVD [129]. Figures 3.5 and 3.6 show the model fit for EVD data from Sierra Leone and Liberia, collected by the Centers for Disease Control and Prevention (CDC) [129]. At the national level, the maximum number of beds for hospitalisation of EVD patients was very large.

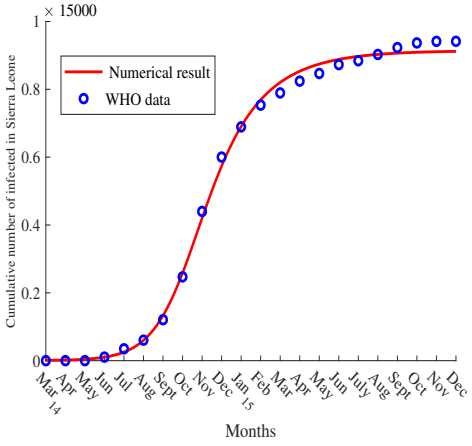

Figure 3.5: Curve fitting for data from Sierra Leone. 14 stands for the year 2014 and 15 stands for the year 2015 on the x-axis.

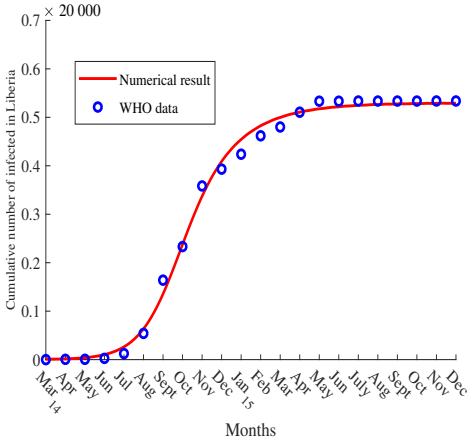

Figure 3.6: Curve fitting for data from Liberia. 14 stands for the year 2014 and 15 stands for the year 2015 on the x-axis.

The estimated parameter values from the fitting process are given in Table 3.2 for each country. The value of the reproduction number in each case is $R_h = 2$ for Liberia and $R_h = 2.5$ for Sierra Leone. These values of the reproduction numbers are comparable to those obtained from the literature. Rivers *et al.* [32] found an overall basic reproduction number of 2.2 for the two considered countries, with improved contact tracing, pharmaceutical interventions and improved infection control. Althaus [38] found the maximum likelihood estimate of the basic reproduction number as 1.59

for Liberia and 2.53 for Sierra Leone in 2014. In the absence of effective control measure, the basic reproduction number of EVD was 2.02 for Liberia according to Xia *et al.* [130], who were investigating the different transmission routes of EVD. Nishiura and Chowell [39] estimated the reproduction number to be between 1 and 2 for Liberia and Sierra Leone, from March to August 2014. These estimations of the secondary number of Ebola infections have been made from different compartmental models, during different periods of the year 2014 and for diverse types of control measures. This could explain the differences in the values of the reproduction numbers obtained.

Parameters	Λ	β	c	α	μ	ω	δ_1	δ_2	ρ	η_1	η_2	μ_0	μ_1	π	$bmax$	ETU
Liberia	2.1	0.48	4.3	0.5	2.1	0.2	0.37	0.01	0.7	0.16	1.7	0.008	0.4	0.5	45	30
Sierra Leone	3.53	0.47	2.9	0.5	3.53	0.2	0.6	0.009	0.7	0.5	3.43	0.0076	0.52	0.5	50	20

Table 3.2: Estimated parameters' value obtained from the fitting process. b_{max} is the maximum bed capacity of an ETU.

Figures 3.5 and 3.6 show that the model formulated in this work fits well to data for parameter values given in Table 3.2. We notice from the estimated parameters in Table 3.2 that Sierra Leone had a larger hospitalisation rate. This is consistent with the fact that the country had the highest number of infected individuals [129]. The efficacy of hospitalisation is indicated by death rate, which is lower with hospital admission of EVD infected individuals in both countries. However, despite the utility of hospitalisation, in Liberia more patients died in these hospitals than in Sierra Leone. This could mean that Liberia had more difficulties in handling its patients in ETU than Sierra Leone. This could have been due to a shortage of beds for a proper hospital admission or insufficient drugs for treatment.

The period during which new ETUs with more available beds were built was an important factor in the limitation of EVD transmission. In fact, Kucharski *et al.* [35] and Dubois *et al.* [131] claim that an early allocation of sufficient beds for treatment or holding centers would have helped to avoid many transmissions and deaths. Figures 3.7 and 3.8 indicate the monthly number of new Ebola infected [132]. They also indicate the total number of available beds per country for a period of eight months. Ebola incidence

here represents the number of new cases reported the 25*th* of the indicated month [133]. The number of beds is the total sum of beds available in Ebola CCCs, ETUs and Ebola holding centers. The maximum number of beds for each month is represented on the graphs and WebPlotDigitizer was used to extract data from the plots in [35]. Data from March to May 2014 were missing in [35] and this explains the absence of some data points in Figures 3.7 and 3.8.

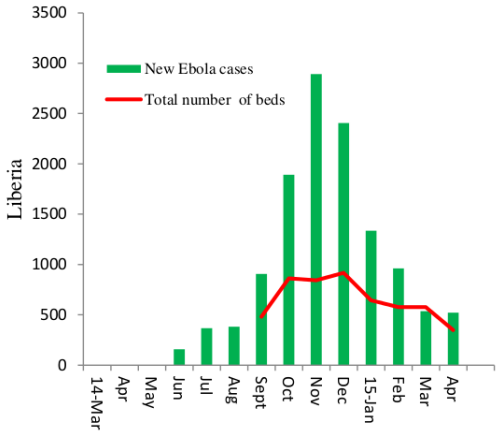

Figure 3.7: Comparison between the moments when the maximum number of infected and beds are reached in Liberia. 14 stands for the year 2014 and 15 stands for the year 2015 on the x-axis.

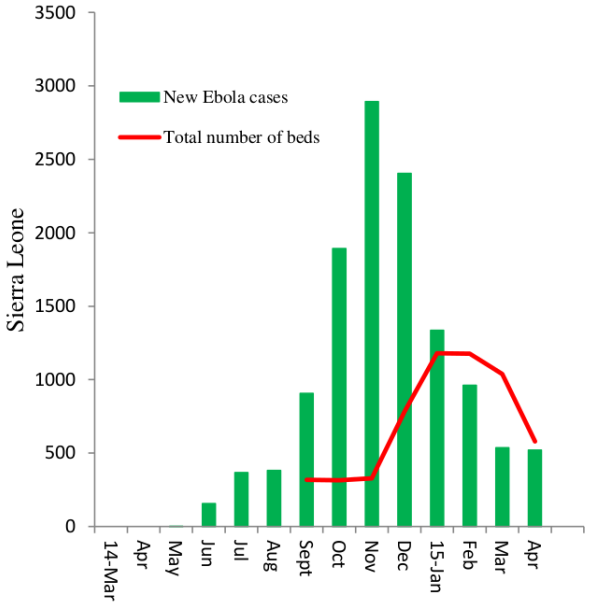

Figure 3.8: Comparison between the moments when the maximum number of infected and beds are reached in Sierra Leone. 14 stands for the year 2014 and 15 stands for the year 2015 on the x-axis.

We notice in Figures 3.7 and 3.8 that the maximum number of infected and beds do not always coincide. In Liberia, the maximum number of beds is reached one month after the maximum number of infected is reached. In, Sierra Leone, many beds were expected during two months, from November 2014 when the maximum number of infected was reached, to December 2014 when the maximum number of available beds was reached. This delay of two months certainly led to more infections and deaths, since the time from infection to death of EVD was estimated to be only 10 days in Liberia and sierra Leone [32]. This emphasises the necessity of timely allocation of funds and implementation of recommendations to build enough Ebola health care facilities with sufficient beds early.

The aim of providing beds for EVD exposed individuals is to limit the disease transmission within the hospital setting and increase access to treatment. This can be attained when beds are allocated according to the needs of each affected country and if proper maintenance of these beds is implemented. Our results suggest a more balanced distribution and maintenance of hospital beds.

3.7 Conclusion

EVD emerged in 2014 in West African countries with poor or insufficient health care facilities [108]. A set of control measures like quarantine into ETUs and contact tracing were implemented to stop the disease spread. Admission into ETUs was determined by the availability of personnel and beds. The limited number of new beds reduced the hospitalization rate into these units. We formulated a deterministic compartmental model with a time dependent number of beds available. The analysis of the model shows the existence of an unstable DFE E_1^0, when there are no hospital bed, for values of the reproduction number less than one or the existence of a globally stable DFE E_2^0 for values of the reproduction number less than a threshold R_h^c when $b = b_{max}$ at equilibrium. We have also proven that the number of beds available in ETU is a determining factor in the disease control. It has been shown that, when there are no beds or a limited number of available beds, controlling EVD is more difficult because of the presence of a backward bifurcation. When the maximum capacity of an ETU is increased, a forward bifurcation appears and reducing the reproduction number to values less than 1 will stop EVD. As part of the model validation, the model was fitted to data from Liberia and Sierra Leone. We recommend a timely supply of beds into Ebola health care units and highlight the need for upgraded infrastructures in countries affected by the last EVD outbreak.

The model formulated in this work is consistent with the dynamics of EVD in Liberia and Sierra Leone, but is not without shortcomings. In fact, the lack of sufficient data on the number of beds supplied into Ebola care units in the affected countries, limited the numerical analysis and interpretation. We have only considered the number of beds in this work, but other aspects like personal protective equipment and materials for laboratories have been useful in Ebola patients management and care. These tools could also be taken into account. It is well documented that the goodness of fit measures the discrepancy between observed data and values expected from the model. In this work, no goodness of fit tests are done but we relied on the least squares method for the model fitting. We however argue that the least squares method of fitting models to data, provides useful insights into how the model can be linked to data despite the challenge of using statistics tools to test the goodness of fit of the model.

Chapter 4

A qualitative analysis of a simple Ebola virus disease model with a non linear incidence rate

4.1 Introduction

Population growth and density in health risk areas of our societies do not facilitate the management of disasters, whose number keeps growing as time evolves [134]. When a catastrophe arises, people can exhibit a controlled behaviour which can take the form of intelligent and reasoned reactions. However, panic or lack of knowledge can lead to a less controlled behaviour demonstrated by sideration or automate behaviour such as washing the corpses of the deceased [134]. The efficacy of behaviour change can then be evaluated by the level of control in the behaviour of the affected population. During the last Ebola virus disease (EVD) outbreak of 2014 – 2016, the poor economic situation of the affected countries and some cultural beliefs impacted the level of control in the populations' behaviour, especially at the early stage of the epidemic. Uncontrolled behaviours such as washing and touching the deceased and bush-meat consumption, practised in West Africa helped to fuel EVD spread [7].

Mathematical models of EVD can be divided into two groups: models that do not account for infection due to EVD deceased and models that do. Models ignoring the deceased are classified as $SEIR$ or SIR models, see for instance [35, 39, 44, 54, 55, 135, 136]. The incidence rate of these models is

generally bilinear, i.e. of the form βSI. The formulation of such an incidence function increases the ease of analysing the models, including the global stability analysis of the fixed points using Lasalle's invariance principle [44, 135, 136]. However, neglecting the contribution of the deceased in the force of infection of EVD underestimates the number of Ebola cases [137].

Several models of EVD including a compartment for the deceased have been formulated and analysed, see for instance [32, 36, 45, 57, 58, 138]. The mathematical analysis of the equilibria of such models mostly focuses on the determination of the reproduction number and local stability analysis of equilibria [57, 58]. The proof of the global stability of the equilibria is often neglected because of the nonlinearity of the incidence rate. Rivers *et al.* [32] modelled the impact of interventions on an epidemic of Ebola using a model that accounts for infection during funerals (F). The total population N, in this case, was made up of susceptibles (S), exposed (E), infected (I), hospitalized (H) and recovered (R) individuals. The incidence rate of the model which was given by $(\beta SI + \beta_H SH + \beta_F SF)/N$, accounted for infection during hospitalisation and burials. A similar structure of the incidence rate was used by Djiomba and Nyabadza [57] to investigate an optimal control of EVD with educational campaigns, active case finding and pharmaceutical interventions and Xia *et al.* [139] who modelled the transmission dynamics of Ebola in Liberia.

More complex incidence rates or forces of infection are found in disease models, especially those that incorporate behaviour change. Stopping a disease outbreak, in general, relies on the technical implementation of control strategies like vaccination, treatment or educational campaigns. In the absence of treatment, a change in human behaviour will be the only hope to stop the disease spread. So, human behaviour remains the mainstay of any disease eradication, including EVD [60].

Psychology and anthropology are not the only domains interested in human behaviour. Mathematical modelling has also focused on the effects of human behaviour on various diseases' evolution, see for instance [60, 61, 62, 63, 64]. However, the quantification of human behaviour remains a challenge and its effects on a disease evolution is often represented

by probabilities or by a modified incidence rate of the disease, see for instance [61]. Del Valle *et al.* [75] formulated a model to investigate the effects of behavioural changes in a smallpox attack. They assumed that individuals within a community change their behaviour and move from a normal active group to a less active group, reducing their average number of contacts, in response to a high prevalence of smallpox in the community. The per-capita transfer rate between compartments was modelled by the function $\phi_i = a_i(I_n + I_l)/\left(1 + b_i(I_n + I_l)\right)$ per day with $i = S, E, I$ and where $n =$ normally active, $l =$ less active, a_i and b_i being positive constants that modulate the rate of change. Behavioural change was thus taken to vary with the ϕ_i values and the transmission rate of smallpox. The force of infection for the normally active and less active was given by

$$\lambda_j = \frac{\gamma_n I_n + \gamma_l I_l + \gamma_c W}{\gamma_n A_c + \gamma_l A_l + \gamma_c A_c}$$

where A_c and W were respectively the confined and quarantined individuals, $j = (n, l)$. They concluded that, besides the standard intervention procedure that would affect the extend and duration of a smallpox epidemic, the reduction in contacts of people in response to information about the epidemic was another contribution to smallpox control [75]. Wang *et al.* [78] modelled the influence of human behaviour on cholera dynamics with a disease prevalence contact rate $\beta_i = a_i - b_i\, m_i(I)$, where a_i is the contact rate without considering the influence of human behaviour, b_i is the maximum reduced contact rate due to human behaviour and $m_i(I) = \dfrac{I}{I + \kappa_i}$, $i = 1, 2, 3$ where κ_i is the half saturation constant function. The contact rate was driven by a saturation function of the Michaelis Menten type. They concluded that human behaviour can reduce the endemic and epidemic levels, cholera spreading speeds and the risk of infection [78].

The impact of behaviour change on the spread of EVD with a linear force of infection has been done in [80]. Most of EVD models that have been formulated to date are of the types $SEIR$, SIR, $SIRF$, $SEIRF$ and $SEIHRF$. In this work, we consider a simple $SIRD$ model, where D is the class of the deceased with a non linear incidence function.

In general, people abandon good behaviour when the perceived risk of a disease is reduced or because of limited funds to continue [140]. In the case of EVD, we assume that when the number of infected cases is well pro-

nounced, the fear of contracting the disease obliges people to change their behaviour and a decline in the number of cases follows. Disease incidence or prevalence in a population has already been mentioned as a motivator of behaviour change during an epidemic for the case of influenza [75, 140]. Exponential functions have been suggested to represent the probability of disease transmission in the case of alertness to a disease by Lio *et al.* [141]. Fast *et al.* [142] used a decreasing exposition probability, due to behaviour change between susceptible and infected individuals, to assess the role of social mobilisation in EVD control in Lofa.

The absence of treatment against EVD is a source of fear within the affected population and motivates a change in their behaviour leading to reduced disease transmission, especially when the number of infected cases reaches unexpected high values. In this model, we innovatively introduce a non linear force of infection that considers human behaviour. EVD started in a rural area where it had been unnoticed for few months, causing the force of infection to initially grow exponentially and later declined as the epidemic progressed [143]. Concave exponential functions are thus suitable to represent the force of infection. Among all the existing exponential functions, we propose the Ricker function to represent the force of infection for our model. The function models the infection growth in the presence of behaviour change and the model fits better to EVD data from the two countries considered, see also [144]. The effective transmission rate of EVD is represented by the parameter β and the efficacy of behaviour change is represented by a parameter $p\left(p \in [0,1]\right)$ such that $p = 0$ corresponds to an uncontrolled behaviour that fuels EVD spread and $p = 1$ correspond to a perfectly controlled behaviour that stops EVD spread. We also introduce a parameter K that represents the speed at which individuals change their behaviour. The parameter K helps to track how fast individuals change their behaviour in response to EVD. $K = 0$ corresponds to no behaviour change and greater values of K indicate a positive change in the affected population's behaviour. A total eradication of EVD corresponds to a zero force of infection for very high values of $K\left(K \to \infty\right)$.

We propose a force of infection given by

$$\lambda(t) = \beta\,(1-p)\Big(I(t) + \epsilon D(t)\Big)\exp\Big[-\Big(I(t) + \epsilon D(t)\Big)\,K\Big]$$

where ϵ indicates the infectivity of the deceased when compared to that of the infected individuals, with $\epsilon > 1$ and $\lim_{K\to\infty} \lambda = 0$.

The intent of this work is to study the dynamics of an EVD model with a non linear force of infection innovatively described by a Ricker function. We also present the global stability analysis of the model steady states.

This work is arranged as follows: in Section 4.2 we formulate the model. Section 4.3 is reserved for the model analysis and in Section 4.4 we focus on the steady states and their global properties. Section 4.5 is reserved for the numerical simulations and section 4.6 contains some concluding remarks.

4.2 Model formulation and equations

A deterministic model, consisting of individuals with different EVD status is formulated to represent the population dynamics when there is a change of behaviour due to the high prevalence of the disease. Susceptible individuals (in compartment S) represent individuals that are at risk of contracting the infection through contact with the infected (in compartment I) and the deceased (in compartment D). Susceptible individuals are recruited into a homogeneous population at a constant rate Λ. Infected individuals may recover at the rate α or may succumb to the Ebola virus and die at a rate φ. Individuals in each compartment are assumed to die naturally at a rate μ and dead bodies of EVD infected individuals deceased are buried at a rate ρ. Dead bodies of infected individuals are assumed to be infectious. We thus assume here that even the infected who do not die from EVD contribute to EVD spread [145] and we set $\delta = \varphi + \mu$.

The total population size is given by

$$N(t) = S(t) + I(t) + R(t) + D(t).$$

Figure 4.1 below represents the movements between different classes, as their infection status with respect to the disease changes.

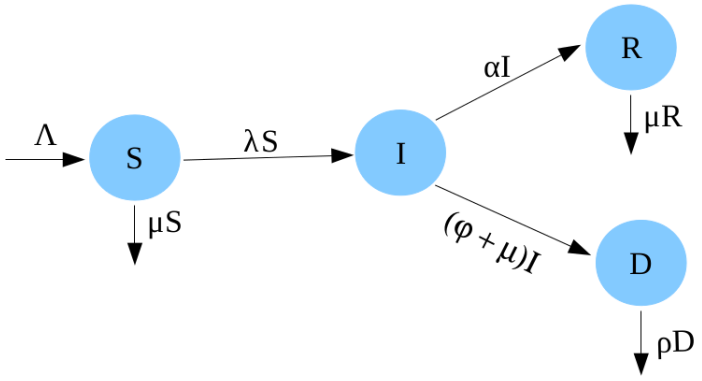

Figure 4.1: Flow chart diagram of the model

The governing equations that describe the dynamics of EVD as described are as following:

$$\frac{dS(t)}{dt} = \Lambda - \Big(\lambda(t) + \mu\Big)\, S(t), \tag{4.2.1}$$

$$\frac{dI(t)}{dt} = \lambda(t)\, S(t) - Q_1\, I(t), \tag{4.2.2}$$

$$\frac{dR(t)}{dt} = \alpha\, I(t) - \mu\, R(t), \tag{4.2.3}$$

$$\frac{dD(t)}{dt} = \delta\, I(t) - \rho\, D(t), \tag{4.2.4}$$

where $Q_1 = (\alpha + \delta)$, with $S(0) > 0$, $I(0) \geq 0$, $R(0) \geq 0$ and $D(0) \geq 0$.

4.3 Model properties: existence, positivity and uniqueness of solutions

The right hand side of the system of differential equations (4.2.1)-(4.2.4) is made of Lipschitz continuous functions. According to Picard's existence Theorem, with given initial conditions, the solutions of our system exist and they are unique [113].

Theorem 4.3.1. *Solutions to system* (4.2.1)-(4.2.4) *with non-negative initial conditions are all non-negative.*

Proof. We suppose that there exists $\hat{t} > 0$ such that $S(\hat{t}) < 0$. From the intermediate value Theorem, there exists $t_1 \in [0, \hat{t}]$ such that $S(t_1) = 0$.

From equation (4.2.1),

$S(t) \geq S(t_1)\exp\left(-\left(\int_0^t \lambda(u)\,du + \mu\,t\right)\right)$ for all $t \in [t_1, \hat{t}]$. $S(t_1) = 0$ implies that $S(t) \geq 0$ for $t \geq t_1$. Since $\hat{t} > t_1$, $S(\hat{t}) \geq 0$ and this contradicts the initial assumption. Thus $S(t) \geq 0$ for all $t \geq 0$. The same principle is applied to I, R and D, and from equation (4.2.2) we obtain $I(t) \geq I(t_1)\exp\left(-Q_1\,t\right)$, from equation (4.2.3) we obtain $R(t) \geq R(t_1)\exp\left(-\mu\,t\right)$, from equation (4.2.4) we obtain $D(t) \geq D(t_1)\exp\left(-\rho\,t\right)$. We can then conclude that solutions of the system (4.2.1)-(4.2.4) are non-negative. □

Theorem 4.3.2. *The system makes biological sense in the entire non-negative orthant*

$$\Omega = \left\{\left(S(t), I(t), R(t), D(t)\right) \in \mathbb{R}^4_+ : S(t) + I(t) + R(t) \leqslant \frac{\Lambda}{\mu} \text{ and } D(t) \leq \frac{\delta\,\Lambda}{\mu\,\rho}\right\}$$

which is attracting and positively invariant with respect to the flow of system (4.2.1)-(4.2.4).

Proof. We set $H(t) = S(t) + I(t) + R(t)$. By adding all the equations of system (4.2.1)-(4.2.3) we obtain:

$$\frac{\mathrm{d}H(t)}{\mathrm{d}t} \leqslant \Lambda - \mu\,H(t). \tag{4.3.1}$$

Using Gronwall inequality [114] and integrating (4.3.1) we obtain the following solution

$$H(t) \leqslant \left(H(0) - \frac{\Lambda}{\mu}\right)\exp\left(-\mu\,t\right) + \frac{\Lambda}{\mu}, \quad \forall\ t \geqslant 0.$$

If $H(0) \leqslant \frac{\Lambda}{\mu}$, then the upper bound of $H(t)$ is $\frac{\Lambda}{\mu}$ when $t \to \infty$. If $H(0) \geq \frac{\Lambda}{\mu}$, then $H(t)$ decreases to $\frac{\Lambda}{\mu}$ when $t \to \infty$ and enters Ω or approaches Ω asymptotically.

Integrating (4.2.4) gives $D(t) \leqslant \left(D(0) - \frac{\Lambda\,\delta}{\rho\,\mu}\right)\exp\left(-\rho\,t\right) + \frac{\Lambda\,\delta}{\rho\,\mu}, \quad \forall\ t \geqslant 0$. If $D(0) \leqslant \frac{\Lambda\,\delta}{\rho\,\mu}$, then $\frac{\Lambda\,\delta}{\rho\,\mu}$ is the upper bound of $D(t)$ when $t \to \infty$. If $D(t) \geq \frac{\Lambda\,\delta}{\rho\,\mu}$, then $D(t)$ decreases to $D(t) \geq \frac{\Lambda\,\delta}{\rho\,\mu}$ when $t \to \infty$ and enters Ω.

Besides, any sum or difference of variables in Ω with positive initial values will remain in Ω or in a neighbourhood of Ω. Thus Ω is bounded, positively invariant and attracting with respect to the flow of system (4.2.1)-(4.2.4). □

4.4 Steady states and global properties

Equations (4.2.1)-(4.2.2) and (4.2.4) are decoupled from (4.2.3) so that

$$\frac{dS(t)}{dt} = \Lambda - \Big(\lambda(t) + \mu\Big) S(t), \tag{4.4.1}$$

$$\frac{dI(t)}{dt} = \lambda(t)\, S(t) - Q_1\, I(t), \tag{4.4.2}$$

$$\frac{dD(t)}{dt} = \delta\, I(t) - \rho\, D(t). \tag{4.4.3}$$

Theorem 4.4.1. *Solutions to system (4.4.1)-(4.4.3) exist and are non-negative for non-negative initial conditions. Besides, system (4.4.1)-(4.4.3) makes biological sense in the entire non-negative orthant*

$$\Theta = \left\{ \Big(S(t), I(t), D(t)\Big) \in \mathbb{R}^3_+ : S(t) + I(t) \leqslant \frac{\Lambda}{\mu} \text{ and } D(t) \leq \frac{\delta\,\Lambda}{\mu\,\rho} \right\}.$$

Proof. The proof follows directly from the proof of Theorem 4.3.2. □

At equilibrium $\Big(\frac{dS(t)}{dt} = \frac{dI(t)}{dt} = \frac{dD(t)}{dt} = 0\Big)$, we can either have the disease free equilibrium (DFE) when $I = D = 0$ and $S = \frac{\Lambda}{\mu}$ which is obtained by solving equation (4.4.1) for S; or we can have the endemic equilibrium.

At the DFE, (4.4.1) $\iff \frac{dS(t)}{dt} = 0 \Longrightarrow S = \frac{\Lambda}{\mu}$.

Equations (4.4.1)-(4.4.3) admit a DFE denoted by $E^0 = \Big(\frac{\Lambda}{\mu}, 0, 0\Big)$ and the next generation matrix method (see [115]) yields a reproduction number R_0 given by

$$R_0 = \beta\,(1-p)\,\frac{\Lambda}{\mu}\left(\frac{1}{Q_1} + \epsilon\,\frac{\delta}{\rho\, Q_1}\right).$$

From the expression of the reproduction number, we can state that a more effective behaviour change reduces the number of secondary EVD infections.

The endemic equilibrium $E^* = \left(S^*, I^*, D^*\right)$ is given by

$$S^* = \frac{\Lambda\,\rho}{\left(\mu\,\rho + \beta\,(1-p)\,I^*\,(\delta\,\epsilon + \rho)\,\exp\left(-I^*\left(1+\frac{\epsilon\delta}{\rho}\right)K\right)\right)} \tag{4.4.4}$$

$$D^* = \frac{\delta}{\rho}\,I^* \tag{4.4.5}$$

which is obtained at equilibrium by solving equation (4.4.3) for D to get D^* and solving equation (4.4.1) for S to obtain S^*.

$$(4.4.3) \Longleftrightarrow \dot{D}(t) = 0 \Longrightarrow D = D^*,$$
$$(4.4.1) \Longleftrightarrow \dot{S}(t) = 0 \Longrightarrow S = S^*.$$

I^* is a **positive** solution of the equation

$$\Gamma(I^*) - y = 0, \tag{4.4.6}$$

where $y = Q_1$, obtained by substituting equations (4.4.4) and (4.4.5) into equation (4.4.2) and discarding the case $I^* = 0$ with

$$\Gamma(I^*) = \beta\,(1-p)\,S^*\left(1+\epsilon\,\frac{\delta}{\rho}\right)\exp\left(-I^*\left(1+\frac{\delta\,\epsilon}{\rho}\right)K\right).$$

The exponential function does not facilitate the algebraic resolution of equation (4.4.6). We have

$$\frac{\mathrm{d}\Gamma(I^*)}{\mathrm{d}I^*} = -\frac{\beta\,(1-p)\,\Lambda\,(\delta\,\epsilon+\rho)^2\left(\beta\,(1-p) + \mu\,K\,\exp\left(I^*\left(1+\frac{\delta\,\epsilon}{\rho}\right)K\right)\right)}{\left(I^*\,\beta(1-p)\,(\delta\,\epsilon+\rho) + \mu\,\rho\,\exp\left(I^*\left(1+\frac{\delta\,\epsilon}{\rho}\right)K\right)\right)^2} < 0$$

and $\Gamma(0) = R_0\,Q_1$, $\lim\limits_{I^*\to\infty}\Gamma(I^*) = 0$.
So $\Gamma(I^*)$ is a monotone decreasing and positive function which intercepts the line $y = Q_1$ only once when $R_0 > 1$. In fact, the graph of Γ can intercept the line $y = Q_1$ if $\Gamma(0) \geq y(0)$ because Γ is a decreasing function. Since $\Gamma(0) = R_0\,Q_1$, $\Gamma(0)$ is above Q_1 when $R_0 > 1$. If $R_0 < 1$, $\Gamma(0)$ is below Q_1, implying that we have no endemic equilibrium. We can then conclude that our model has a unique endemic equilibrium point when $R_0 > 1$.

Note that for any $I, D \in \Theta$, inequality (4.4.7) is valid i.e.

$$\exp\left(-\psi\right) \leq \exp\left(-\left(I+\epsilon\,D\right)K\right) \leq 1, \quad \text{where} \quad \psi = \frac{\Lambda}{\mu}\left(1+\epsilon\,\frac{\delta}{\rho}\right)K. \tag{4.4.7}$$

4.4.1 The disease free equilibrium

Theorem 4.4.2. *The DFE is globally asymptotically stable when* $R_0 < 1$ *and unstable otherwise.*

Proof. We set $V = I + D$ as the Lyapunov function and $\dot{V} = \frac{dV}{dt}$. Using equations (4.4.2), (4.4.3) together with inequality (4.4.7), we can write $\dot{V} \leq Q_1 I \left(R_0 - 1\right)$ since $D = \frac{\delta}{\rho} I$ at equilibrium. So, $\dot{V} < 0$ if $R_0 < 1$. Finally V is positive definite and V is equal to zero only at the DFE. Besides, $\dot{V} \leq 0$ when $R_0 < 1$. We can conclude from Lassale's invariance principle (see [116]) that the DFE is globally asymptotically stable for values of the reproduction number less than one. □

A globally stable DFE is the main target of any disease control program. We have just proven that in the case of EVD, reducing the reproduction number to values less than one, by using the appropriate behaviour change, is a sufficient condition required to eradicate the disease.

4.4.2 The endemic equilibrium

This steady state indicates the persistence of EVD in the human population.

Theorem 4.4.3. *The unique EE is globally asymptotically stable for non-negative initial conditions.*

Proof. In order to prove the global stability of the EE, we set F as a candidate Lyapunov function and we give conditions under which $\dot{F}$ is non-positive.

$$F = \left(S - S^* - S^* \ln\left(\frac{S}{S^*}\right)\right) + A\left(I - I^* - I^* \ln\left(\frac{I}{I^*}\right)\right) + G\left(D - D^* - D^* \ln\left(\frac{D}{D^*}\right)\right),$$

where A and G are positive constants to be calculated with $F = 0$ at the endemic equilibrium E^*.

The right hand side of system (4.4.1)-(4.4.3) at equilibrium yields

$$\begin{aligned} \Lambda &= \left(\beta\left(1-p\right)\left(I^* + \epsilon D^*\right)\exp\left(-\left(I^* + \epsilon D^*\right)K\right) + \mu\right) S^*, \\ Q_1 &= \frac{S^*}{I^*}\beta\left(1-p\right)\left(I^* + \epsilon D^*\right)\exp\left(-\left(I^* + \epsilon D^*\right)K\right), \\ D^* &= g\, I^* \end{aligned} \tag{4.4.8}$$

where $g = \frac{\delta}{\rho}$.
The derivatives of F with respect to each state variable are

$$\frac{\partial F}{\partial S} = \left(1 - \frac{S^*}{S}\right), \frac{\partial F}{\partial I} = A\left(1 - \frac{I^*}{I}\right), \frac{\partial F}{\partial D} = G\left(1 - \frac{D^*}{D}\right),$$

$$\frac{\partial^2 F}{\partial S^2} = \left(\frac{S^*}{S^2}\right), \frac{\partial^2 F}{\partial I^2} = A\left(\frac{I^*}{I^2}\right), \frac{\partial^2 F}{\partial D^2} = G\left(\frac{D^*}{D^2}\right).$$

E^* is then the unique critical point of F and since the second derivative of F is positive at any point of Θ, the Lyapunov function F is concave up and the unique endemic equilibrium point is the global minimum of F.

The derivative of F with respect to time t, denoted $\dot{F}$ is

$$\dot{F} = \left(1 - \frac{S^*}{S}\right)\dot{S} + A\left(1 - \frac{I^*}{I}\right)\dot{I} + G\left(1 - \frac{D^*}{D}\right)\dot{D}.$$

Considering the system of equations (4.4.1)-(4.4.3) together with inequality (4.4.7) and the fact that E^* is the global minimum of F, we obtain

$$\begin{aligned}\dot{F} \leq & \left(1 - \frac{S^*}{S}\right)\left(\Lambda - \left(\beta\,(1-p)\,(I + \epsilon\,D)\,\exp\left(-\psi\right) + \mu\right)S\right) \\ & + A\left(1 - \frac{I^*}{I}\right)\left(\beta\,(1-p)\,(I + \epsilon\,D)\,S - Q_1\,I\right) + G\left(1 - \frac{D^*}{D}\right)(\delta\,I - \rho\,D).\end{aligned} \tag{4.4.9}$$

We set

$$x = \frac{S}{S^*}, y = \frac{I}{I^*}, u = \frac{D}{D^*}$$

and rewrite (4.4.9) as

$$\dot{F} \leq -\mu\,\frac{(S - S^*)^2}{S} + \beta\,(1-p)\,I^* L(x,y,u)$$

where

$$\begin{aligned}L(x,y,u) = & \left(1 - \frac{1}{x}\right)S^*\left(\left(1 - x\,y\,\exp\left(-\psi\right)\right) + g\,\epsilon\left(1 - u\,x\,\exp\left(-\psi\right)\right)\right) \\ & + A\left(1 - \frac{1}{y}\right)S^*\left(y\,(x-1) + \epsilon\,g\,(u\,x - y)\right) \\ & + \frac{G\,\delta}{\beta\,(1-p)}\left(1 - \frac{1}{u}\right)(y - u).\end{aligned} \tag{4.4.10}$$

The expression of L is obtained by replacing Λ, Q_1 and g in equation (4.4.9) by their expressions from equations (4.4.8).

Expanding the expression of $L(x, y, u)$ from system (4.4.10) and grouping the coefficients with the same variable give

$$\begin{aligned} L(x,y,u) = & \frac{G\,\delta}{\beta\,(1-p)} + S^*\,(A+1) + S^*\,\epsilon\,g\,(A+1) \\ & + y\left(\frac{G\,\delta}{\beta\,(1-p)} + S^*\left(\exp\left(-\psi\right) - A\right) - \epsilon\,g\,A\,S^*\right) \\ & + u\left(-\frac{G\,\delta}{\eta\,(1-p)} + \epsilon\,g\,S^*\exp\left(-\psi\right)\right) \\ & + \frac{y}{u}\left(-\frac{G\,\delta}{\beta\,(1-p)}\right) + \frac{1}{x}\left(-S^* - \epsilon\,g\,\exp\left(-\psi\right)S^*\right) - x\,A\,S^* \\ & + x\,y\left(-S^*\exp\left(-\psi\right) + A\,S^*\right) \\ & + u\,x\left(-\epsilon\,A\,g\,S^* + \epsilon\,A\,g\,\exp\left(-\psi\right)S^*\right) + \frac{u\,x}{y}\left(-A\,g\,S^*\,\epsilon\right). \end{aligned} \tag{4.4.11}$$

Since we already have $-\mu\,\dfrac{(S-S^*)^2}{S} \leq 0$ from the expression of $\dot{F}$, it remains to prove that $L \leq 0$ in order to get $\dot{F} \leq 0$.

From the expression of L in (4.4.11), we will first set the terms containing variables and with non negative coefficients to zero in order to get rid of the positive and non constant part of L. The coefficients of $y, u, x\,y$ and $u\,x$ are thus set to zero and solved for A and G. We obtain

$$A = \exp\left(-\psi\right),\; G = \frac{\epsilon\,g\beta\,(1-p)}{\delta}S^*\exp\left(-\psi\right)$$

and

$$\begin{aligned} L(x,y,u) = & \frac{G\,\delta}{\beta\,(1-p)}\left(1-\frac{y}{u}\right) + \epsilon\,g\,S^*\left(A\left(1-\frac{1}{x}\right) + 1 - \frac{u\,x}{y}\right) \\ & + \left(A(1-x) + 1 - \frac{1}{x}\right)S^*. \end{aligned}$$

So L is negative and will be equal to zero if $x = y = u = 1$ which is in the set

$$\mathsf{C} = \left\{ \left(S, I, D\right) : S = S^*, I = I^*, D = D^* \right\}.$$

LaSalle's extension implies that each solution which intersects $\mathbb{R}^3_+$ limits to the endemic equilibrium and E^* is globally asymptotically stable on Θ (see [116]). □

Global stability of the EE indicates that EVD persists as long as the value of the reproduction number is greater than one. Programs aiming at eradicating EVD should limit the disease transmission in such a way that the value of the reproduction number remains less than one.

4.5 Numerical simulations

4.5.1 Model validation

We fit the number of new EVD cases $I(t)$ from our model to data from Liberia and Sierra Leone [4]. The values of the parameters estimated through the least-squares fitting process are given in Tables 4.1. A comprehensive description of the least-squares fitting method is given in [45].

For Liberia, the initial conditions used for the fitting process are

$$S(0) = 4600000, I(0) = 1, D(0) = 0$$

and for Sierra Leone these conditions are

$$S(0) = 7396000, I(0) = 1, D(0) = 0.$$

The value of $S(0)$ is chosen as the total population of the corresponding country in 2018.

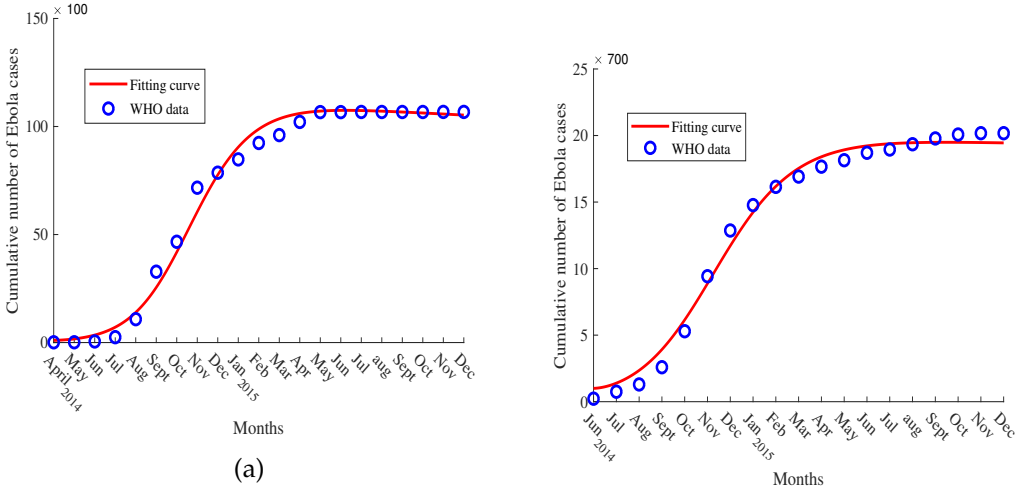

Figure 4.2: Curve fitting with data collected from Liberia in (a) and from Sierra Leone in (b).

Figures 4.2 show that our model closely fits to the data and indicate that behaviour change during EVD outbreak of $2014 - 2016$ was motivated by an increased number of EVD cases for the set of parameters value used. They also show that an efficacious behaviour change ($p = 0.8$) was necessary to stop EVD spread. The controlled or efficacious behaviour adopted by populations in order to limit EVD spread consisted of practising careful hygiene, avoiding contact with infected animals and humans, collaborating with case tracking, not fleeing from isolation areas, safely burying those who died from EVD, etc [57, 146]. If the efficacy of behaviour change is allowed to be zero, then higher values of β are obtained for the model to fit to the data

Parameters (units)	**Liberia**	**Sierra Leone**
Λ	30 000	59 770
ϵ	2	2
p	0.8	0.8
K	4.6×10^{-3}	0.0044
φ (month^{-1})	0.52	0.58
ρ (month^{-1})	0.89	0.8
μ (month^{-1})	10^{-2}	10^{-2}
α (month^{-1})	10^{-2}	10^{-2}
β (ind^{-1}.month^{-1})	1.23×10^{-6}	5.2×10^{-7}

Table 4.1: Estimated value of the parameters for each country with behaviour change. ind stands for individual.

The values of the estimated parameters in Table 4.1 yield a reproduction number equal to 2.3 in Liberia and 2.5 in Sierra Leone when there is a controlled change in human behaviour. These values are comparable to those obtained by several authors. Rivers *et al.* [32] found that the value of the reproduction number for the two countries on an average is 2.2. Althaus [38] found $R_0 = 1.59$ for Liberia and $R_0 = 2.53$ for Sierra Leone in 2014. Xia *et al.* [130] found $R_0 = 2.02$ for Liberia when investigating the different transmission routes of EVD. Nishiura and Chowell [39] estimated the value of the reproduction number between 1 and 2 in Liberia and Sierra Leone, from March to August 2014. The difference between the estimated and cited values of the reproduction number might come from the fact that they are calculated during different periods of EVD epidemics and the models built by the authors have different structures and they integrate different control measures in some instances.

Behaviour change influenced several factors such as EVD transmission rate, death rate, recovery rate and even the burial rate of the deceased. Avoiding contact between susceptible and infected individuals for example, contributed to a reduction in the transmission rate of EVD. This may explain the higher value of β estimated for Liberia in Table 4.1, since behaviour change was a slower process (lower value of K) in the country when compared to Sierra Leone. Other researchers also concluded that the transmission rate of EVD is higher without behaviour change [32, 130]. The recovery rate and death rate of EVD are influenced by the collaboration between populations and authorities through active case finding or hospitalisation for example.

Recovering from EVD without treatment was very rare and can explain the low values of α estimated. The case fatality rate of the last EVD epidemic was greater than 50% [32, 130, 145], indicating a high risk of death for EVD patients which can be greater in case of inappropriate behaviour. This supports the higher values of φ in Table 4.1 in the absence of behaviour change. In [147], the values of φ are greater without a controlled behaviour, highlighting the importance of adopting disease reducing behaviours like visiting the appropriate health centers to receive pharmaceutical interventions that help to increase the chances of recovering from EVD. Dead bodies of EVD deceased are twice more infectious than the living infected individuals according to the estimation of ϵ. Some authors found that this infectivity could be even four times higher for the deceased [130]. Quick and safe burials of EVD deceased have helped to limit EVD spread and the high values of ρ from Table 4.1 indicate that a high burial rate helped to limit the disease spread. The estimated values of p indicate that a highly efficacious behaviour change, adapted to health authorities instructions for example, was necessary to halt EVD spread. The estimated values of K indicate how fast a behaviour change occurred during the last EVD epidemic in Liberia and Sierra Leone. However, the values of k in Table 4.1 are low and this implies that behaviour change was a slow process during the outbreak. This could explain the long duration of the outbreak and its extent in terms of number of deaths. In fact, cultural beliefs and poor economic conditions build mistrust between rural populations and authorities in West Africa [7]. This situation led to a slow application of instructions from authorities during the outbreak. So, building confidence and improving people's living conditions is essential in motivating people to quickly react in case of an epidemic of EVD.

4.5.2 Sensitivity analysis

The reproduction number R_0 is made of different parameters and their correlations to R_0 differs as well. Sensitivity analysis helps to assess the variability in the model predictions introduced by uncertainty in the parameters value [122]. We use Latin Hypercube Sampling (LHS) and Partial Correlation Coefficient (PRCC) to explore the parameter space of the model with 1000 simulations [123]. We choose a uniform distribution to implement LHS sampling scheme. The PRCC value for a specific parameter is a Pearson cor-

relation coefficient for the residuals from two regression models [122]. The most important parameters have a PRCC value greater than 0.5 or less than -0.5. Figure 4.3 represents the sensitivity analysis of R_0.

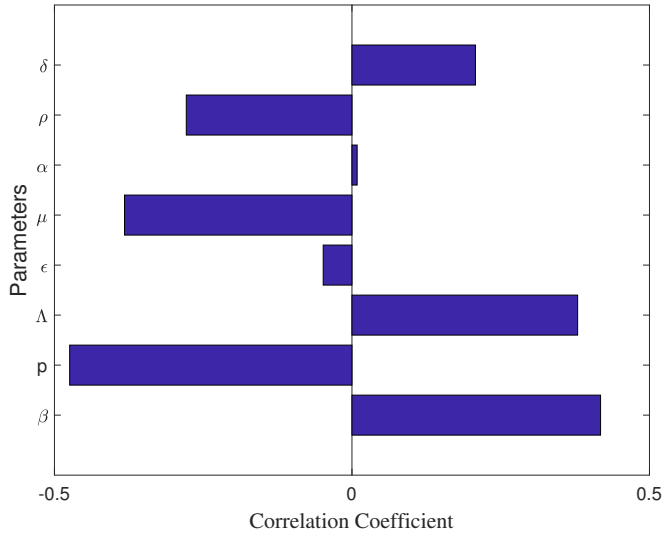

Figure 4.3: Tornado plot of the sensitivity analysis of R_0

We observe in Figure 4.3 that the parameters with the most important positive correlations to R_0 are δ, Λ, β and those with the negative correlations are ρ, μ and p. The results show that when the transmission rate and death rate of EVD increase, the number of new infections increases since the deceased and infected individuals are both infectious. When the recruitment rate is increased, more individuals are exposed to Ebola virus and this increases their chances of contracting the virus and contribute to the disease spread. Natural death reduces the size of the population and thus limits the number of people who might be infected by EVD. Disposing of the corpses of EVD deceased rapidly and safely stops contamination during funerals and reduces the potential number of EVD cases. The negative correlation between R_0 and p is certainly due to the fact that adopting a controlled behaviour that limits or stops EVD spread, reduces the reproduction number and is represented by an increase of the value of p.

4.6 Conclusion

The global stability analysis of the steady states of a model of EVD with a non linear incidence function is presented in this chapter. The global stability of equilibria is presented through suitably chosen Lyapunov functions. The non linear incidence function is chosen to represent the influence of human behaviour on EVD evolution. Data from Liberia and Sierra Leone are used in the fitting process whose results show how closely the model describes the evolution of EVD with human behaviour and support the idea that behaviour change is motivated by disease prevalence. As soon as an epidemic starts, individuals affected should trust the authorities and do as instructed to avoid deaths and disaster due to a slow reaction.

The work presented in this chapter is not without shortcomings. The modelling of human behaviour through any mathematical function is a challenge as human behaviour is complex and unpredictable. In fact, a stochastic version of the incidence function may be worth looking at as an alternative albeit the challenges associated with its formulation and the mathematical analysis. The use of individual based models or network models could potentially solve the inadequacies of dealing with deterministic models. The discrepancy between observed data and values expected from the model is well measured by the goodness of fit. In this work, no goodness of fit tests are done but we relied on the least-squares method for the model fitting. We however argue that the least-squares method of fitting models to data, provides useful insights into how the model can be linked to data despite the challenge of using statistics tools to test the goodness of fit of the model. We still however argue that this model presents some interesting mathematical results on the global stability of an EVD model with human behaviour and a non linear incidence rate.

Chapter 5

Modelling the potential influence of human migration and multiple strains on Ebola virus disease dynamics

5.1 Introduction

More than 20 Ebola Virus Disease (EVD) outbreaks hit the African continent in recent decades and different ebolavirus strains have caused these outbreaks. There are five different strains of ebolaviruses and the most devastating are the Zaire ebolavirus strain, the Sudan ebolavirus strain and the Bundibugyo ebolavirus strain [5]. Before the year 2013, these species affected countries like Gabon, Congo, Sudan or Uganda. But in 2013, the most devastating EVD outbreak ever hit West Africa, killing more than 11000 people and was driven by the Zaire ebolavirus strain [148]. Among all the theories explaining how a Central African virus moved to West Africa, one of them supports the idea that migrating bats that can fly over hundreds of kilometres might have brought the virus there [149]. Migration of the natural reservoir of ebolavirus in this case is a key element in the transportation of the Zaire ebolavirus strain within different parts of the continent. Economic activities such as hunting or mining have increased the contacts between humans and infected animals such as bats, chimpanzees or monkeys living in tropical forests [3, 150]. An eventual mutation of the Zaire ebolavirus strain was suspected as well because of the large death toll of the

outbreak.

The African tropical forest that hosts Ebola viruses natural reservoirs ranges from East to West Africa [151]. The Zaire, Sudan and Bundibugyo ebolavirus strains have been linked to the animal population during the past outbreaks and this might explain the fact that different species have hit several countries already [3, 150]. The Democratic Republic of Congo (DRC) generally hit by the Zaire strain was affected by the Bundibugyo strain in 2012, showing the possibility of one region being affected by a different strain. Uganda naturally hosts the Bundibugyo ebolavirus strain and was hit by the Sudan strain in 2000 and $2011-2013$. Besides, DRC, Uganda and Sudan share common boundaries [5]. So, as of May 2017, two ebolavirus strains existed in DRC and Uganda and the possibility of having an outbreak caused simultaneously by these strains is a reality.

Movements within the African continent are motivated by labour and livelihoods, social and familial connections, cultural ceremonies, disasters and conflicts [152]. Eastern and Western Africa have a long history of labour migration between and within countries to plantations (cotton and coffee in Uganda, cocoa and coffee in Ivory Coast) or to mines (in DRC and Uganda) during the appropriate seasons [153]. Pastoralist communities in Kenya, Tanzania, and Uganda for example, move to feed their animals [153]. In West Africa, the labour force from Mali, Burkina Faso and Guinea frequently move to Ivory Coast to harvest cocoa [154, 155]. This movement is observed either during the big harvesting period from October to March, or during the small harvesting period from April to August [154, 155]. This type of migration is often seasonal and happens during the harvesting period and is somehow similar to impulsive migration. Tourists' movements are also a typical example of impulsive migration and in Uganda for example, intra-African migrant birds and the tourists coming to see them arrive in July and start leaving in December [156]. Borders and boundaries in West Africa, including land borders, are difficult to control and make it difficult to track people's movements [152]. Fear, stigmatization or the non-access to close Ebola health care centers unexpectedly increased populations' mobility during the outbreak of $2013-2016$ [152]. So, despite the control measures installed at the airports, ports and main roads of entry in the affected countries, uncontrolled movement of people was still possible during the EVD epidemic. Given that different strains exist in the West and Central

African regions, with free movement of persons, the potential of new strain exportation exists. This phenomenon can be viewed as migration of infectives in mathematical modelling of communicable diseases and we consider the potential of such migration into the spread of EVD.

Migration can encourage the spread of communicable diseases as people carry viruses over long distances [154]. For example, a successful immunization program against measles in Burkina Faso was achieved. But later on, a large outbreak of measles among the target population arose [154]. This was the first reported failure of a widely successful strategy for controlling measles. On investigation, it became clear that the immigration of non immunized children from Ivory Coast caused the failure of the programme [154]. Migration in West Africa has been seen as a challenge to stopping Ebola because researchers believe that it has contributed to the disease spread in the region [90]. EVD is a fluid borne disease transmitted via contact with an infected individual or its fluids. So, movements of individuals especially in the affected areas during EVD outbreak has the potential of spreading the disease to unaffected areas. During the West African outbreak of $2013 - 2016$, human movement was limited by the authorities and several quarantines were observed during that period [152]. But the free movement of persons and goods in West Africa is a reality and up to 14% of people live outside their countries of origin [152]. It is common in West Africa to find families living across the boundaries between different countries.

Mathematical models of EVD that include migration of individuals have been formulated and analysed by several authors. Valdez *et al.* [157] considered a stochastic model to evaluate the extension of Ebola spreading in Liberia. They assumed that travel between countries propagated EVD in Liberia and used the model to quantify how mobility of humans between regions affected impacted EVD epidemic. They concluded that reduced mobility between countries delays the spread of EVD but does not stop it and an early response would have been more effective in containing EVD [157]. Kramer *et al.* [158] stated that the probability of EVD transmission between locations depends on distance, population density and international border closures. They considered Guinea, Liberia, Sierra Leone and neighbouring countries for their study and concluded that border closures between affected countries has the potential to limit the disease spread.

Brauer and Van Den Driessche [159] modelled the transmission of diseases with immigration of infectives and with an application to HIV transmission. They considered two main cases: first, a constant transmission rate and second, a transmission rate that depends on the total population size. They used Bendixson-Dulac criterion to analyse the stability of the models and concluded that in the presence of immigration of infectives, there is no disease free equilibrium and the steady states are locally asymptotically stable. In a model of HIV transmission in a prison system, they suggested screening and quarantining as control measures to reduce the number of infective immigrants [159]. Similar results were found by Tripathi et al. [160], who incorporated treatment and time delay into a model of HIV/AIDS with immigration of infectives.

As Africa develops, human movement from different regions is bound to increase. Because different regions have different strains, the possibility of strains being transported between regions is highly likely. This work considers the possibility of strain importation through human migration and strain mutation, and therefore present a possibility that is highly likely in the distant future. We formulate a model of EVD with a resident strain that either mutates or is invaded by a new strain of ebolavirus and evaluate the potential influence of strain importation or mutation on the disease dynamics. If the new strain is a mutant of the resident strain, then we have a scenario where the possibility of an invasion by the new strain is possible. If the new strain is imported from a different region, then we consider the cases where we have a continuous or an impulsive migration of infectives. We assume in this work that movements of populations on the African continent could import a new strain of EVD into a country already affected by a different strain. We also assume that recovered individuals acquire immunity during the modelling period.

This work is arranged as follows: we start by the model formulation in Section 5.2, then follows the analysis of the model first with continuous migration of infectives in Section 5.3 and second with impulsive migration of infectives in Section 5.4. Numerical simulations are done in Section 5.5 and we give concluding remarks in Section 5.6.

5.2 Model formulation

We formulate a model of EVD with two strains, strain 1 $\big(\text{EVD1}\big)$ and strain 2 $\big(\text{EVD2}\big)$. Strain 1 is considered to be the resident strain while strain 2 is either an imported or mutant strain. In a given region or country, we assume that susceptible individuals, at any time t, denoted by $S(t)$, are recruited at a constant rate Λ either through births or immigration. Susceptible individuals can be infected by either strain 1 or strain 2 at a time. We thus do not assume co-infection by different strains. Susceptible individuals infected by strain i $\big(i = 1, 2\big)$, move to compartment I_i and can transmit EVD. An infectious individual can either die of the disease or recover. Those that die of strain i are denoted D_i and those that recover are assumed to belong to the class R that is independent of the strain they were suffering from. The flow of the individuals between compartments is shown in Figure 5.1. Susceptible, infected and recovered individuals die naturally at a rate μ with the infected dying at rates φ_1 and φ_2 from strain 1 and 2 respectively. Individuals are assumed to recover from strain 1 and strain 2 at a rates α_1 and α_2 respectively. The deceased are assumed to contribute to infection and the force of infection for the respective strains is

$$\lambda_i = \beta_i\Big(I_i + \eta_i D_i\Big) \quad \text{for} \quad i = 1, 2$$

where η_i is a parameter that measures the relative infectivity of the deceased compared to the infected. To model migration that leads to the importation of strains, we consider that a group of individuals made of infectious individuals at a proportion p (infected by strain 2) and susceptibles, moves into a community affected by EVD strain 1 at a constant rate σ. Ebola epidemics are usually short and we do not assume migration of the recovered and deceased during an epidemic. It is important to note that the constant Λ incorporates migrants and births in a community. The corpses of the deceased are buried at rates ρ_i depending on the strain that caused the death.

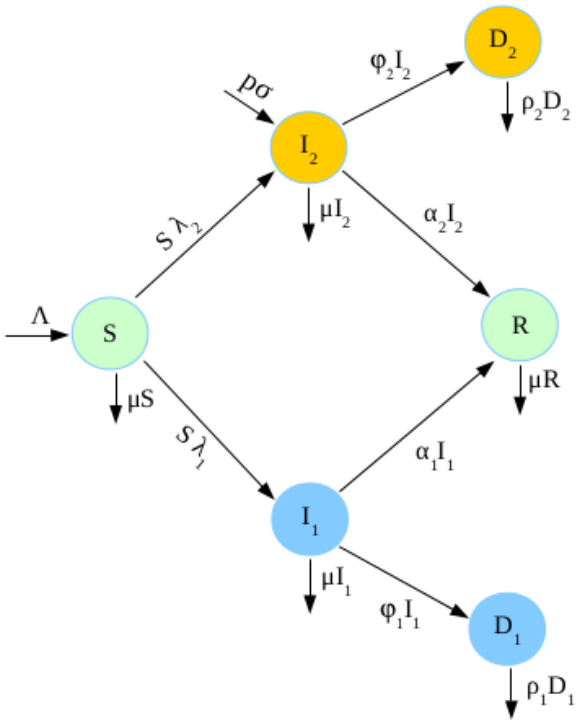

Figure 5.1: Flow chart diagram of the model with migration of infectives

The differential equations that model the described disease dynamics are

$$\begin{aligned}
\frac{dS}{dt} &= \Lambda - \left(\lambda_1 + \lambda_2 + \mu\right) S, \\
\frac{dI_1}{dt} &= \lambda_1 S - Q_1 I_1, \\
\frac{dD_1}{dt} &= \varphi_1 I_1 - \rho_1 D_1, \\
\frac{dI_2}{dt} &= \pi + \lambda_2 S - Q_2 I_2, \\
\frac{dD_2}{dt} &= \varphi_2 I_2 - \rho_2 D_2, \\
\frac{dR}{dt} &= \alpha_1 I_1 + \alpha_2 I_2 - \mu R,
\end{aligned} \tag{5.2.1}$$

with initial conditions

$$S(0) > 0, I_i(0) \geq 0, D_i(0) \geq 0, R(0) \geq 0 \quad \text{for} \quad i = 1, 2$$

and where $Q_1 = \mu + \alpha_1 + \varphi_1$, $Q_2 = \mu + \alpha_2 + \varphi_2$. We redefine $\Lambda = \theta + (1 - p)\sigma$ and $\pi = p\sigma$ where θ is the recruitment rate of susceptibles through

other means, other than immigration. We consider the equation for R to be redundant. To analyse (5.2.1), we consider three cases: first, a case with a constant immigration of infectives who come with strain 2, second a case in which we have impulsive migration, and third a case in which we have a mutant strain 2 that comes from strain 1.

5.3 Model of Ebola dynamics with continuous immigration of infectives

West Africa is the most mobile part of the continent and improving the living conditions of the migrants is the main motivation of populations' movement [154, 161]. Continuous migration in Africa is observed at any period of the year, when individuals or even whole families choose to move to other African countries. This is the case of refugees for example, who have to flee from conflicts' regions and live outside their homes for an undetermined period of time. During the last decades, waves of refugees were noticeable all over the African continent, especially in West Africa where Ivory Coast has taken the lead in hosting refugees [162]. We consider the case where individuals infected by strain 2 of ebolavirus are constantly recruited into a country already affected by strain 1 of ebolavirus. The flow between the compartments of the model representing Ebola dynamics in this case is given by

$$\frac{\mathrm{d}S}{\mathrm{d}t} = \Lambda - \left(\lambda_1 + \lambda_2 + \mu\right) S, \tag{5.3.1}$$

$$\frac{\mathrm{d}I_1}{\mathrm{d}t} = \lambda_1 S - Q_1 I_1, \tag{5.3.2}$$

$$\frac{\mathrm{d}D_1}{\mathrm{d}t} = \varphi_1 I_1 - \rho_1 D_1, \tag{5.3.3}$$

$$\frac{\mathrm{d}I_2}{\mathrm{d}t} = \pi + \lambda_2 S - Q_2 I_2, \tag{5.3.4}$$

$$\frac{\mathrm{d}D_2}{\mathrm{d}t} = \varphi_2 I_2 - \rho_2 D_2. \tag{5.3.5}$$

5.3.0.1 Existence and positivity of solutions

System (5.3.1)-(5.3.5) makes biological sense if its solutions exist and are positive in an invariant region.

Theorem 5.3.1. *Picard's existence theorem is sufficient to conclude the existence and uniqueness of solutions of system (5.3.1)-(5.3.5), for given initial conditions. The invariant region is given by*

$$\Omega = \left\{ \left(S, I_1, D_1, I_2, D_2\right) \in \mathbb{R}^5_+ : S + I_1 + I_2 \leq \frac{(\Lambda+\pi)}{\mu}, D_1 \leq \frac{(\Lambda+\pi)\,\varphi_1}{\mu\,\rho_1} \text{ and } D_2 \leq \frac{(\Lambda+\pi)\,\varphi_2}{\mu\,\rho_2} \right\}.$$

Proof. In fact, the right hand side of system (5.3.1)-(5.3.5) is made of Lipschitz continuous functions, which is a necessary and sufficient condition in Picard's existence Theorem [113] for the solutions to exist and the system (5.3.1)-(5.3.5) has positive and bounded solutions in the region.
Let us set $M(t) = S(t) + I_1(t) + I_2(t)$. Adding equations (5.3.1), (5.3.2) and (5.3.4) yields $\frac{\mathrm{d}M(t)}{\mathrm{d}t} \leq \pi + \Lambda - \mu M(t)$. Solving the corresponding differential equation $\frac{\mathrm{d}M(t)}{\mathrm{d}t} = \pi + \Lambda - \mu M(t)$ and using Gronwall inequality yield $M(t) \leq \frac{\Lambda+\pi}{\mu}$. Similarly, since $I_1(t) < M(t) \leq \frac{\Lambda+\pi}{\mu}$, equation (5.3.3) yields $\frac{\mathrm{d}D_1}{\mathrm{d}t} \leq \varphi_1 \frac{(\Lambda+\pi)}{\mu} - \rho_1 D_1$ and Gronwall inequality gives $D_1 \leq \frac{(\Lambda+\pi)\,\varphi_1}{\mu\,\rho_1}$. Since $I_2(t) < M(t) \leq \frac{(\Lambda+\pi)}{\mu}$, equation (5.3.5) yields $\frac{\mathrm{d}D_2}{\mathrm{d}t} \leq \varphi_2 \frac{(\Lambda+\pi)}{\mu} - \rho_2 D_2$ and similarly we obtain $D_2 \leq \frac{(\Lambda+\pi)\,\varphi_2}{\mu\,\rho_2}$. □

Theorem 5.3.2. *All the solutions of the system (5.3.1)-(5.3.5) are non-negative for non-negative initial conditions.*

Proof. We set $A(t) = \lambda_1(t) + \lambda_2(t) + \mu$. Solving equation (5.3.1) for $S(t)$ yields

$$S(t) = \left[S(0) + \left(\int_0^t \Lambda \exp\left(\int_0^s A(\tau) d\tau \right) ds \right) \right] \exp - \left(\int_0^t A(\tau) d\tau \right).$$

So, $S(t) \geq 0$ for all $t \geq 0$ whenever $S(0) \geq 0$. System of equations (5.3.2)-(5.3.5) can be rewritten as $\frac{\mathrm{d}Y(t)}{\mathrm{d}t} = Z\,Y(t) + B$ where

$$Y(t) = \begin{bmatrix} I_1(t) \\ D_1(t) \\ I_2(t) \\ D_2(t) \end{bmatrix}, \; B = \begin{bmatrix} 0 \\ 0 \\ \pi \\ 0 \end{bmatrix} \text{ and } Z = \begin{bmatrix} \beta_1 S - Q_1 & \eta_1 \beta_1 S & 0 & 0 \\ \varphi_1 & -\rho_1 & 0 & 0 \\ 0 & 0 & \beta_2 S - Q_2 & \eta_2 \beta_2 S \\ 0 & 0 & \varphi_2 & -\rho_2 \end{bmatrix}.$$

Since all the off diagonal elements of Z are non-negative, Z is a Metzler matrix and Y is monotone and positive, see [145, 163]. So, $\mathbb{R}^4_+$ is invariant under $\dfrac{dY(t)}{dt}$ and $Y(t)$ is non-negative. □

5.3.0.2 Reproduction number

The disease free equilibrium $\left(\text{DFE}\right)$ E^0 is a steady state without any existing case of EVD irrespective of the strain and no migration of infectives ($\pi = 0$). $E^0 = \left(S^0, 0, 0, 0, 0\right)$, where $S^0 = \dfrac{\Lambda}{\mu}$ is obtained by solving equation (5.3.1) for S at equilibrium ($\dfrac{dS(t)}{dt} = 0$).

At the DFE,

$$\begin{aligned} (5.3.1) &\iff \frac{dS(t)}{dt} = 0 \\ &\implies S = S^0, \end{aligned}$$

The reproduction number R_0 is calculated by using the next generation matrix method $\left(\text{see [115]}\right)$. The renewal and transfer matrices are respectively given by

$$F = \begin{bmatrix} \beta_1 S^0 & \beta_1 \eta_1 S^0 & 0 & 0 \\ 0 & 0 & 0 & 0 \\ 0 & 0 & \beta_2 S^0 & \beta_2 \eta_2 S^0 \\ 0 & 0 & 0 & 0 \end{bmatrix}, \; V = \begin{bmatrix} Q_1 & 0 & 0 & 0 \\ -\varphi_1 & \rho_1 & 0 & 0 \\ 0 & 0 & Q_2 & 0 \\ 0 & 0 & -\varphi_2 & \rho_2 \end{bmatrix}.$$

The reproduction number is the largest eigenvalue of the matrix $F.V^{-1}$ and after calculation we obtain $R_0 = \max\left\{R_1, R_2\right\}$ where

$$R_1 = \frac{\Lambda}{\mu}\beta_1\left(\frac{\rho_1 + \eta_1\varphi_1}{\rho_1 Q_1}\right) \quad \text{and} \quad R_2 = \frac{\Lambda}{\mu}\beta_2\left(\frac{\rho_2 + \eta_2\varphi_2}{\rho_2 Q_2}\right).$$

$\pi = 0$ is a necessary condition in order to reach the total absence of EVD. In this case, global stability of the equilibrium point is not guaranteed as long as infected immigrants continue to move into the country. This emphasizes the complexity of the control of EVD in the African setting where road boundaries particularly, are most of the time porous and migration is not always well controlled.

5.3.0.3 Strain 2 free equilibrium

In the absence of EVD2 $\left(I_2 = D_2 = 0\right)$, the reproduction number is R_1 and the endemic equilibrium is $E_1^* = \left(S^*, I_1^*, D_1^*\right)$ where $S^* = \dfrac{\Lambda}{\mu R_1}, I_1^* = \dfrac{\Lambda}{Q_1 R_1}\left(R_1 - 1\right), D_1^* = \dfrac{\varphi_1}{\rho_1} I_1^*$.
At equilibrium $\left(\dfrac{\mathrm{d}S}{\mathrm{d}t} = 0, \dfrac{\mathrm{d}I_1}{\mathrm{d}t} = 0, \dfrac{\mathrm{d}D_1}{\mathrm{d}t} = 0\right)$, we solve equation (5.3.1) for S to obtain S^* and we solve equation (5.3.3) for D_1 to obtain D_1^*. We set $D_1 = D_1^*$ in equation (5.3.2) and solve for I_1 to get I_1^*. We obtain the final results by replacing the final value of I^* into S^*.
At the endemic equilibrium in this case,

$$\begin{aligned}
(5.3.1) &\iff \frac{\mathrm{d}S(t)}{\mathrm{d}t} = 0 \\
&\implies S = S^*, \\
(5.3.3) &\iff \frac{\mathrm{d}D_1(t)}{\mathrm{d}t} = 0 \\
&\implies D_1 = D_1^*, \\
(5.3.2) &\iff \frac{\mathrm{d}I_1(t)}{\mathrm{d}t} = 0 \\
&\implies I_1 = I_1^*.
\end{aligned}$$

Theorem 5.3.3. *The endemic equilibrium E_1^* exists for $R_1 > 1$. Before the invasion of strain 1 by strain 2, E_1^* is globally asymptotically stable. When the invasion occurs, E_1^* is locally stable.*

Proof. Strain 2 can invade strain 1 when the latter is at equilibrium and the invasion reproduction number of strain 2 denoted by R_{12}^{inv} is computed using the next generation matrix method for $S = S_1^*$ and $I_2 = D_2 = \pi = 0$. We

obtain

$$R_{12}^{inv} = S_1^* \beta_2 \left(\frac{\rho_2 + \eta_2 \varphi_2}{\rho_2 Q_2} \right) = \frac{R_2}{R_1}.$$

In a country where EVD1 exists already, immigration of individuals infected by EVD2 may lead to an invasion and the invasion reproduction number is R_{12}. If $R_1 > R_2$, then EVD1 is spreading faster than EVD2. $R_1 < 1$ (which implies that I_1^* does not exist) is necessary to stop EVD1 but not EVD2. $\pi = 0$ is necessary for the total eradication of EVD2. If $R_2 > R_1$, then EVD2 totally invades the country ($R_{12} > 1$) and reducing R_2 to values less than one can help to limit the spread of strain 1 since $R_2 < 1$ implies $R_1 < 1$ in this case. So, in order to stop the invasion, immigration of individuals infected by EVD2 should be prohibited (in order to have $\pi = 0$) and other control measures such as quarantine and hospitalisation should be introduced to limit the spread of EVD1 and EVD2 in the population. When EVD1 is the only strain of EVD existing in the country, its eradication is easier because health authorities only focus on limiting the spread of one strain of EVD.

The use of the next generation matrix method to compute R_{12}^{inv} guarantees the local stability of the equilibrium point E_1^*. The proof of the global asymptotic stability of E_1^* before the invasion is as follows: we set F_1 as the Lyapunov function with

$$F_1 = \left(S - S^* - S^* \ln \left(\frac{S}{S^*} \right) \right) + A_1 \left(I_1 - I_1^* - I_1^* \ln \left(\frac{I_1}{I_1^*} \right) \right) + B_1 \left(D_1 - D_1^* - D_1^* \ln \left(\frac{D_1}{D_1^*} \right) \right),$$

where A_1 and B_1 are positive constants to be calculated with $F_1(E_1^*) = 0$.

The right hand side of system (5.3.1)-(5.3.5) at equilibrium yields

$$\begin{aligned} \Lambda &= \beta_1 \left(I_1^* + \eta_1 D_1^* \right) S^* + \mu S^*, \\ Q_1 &= \frac{S^*}{I_1^*} \beta_1 \left(I_1^* + \eta_1 D_1^* \right), \\ D_1^* &= g_1 I_1^*, \end{aligned} \tag{5.3.6}$$

where $g_1 = \dfrac{\varphi_1}{\rho_1}$. $\dot{F}_1$ is the derivative of F_1 with respect to time and is given by

$$\dot{F}_1 = \left(1 - \frac{S^*}{S}\right)\dot{S} + A_1\left(1 - \frac{I_1^*}{I_1}\right)\dot{I}_1 + B_1\left(1 - \frac{D_1^*}{D_1}\right)\dot{D}_1.$$

$\dot{S}$ is obtained from equation (5.3.1), $\dot{I}_1$ is obtained from equation (5.3.2) and $\dot{D}_1$ is obtained from equation (5.3.3). We then have

$$\begin{aligned}\dot{F}_1 = &\left(1 - \frac{S^*}{S}\right)\left(\Lambda - \left(\beta_1\left(I_1 + \eta_1 D_1\right) + \mu\right)S\right) + B_1\left(1 - \frac{D_1^*}{D_1}\right)\left(\varphi_1 I_1 - \rho_1 D_1\right)\\ &+ A_1\left(1 - \frac{I_1^*}{I_1}\right)\left(\beta_1\left(I_1 + \eta_1 D_1\right)S - Q_1 I_1\right). \qquad (5.3.7)\end{aligned}$$

We set

$$x = \frac{S}{S^*},\ y = \frac{I_1}{I_1^*},\ u = \frac{D_1}{D_1^*}.$$

Using the expressions in (5.3.6) and x, y, u into (5.3.7) yield

$$\dot{F}_1 \ = \ -\mu\frac{(S - S^*)^2}{S} + \beta_1 I_1^* L_1(x, y, u) \qquad (5.3.8)$$

where

$$\begin{aligned}L_1(x, y, u) = &\left(1 - \frac{1}{x}\right)S^*\left(\left(1 - x\,y\right) + g_1\,\eta_1\left(1 - u\,x\right)\right)\\ &+ A_1\left(1 - \frac{1}{y}\right)S^*\left(y\left(x - 1\right) + \eta_1\,g_1\left(u\,x - y\right)\right)\\ &+ \frac{B_1\,\varphi_1}{\beta_1}\left(1 - \frac{1}{u}\right)\left(y - u\right). \qquad (5.3.9)\end{aligned}$$

Equation (5.3.8) implies $\dot{F}_1 \ \leq \beta_1\, I_1^* L_1(x, y, u)$ since $-\mu\dfrac{(S - S^*)^2}{S} \leq 0$.

Expanding the expression of $L_1(x, y, u)$ from system (5.3.9) and grouping the coefficients with the same variable give

$$
\begin{aligned}
L_1(x,y,z,u) = &\frac{B_1\,\varphi_1}{\beta_1} + S^*\left(A_1+1\right) + S^*\,\eta_1\,g_1\left(A_1+1\right)\\
&+u\,x\left(-\eta_1\,A_1\,g_1\,S^* + \eta_1\,A_1\,g_1\,S^*\right) + \frac{u\,x}{y}\left(-A_1\,g_1\,S^*\,\eta_1\right)\\
&+\frac{y}{u}\left(-\frac{B_1\,\varphi_1}{\beta_1}\right) + \frac{1}{x}\left(-S^* - \eta_1\,g_1\,S^*\right) - x\,A_1\,S^*\\
&+y\left(\frac{B_1\,\varphi_1}{\beta_1} + S^*\left(-A_1\right) - \eta_1\,g_1\,A_1\,S^*\right)\\
&+u\left(-\frac{B_1\,\varphi_1}{\beta_1} + g_1\,\eta_1\,S^*\right)\\
&+x\,y\left(-S^* + A_1\,S^*\right). \qquad (5.3.10)
\end{aligned}
$$

To prove that $\dot{F}_1 \leq 0$, we only need to prove that $L_1 \leq 0$ since $\dot{F}_1 \leq \beta_1 I_1^* L_1(x,y,u)$.

The expression of L_1 in (5.3.10) contains positive and negative terms. We set the terms with non-negative coefficients to zero in order to find the final expressions of A_1 and B_1. The coefficients of $y, u, x\,y$ and $u\,x$ are non-negative and then set to zero and solved for A_1 and B_1. We obtain

$$A_1 = 1,\; B_1 = \frac{\eta_1\,g_1\beta_1}{\varphi_1}S^*$$

and L_1 becomes

$$
\begin{aligned}
L_1(x,y,z,u) = &\frac{B_1\,\varphi_1}{\beta_1}\left(1-\frac{y}{u}\right) + \eta_1\,g_1\,S^*\left(A_1\left(1-\frac{1}{x}\right)+1-\frac{u\,x}{y}\right)\\
&+\left(A_1(1-x)+1-\frac{1}{x}\right)S^*. \qquad (5.3.11)
\end{aligned}
$$

So, for $x = y = u = 1$, L_1 is negative and equal to zero. So, $L_1 \leq 0$ for $\left(S, I_1, D_1\right) \in \Gamma$ where

$$\Gamma = \left\{\left(S, I_1, D_1\right) : S = S^*, I_1 = I_1^*, D_1 = D_1^*\right\}.$$

By LaSalle's invariance principle $\left(\text{see } [116]\right)$, E_1^* is globally asymptotically stable on Ω. □

5.3.0.4 Coexistence equilibrium

The coexistence of the two strains leads to the endemic equilibrium $E^{**} = \left(S^{**}, I_1^{**}, D_1^{**}, I_2^{**}, D_2^{**}\right)$ where

$$S^{**} = \frac{\Lambda}{\mu R_1}, I_1^{**} = \mu Q_1^2 \rho_1^2 Q_2 \rho_2 \left(R_1 - \hat{R}_1\right), D_1^{**} = \frac{\varphi_1}{\rho_1} I_1^{**},$$
$$I_2^{**} = \frac{\pi R_1}{Q_2 \rho_2 \left(R_1 - R_2\right)}, D_2^{**} = \frac{\varphi_2}{\rho_2} I_2^{**}, \text{ with } \hat{R}_1 = 1 + \frac{\pi R_1 R_2}{\Lambda \left(R_1 - R_2\right)}.$$

In order to obtain the expressions of the states variables at the endemic equilibrium, we did the following calculations:

$$\begin{aligned}
(5.3.1) &\iff \frac{\mathrm{d}S(t)}{\mathrm{d}t} = 0 \\
&\implies S = S^{**}, \\
(5.3.3) &\iff \frac{\mathrm{d}D_1(t)}{\mathrm{d}t} = 0 \\
&\implies D_1 = D_1^{**}, \\
(5.3.2) &\iff \frac{\mathrm{d}I_1(t)}{\mathrm{d}t} = 0 \\
&\implies I_1 = I_1^{**}, \\
(5.3.5) &\iff \frac{\mathrm{d}D_2(t)}{\mathrm{d}t} = 0 \\
&\implies D_2 = D_2^{**}, \\
(5.3.4) &\iff \frac{\mathrm{d}I_2(t)}{\mathrm{d}t} = 0 \\
&\implies I_2 = I_2^{**}.
\end{aligned}$$

So EVD1 and EVD2 can coexist when EVD1 is dominant. $R_1 > 1$ is not enough for EVD1 to coexist with EVD2. More individuals must be infected by EVD1 for both strains to coexist. The coexistence of the two strains is conditioned by $R_1 > \max\left\{\hat{R}_1, R_2\right\}$. Figure 5.2 shows the region of existence of E^{**} when R_1 and R_2 are varied.

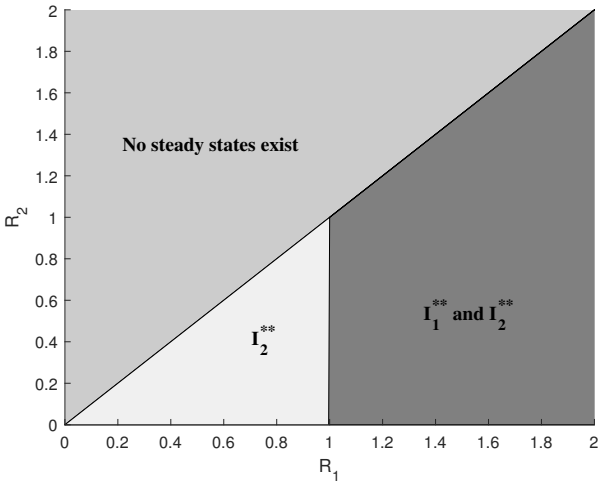

Figure 5.2: Region of existence of I_1^{**} and I_2^{**}

We observe in Figure 5.2 that there is no region of existence of I_1^{**} only and I_2^{**} only exists when $R_2 < 1$. This is due to movements of infectives which always guarantee the presence of individuals infected by EVD2 and suppresses the case where only individuals infected by EVD1 exist. The constant immigration of infectives in this case makes EVD control more difficult since reducing R_2 to values less than one is not enough to reach the DFE.

Theorem 5.3.4. *The endemic equilibrium E^{**} is locally asymptotically stable.*

Proof. To prove the local stability of E^{**}, we set $R_0 = R_1$ since $R_1 > R_2$ is a necessary condition for the existence of E^{**} and $R_0 = \max\left\{R_1, R_2\right\}$. In order to describe the local stability of the endemic equilibrium, we will use the theorem, remark and corollary which are based on the centre manifold theory [121].
We set $\phi = \beta_1$ as our bifurcation parameter, so that for

$$R_0 = 1, \qquad \phi = \phi^* = \frac{\rho_1 Q_1 \mu}{\Lambda\left(\rho_1 + \varphi_1 \eta_1\right)}.$$

In order to linearise system (5.3.1)-(5.3.5), we set

$$S = x_1, I_1 = x_2, D_1 = x_3, I_2 = x_4, D_2 = x_5$$

and

$$\dot{S} = f_1, \dot{I}_1 = f_2, \dot{D}_1 = f_3, \dot{I}_2 = f_4, \dot{D}_2 = f_5.$$

The Jacobian matrix $\mathcal{J}$ of the linearised system (5.3.1)-(5.3.5) at the DFE E^0 and for $\phi = \phi^*$ is given by

$$\mathcal{J} = \begin{bmatrix} -\mu & -\phi^* S^0 & -\phi^* \eta_1 S^0 & -\beta_2 S^0 & -\beta_2 \eta_2 S^0 \\ 0 & \phi^* S^0 - Q_1 & \phi^* \eta_1 S^0 & 0 & 0 \\ 0 & \varphi_1 & -\rho_1 & 0 & 0 \\ 0 & 0 & 0 & \beta_2 S^0 & \beta_2 \eta_2 S^0 \\ 0 & 0 & 0 & \varphi_2 & -\rho_2 \end{bmatrix}.$$

Zero is a simple eigenvalue of $\mathcal{J}$. The left eigenvector of $\mathcal{J}$, $V = \left(v_1, v_2, v_3, v_4, v_5\right)$ and the right eigenvector $W = \left(w_1, w_2, w_3, w_4, w_5\right)'$, both associated to the eigenvalue zero are solutions of the system

$$\begin{cases} \mathcal{J}W = \left[0,0,0,0,0\right]', \\ V\mathcal{J} = \left[0,0,0,0,0\right]', \\ VW = 1, \end{cases} \tag{5.3.12}$$

and we obtain after some algebraic manipulations

$$\begin{aligned} w_1 &= -\frac{Q_1}{\mu}, & v_1 &= 0, \\ w_2 &= 1, & v_2 &= \frac{\rho_1\left(\varphi_1\eta_1 + \rho_1\right)}{\varphi_1\eta_1\left(Q_1 + \rho_1\right) + \rho_1^2}, \\ w_3 &= \frac{\varphi_1}{\rho_1}, & v_3 &= \frac{\rho_1 Q_1 \eta_1}{\varphi_1\eta_1\left(Q_1 + \rho_1\right) + \rho_1^2}, \\ w_4 &= 0, & v_4 &= 0, \\ w_5 &= 0, & v_5 &= 0. \end{aligned}$$

Besides, we notice that for $j = 2,3,4,5$, $E^0(j) = 0$ and $W(j)$ is non-negative. So remark 4 in [121] is verified. Using the formulas defined in [121], we compute the constants a and b and find

$$a = -\frac{2Q_1^2\left(\varphi_1\eta_1 + \rho_1\right)}{\mu S^0\left(\varphi_1\eta_1\left(Q_1 + \rho_1\right) + \rho_1^2\right)} \quad \text{and} \quad b = \frac{S^0\left(\varphi_1\eta_1 + \rho_1\right)^2}{\left(\varphi_1\eta_1\left(Q_1 + \rho_1\right) + \rho_1^2\right)}.$$

The direction of the bifurcation is determined by the signs of a and b. Obviously $b > 0$ and $a < 0$ indicating that E^{**} is locally asymptotically stable and the bifurcation is forward. □

5.4 Model of Ebola dynamics with impulsive immigration of infectives

Impulsive differential equations (IDE) have been produced since 1990 and describe the dynamics of evolving processes subjected to short-term perturbations that act instantaneously or in the form of impulses [164]. We consider in this case that EVD2 is introduced into a population already affected by EVD1 in the form of impulses at specific times t_k, $k = 1, 2, ..., m$ with $m > 0$. During the specific times t_k, the boundaries of the country affected by strain 1 are opened and groups of individuals move in. Individuals infected with EVD2 are recruited at a rate π. The system of IDE describing the flow of individuals is given by

$$\frac{dS}{dt} = \Lambda - \left(\lambda_1 + \lambda_2 + \mu\right) S \tag{5.4.1}$$

$$\frac{dI_1}{dt} = \lambda_1 S - Q_1 I_1, \tag{5.4.2}$$

$$\frac{dD_1}{dt} = \varphi_1 I_1 - \rho_1 D_1, \qquad t \neq t_k \tag{5.4.3}$$

$$\frac{dI_2}{dt} = \lambda_2 S - Q_2 I_2, \tag{5.4.4}$$

$$\frac{dD_2}{dt} = \varphi_2 I_2 - \rho_2 D_2, \tag{5.4.5}$$

$$\triangle I_2(t_k) = I_2(t_k^+) - I_2(t_k^-) = \pi, \qquad t = t_k. \tag{5.4.6}$$

Considering only the state variables affected by the impulse, we obtain system (5.4.7)-(5.4.8).

$$I_2'(t) = \beta_2\left(I_2 + \eta_2 D_2\right) S - Q_2 I_2, \qquad t \neq t_k \tag{5.4.7}$$

$$I_2(t_k^+) = I_2(t_k^-) + \pi, \qquad t = t_k \tag{5.4.8}$$

where $t_{k+1} > t_k$. We assume in this case that there is no individual infected by EVD2 before the first impulse, so $I_1(t_1^-) = 0$ and we set $I_2(t_k^+) = I_k^+$, $I_2(t_k^-) = I_k^-$.

5.4.0.1 Positivity of solutions

For $t \in (t_k, t_{k+1}]$, system (5.4.1)-(5.4.6) is equivalent to (5.4.12)-(5.4.16) when $\pi = 0$ and whose solutions has already been proven non-negative (in Theorem 5.3.2) in the invariant set Ω.

5.4.0.2 Existence and uniqueness of solutions

Theorem 5.4.1. *Solutions of system (5.4.1)-(5.4.6) exist in the sets* $(t_k, t_{k+1}] \times \Omega$ *and are unique for each initial condition* $(t_0, x_0) \in \mathbb{R}_+ \times \Omega$. *Besides, each solution* $\varphi : (\alpha, \beta) \to \mathbb{R}^n$, $\alpha, \beta \in \mathbb{Z}_+$, $\alpha < \beta$, $\beta \neq t_k$, *is continuable to the right of* β. *The general expression of the maximal solution of (5.4.1)-(5.4.6) is given by* $I_2(t_n^-) = \pi \sum_{j=1}^{n-1} \exp\left(Q_2\left(\hat{R}_2 - 1\right)\left(t_n - t_j\right)\right)$ *where* $\hat{R}_2 = \dfrac{(\Lambda + \pi)}{\mu} R_2$.

Proof. The proof is based on the Theorem in [165] stipulating the conditions for the existence and uniqueness of the solutions of a system of non linear IDE with fixed moments of impulses. The Theorem states that given an IDE,

$$\begin{aligned} \frac{\mathrm{d}x}{\mathrm{d}t} &= f(t, x(t)) \quad t \neq \tau_k, \\ \triangle x &= I_k(x) \qquad t = \tau_k, \end{aligned} \tag{5.4.9}$$

where $\tau_k < \tau_{k+1}$ $(k \in \mathbb{Z})$ and $\lim_{k \longrightarrow \infty} \tau_k = \infty$.
Let the function $f : \mathbb{R} \times \Omega \longrightarrow \mathbb{R}^n$ be continuous in the sets $(\tau_k \times \tau_{k+1}] \times \Omega$. For each $k \in \mathbb{Z}$ and $x \in \Omega$, suppose there exists the finite limit of $f(t, y)$ as $(t, y) \longrightarrow (\tau_k, x), t > \tau_k$.
Then, for each $(t_0, x_0) \in \mathbb{R} \times \Omega$, there exists $\beta > t_0$ and a solution $\varphi : (t_0, \beta) \longrightarrow \mathbb{R}^n$ of the initial value problem (5.4.9). Moreover, if the function f is locally Lipschitz continuous with respect to x in $\mathbb{R} \times \Omega$, then this solution is unique. Besides, if $\lim_{t \longrightarrow \beta^-} \varphi(t) = \eta$ and $\eta \in \Omega$ when $\beta \neq \tau_k$, then the solution $\varphi(t)$ is continuable to the right of β. The general solution is in the form

$$x(t) = x_0 + \int_{t_0}^{t} f(s, x(s))dx + \sum_{t_0 < \tau_k < t} I_k\big(x(\tau_k)\big).$$

The right hand side of system (5.4.1)-(5.4.5) is bounded and locally Lipschitz in the sets $(\tau_k \times \tau_{k+1}] \times \Omega$, for $k > 0$ and $\alpha, \beta \in (\tau_k \times \tau_{k+1}]$ with $\beta \neq \tau_k$. $\lim_{t \longrightarrow \beta^-} \varphi(t) = \eta$ belongs to Ω since Ω is positively invariant and we can conclude that the solutions of system (5.4.1)-(5.4.6) exist and are continuable to the right of $\beta \neq \tau_k$. The non linearity of the system of equations (5.4.1)-(5.4.5) makes it difficult to find its algebraic solution. Instead, we give the expression of the maximal solution that does not contain this non linearity.

Calculation of the maximal solution

From the invariant set Ω, $S \leq \dfrac{(\Lambda+\pi)}{\mu}$ and $D_2 \leq \dfrac{\varphi_2\,(\Lambda+\pi)}{\rho_2\,\mu}$. Besides, $D_2 < D_2\,I_2$ and equation (5.4.7) is maximised. We obtain for $t \neq t_k$

$$I_2'(t) \leq \left(\hat{R}_2 - 1\right) Q_2\, I_2, \tag{5.4.10}$$

where $\hat{R}_2 = \dfrac{(\Lambda+\pi)}{\mu}\, R_2$. We solve the equality corresponding to equation (5.4.10) during a single impulsive cycle, $t_k^+ \leq t \leq t_{k+1}^-$ and obtain

$$I_{k+1}^- = I_k^+ \exp\left(Q_2\left(\hat{R}_2 - 1\right)\left(t_{k+1} - t_k\right)\right).$$

From equation (5.4.8), $I_k^+ = I_k^- + \pi$ and this implies that

$$I_{k+1}^- = \left(I_2(t_k^-) + \pi\right) \exp\left(Q_2\left(\hat{R}_2 - 1\right)\left(t_{k+1} - t_k\right)\right).$$

Since $I_1^- = 0$ we can write

$$\begin{aligned}
I_2^- &= \pi \exp\left(Q_2\left(\hat{R}_2 - 1\right)\left(t_2 - t_1\right)\right),\\
I_3^- &= \left(\pi + I_2^-\right) \exp\left(Q_2\left(\hat{R}_2 - 1\right)\left(t_3 - t_2\right)\right),\\
&= \pi \exp\left(Q_2\left(\hat{R}_2 - 1\right)\left(t_3 - t_2\right)\right) + \pi \exp\left(Q_2\left(\hat{R}_2 - 1\right)\left(t_3 - t_1\right)\right),
\end{aligned} \tag{5.4.11}$$

$$\vdots$$

$$I_n^- = \pi \sum_{j=1}^{n-1} \exp\left(Q_2\left(\hat{R}_2 - 1\right)\left(t_n - t_j\right)\right), \quad n \in [1, m].$$

Adding all the equations of the system (5.4.11) yields

$$I_n^- = \pi \sum_{j=1}^{n-1} \exp\left(Q_2\left(\hat{R}_2 - 1\right)\left(t_n - t_j\right)\right)$$

and $\lim\limits_{n\longrightarrow\infty} I_n^- = \begin{cases} 0 & \text{if} \quad \hat{R}_2 < 1, \\ \infty & \text{if} \quad \hat{R}_2 > 1, \end{cases}$ since $\lim\limits_{n\longrightarrow\infty} t_n = \infty$.

$\hat{R}_2 < 1$ implies $R_2 < \dfrac{\mu}{(\Lambda+\pi)}$. So, on the long term, reducing the reproduction number of EVD2 to values less than the ratio $\dfrac{\mu}{(\Lambda+\pi)}$ contributes

to eradicate the strain from the population and values of R_2 greater than the ratio leads to an infinite number of individuals infected by EVD2. But the time duration of two consecutive strains is not constant in this case, and it is uncertain how to determine the number of impulses that will help to limit the number of individuals infected by EVD2. We then introduce a fixed impulse period $\tau = t_{k+1} - t_k$ and obtain from equations (5.4.11),

$$\begin{aligned} I_n^- &= \pi \sum_{j=1}^{n-1} \exp\left(\left(\hat{R}_2 - 1\right) Q_2 \tau j\right), \\ &= \pi \left(\frac{1 - \exp\left(Q_2 \tau \left(n-1\right)\left(\hat{R}_2 - 1\right)\right)}{1 - \exp\left(Q_2 \tau \left(\hat{R}_2 - 1\right)\right)}\right), \end{aligned}$$

and

$$\lim_{n \longrightarrow \infty} I_n^- = \begin{cases} \dfrac{\pi}{1 - \exp\left(Q_2 \tau \left(\hat{R}_2 - 1\right)\right)} & \text{if} \quad \hat{R}_2 < 1, \\ \\ \infty & \text{if} \quad \hat{R}_2 > 1. \end{cases}$$

So, the number of individuals infected by EVD2 is bounded if $\hat{R}_2 < 1$ and reducing R_2 to values less than $\dfrac{\mu}{(\Lambda + \pi)}$ helps to limit the spread of EVD2, but not to clear it from the population. If the total population size is constant $(\Lambda + \pi = \mu)$, then $\dfrac{\mu}{(\Lambda + \pi)} = 1$ and reducing R_2 to values less than one will slow down the spread of EVD2. The maximum number of individuals infected by EVD2 is then

$$I_{max} = \frac{\pi}{1 - \exp\left(Q_2 \tau \left(\hat{R}_2 - 1\right)\right)}.$$

Limiting the number of individuals infected by EVD2 to I_{max} is equivalent to $I_n^- < I_{max}$ which implies that $\tau > \tau_{min}$ with

$$\tau_{min} = \frac{1}{Q_2 \left(\hat{R}_2 - 1\right)} \ln\left(1 - \frac{\pi}{I_n^-}\right).$$

The time lag between two impulses should then be greater than the minimum period τ_{min} if one wants the maximum number of individuals infected by EVD2 to be I_{max}. □

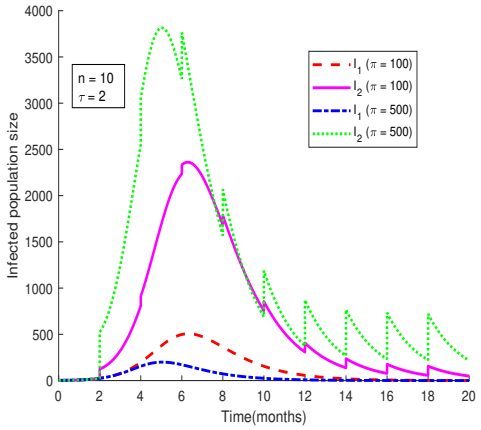

Figure 5.3: Evolution of the number of EVD infected individuals. The parameters' value used are $\Lambda = 8.37$, $\mu = 0.1$, $\beta_1 = \beta_2 = 9 \times 10^{-5}$, $\alpha_1 = \alpha_2 = 0.012$, $\eta_1 = \eta_2 = 2.5$, $\varphi_1 = \varphi_2 = 0.5$, $\rho_1 = \rho_2 = 0.9$

We notice in Figure 5.3 that the graphs representing the number of individuals infected by EVD2 are almost non-existent before the first impulse which is at $t = 2$. But for $t \geq 2$, the impulsive immigration of individuals starts and highly increases the number of individuals infected by EVD2. This graphs highlights then the necessity of permanent control at the borders of any country which can potentially be visited by EVD infected individuals in order to avoid a potential introduction of a new Ebola virus strain into the country.

Between two consecutive impulses, the model dynamics is similar to the following:

$$\frac{dS}{dt} = \Lambda - \left(\lambda_1 + \lambda_2 + \mu\right) S, \tag{5.4.12}$$

$$\frac{dI_1}{dt} = \lambda_1 S - Q_1 I_1, \tag{5.4.13}$$

$$\frac{dD_1}{dt} = \varphi_1 I_1 - \rho_1 D_1, \tag{5.4.14}$$

$$\frac{dI_2}{dt} = \lambda_2 S - Q_2 I_2, \tag{5.4.15}$$

$$\frac{dD_2}{dt} = \varphi_2 I_2 - \rho_2 D_2. \tag{5.4.16}$$

The reproduction number in this case is $R_0 = \max\left\{R_1, R_2\right\}$.

Theorem 5.4.2. *The solutions of the system of equations* (5.4.12)-(5.4.16) *exist and are non-negative for non-negative initial conditions. The invariant set is*

$$\Upsilon = \left\{ \left(S, I_1, D_1, I_2, D_2\right) \in \mathbb{R}_+^5 : S + I_1 + I_2 \leq \frac{\Lambda}{\mu}, D_1 \leq \frac{\Lambda\,\varphi_1}{\mu\,\rho_1} \text{ and } D_2 \leq \frac{\Lambda\,\varphi_2}{\mu\,\rho_2} \right\}.$$

Proof. The proof follows that of Theorems 5.3.1 and 5.3.2. □

5.4.0.3 Coexistence equilibrium

To obtain the equilibrium points, we first set all the differential equations in system (5.4.12)-(5.4.16) to zero. Then we solve equation (5.4.12) for S to get $\hat{S}^{**}$, we solve equation (5.4.13) for I_1 to get $\hat{I}_1^{**}$, we solve equation (5.4.14) for D_1 to get $\hat{D}_1^{**}$, we solve equation (5.4.15) for I_2 to get $\hat{I}_2^{**}$ and we solve equation (5.4.16) for D_2 to get $\hat{D}_2^{**}$.

$\hat{E}^{**} = \left(\hat{S}^{**}, \hat{I}_1^{**}, \hat{D}_1^{**}, \hat{I}_2^{**}, \hat{D}_2^{**}\right)$ is the solution of system (5.4.12)-(5.4.16) at equilibrium with $\hat{S}^{**} = \dfrac{\Lambda}{\mu + \lambda_1^{**} + \lambda_2^{**}}$, $\hat{I}_1^{**} = \dfrac{\Lambda^2\left(R_1 - 1\right) - Q_2\,R_2\,\hat{I}_2^{**}\,\mu}{\mu\,Q_1\,R_1}$, $\hat{D}_1^{**} = \dfrac{\varphi_1}{\rho_1}\,\hat{I}_1^{**}$, $\hat{I}_2^{**} = \dfrac{\Lambda^2\left(R_2 - 1\right) - Q_1\,R_1\,\hat{I}_1^{**}\,\mu}{\mu\,Q_2\,R_2}$, $\hat{D}_2^{**} = \dfrac{\varphi_2}{\rho_2}\,\hat{I}_2^{**}$.

$\hat{E}^{**}$ is the unique endemic equilibrium point in this case. $R_1 > 1$ and $R_2 > 1$ are necessary but not sufficient conditions for the two strains to co-exist at an endemic state.

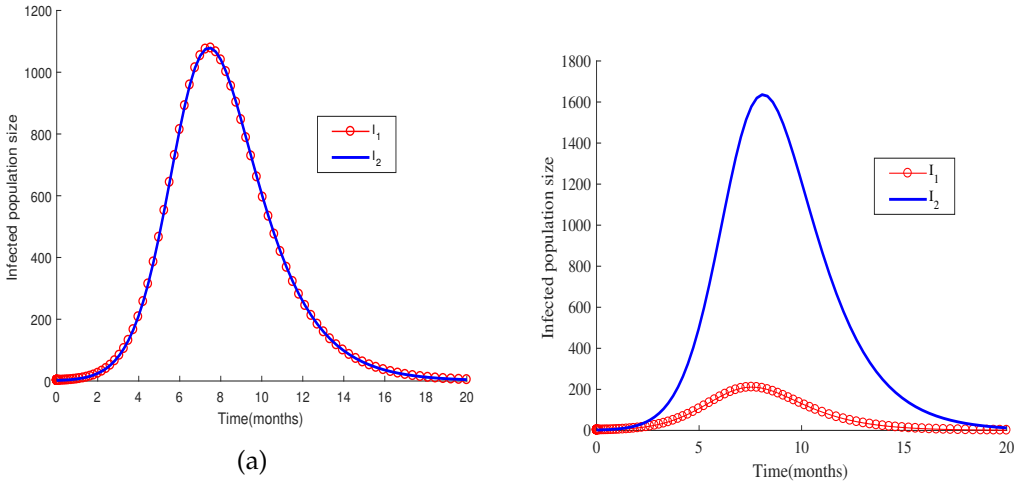

Figure 5.4: Dynamics of the number of EVD infected individuals with two strains. The parameters' value used are the same as in Figure 5.5 with $\beta_1 = \beta_2 = 9 \times 10^{-5}$ in (a) and $\beta_1 = 7 \times 10^{-5}$, $\beta_2 = 9 \times 10^{-5}$ in (b).

Figure 5.4 illustrates the coexistence of two EVD strains. Figure 5.4(a) shows the case where the two strains are equally infectious. We observe a rapid decrease of the number of infected individuals for both strains from the $8th$ month and EVD free equilibrium is reached after 18 months for the chosen parameter values. Figure 5.4(b) illustrates the case where EVD2 is more infectious than EVD1 and we notice the very high number of individuals infected by EVD2 when compare to those infected by EVD1. The most infectious strain is then the most dangerous and health authorities should prioritise control measures that limit the spread of the most infectious strain in the case of an EVD epidemic caused simultaneously by two strains.

5.5 Numerical simulations

Seasons and poor economic conditions motivate frequent movements across borders in Africa, which are similar to impulsive movements of populations. For illustrative purposes, we simulate these scenarios in this section, focusing on the effect of increased immigration rate of infectives, increased immigration frequency of infectives and increased infectivity of Ebolavirus strains.

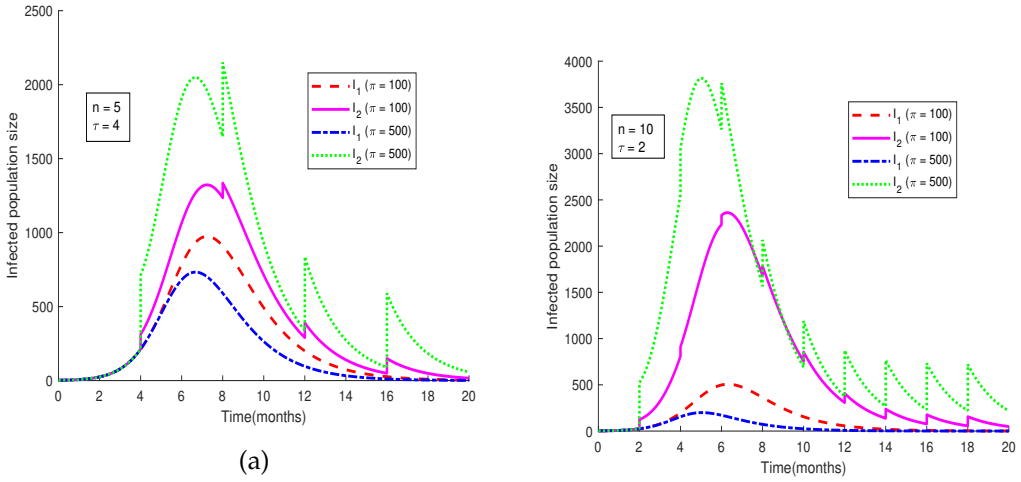

Figure 5.5: Evolution of the number of EVD infected individuals. The parameters' value used are $\Lambda = 8.37$, $\mu = 0.1$, $\beta_1 = \beta_2 = 9 \times 10^{-5}$, $\alpha_1 = \alpha_2 = 0.012$, $\eta_1 = \eta_2 = 2.5$, $\varphi_1 = \varphi_2 = 0.5$, $\rho_1 = \rho_2 = 0.9$

We simulate a scenario where an impulsive immigration of infectives introduces strain 2 is in a country already affected by strain 1. We consider a fixed period of impulse τ during which n impulses occur. We vary the immigration rate of individuals affected by EVD2 and the period of the impulses is varied as well. The results are given in Figures 5.5(a) and 5.5(b). In both figures, we observe that the number of individuals infected by EVD2 is larger when π is increased. This is an expected result since the number of individuals infected by EVD2 is fed by the immigration of infectives and the disease contamination.

The number of impulses during a fixed period affects the extent of EVD epidemic. In Figure 5.5(a), we have 5 impulses within 20 months whereas in Figure 5.5(b) we have 10 impulses within the same period. Irrespective of the strain, the maximum number of infected individuals is 3000 in Figure 5.5(a) and 4000 in Figure 5.5(b). Increasing the frequency of the impulses has thus increased the number of infected individuals. The maximum number of individuals infected by EVD2 is reached a bit earlier when the number or frequency of the impulses is increased. Delayed and less intensive immigration of infectives is then advocated. Although a reduced number of impulses allows more infections due to EDV1, a total eradication of EVD2 gives the possibility of reaching a globally stable DFE. The formu-

lation of control measures to eradicate EVD1 is easier in this case. Because road boundaries in Africa are difficult to control, we advocate for more educational campaigns, economic development and good governance so as to limit the movements of populations which is often due to these causes.

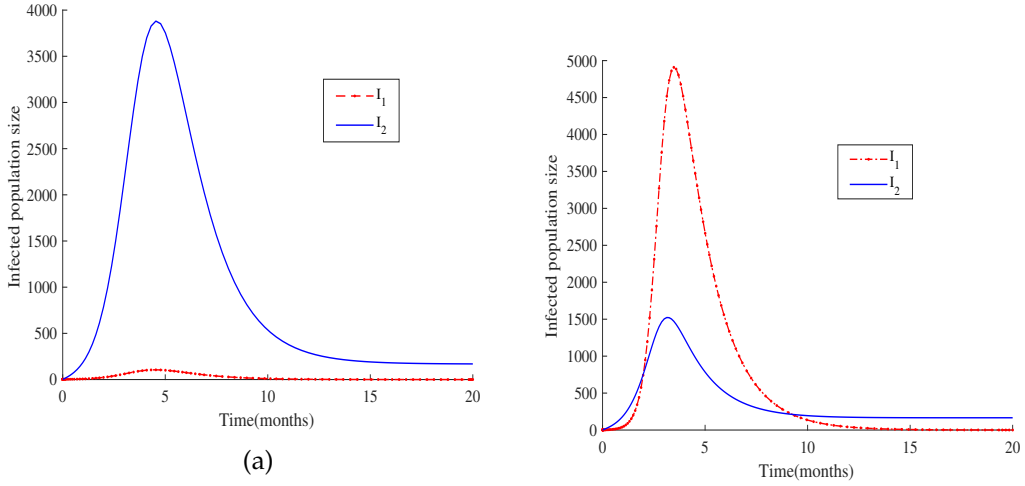

Figure 5.6: The parameters have the same value as in Figure 5.5 with $\beta_1 = \beta_2 = 9 \times 10^{-5}$ in (a), $\beta_1 = 2 \times 10^{-4}$ and $\beta_2 = 9 \times 10^{-5}$ in (b), $\pi = 100$

We simulate the constant migration of infectives scenario and obtain Figure 5.6. Figure 5.6(a) shows that more individuals are infected by EVD2 when the two strains are equally infectious for the chosen parameter values. This result is due to the constant immigration of infectives. In Figure 5.6(b), we observe that the most infectious strain infects more people for about 9 months although immigration of infectives is continuous, for the chosen parameter values. From the $10th$ month onwards, we observe that strain 1 reaches the DFE point while strain 2 remains endemic although it is the less infectious strain. This can be explained by the fact that the susceptible population during the previous months was depleted so that EVD1 has less people to infect. Besides, the recruitment of infectives immigrant is constant and continuously feeds the population of individuals infected by EVD2. This is why EVD2 remains endemic even when there are fewer susceptible individuals to infect. Controls aiming at stopping EVD1 and EVD2 must then also consider the degree of infectivity of each ebolavirus strain. The most infectious strain should be first eliminated as it infects

and certainly kills more individuals. Besides, very strict controls at the different entries of a country are necessary to completely stop both strains of Ebolavirus from invading the population.
The dynamics of EVD represented in Figures 5.5 and 5.6 shows that the highest number of individuals infected by EVD2 is 4000 in Figure 5.6 and 3700 in Figure 5.5. We also observe on these Figures that the DFE is reached earlier in the case of continuous migration of infectives for EVD1. This is an expected result since continuous migration of infectives feeds EVD2 infected population and depletes the susceptible population so that EVD1 has less people to infect. In the case of impulsive migration of infectives, the time lag between two consecutive impulses allows for the susceptible population size to increase and results in higher number of individuals exposed to EVD2 as shown in Figure 5.5(b). The main advantage of impulsive migration of infectives when compared to the continuous one in this case is that the continuous migration does not rapidly depletes the susceptible population and then gives time for control measures implementation. We then suggest that once a new strain is noticed within the boundaries of a country or in his neighbourhood, migration services should privilege impulsive movement to continuous movement of populations at their boundaries. A total closure of the boundaries can be considered if the control cannot be well conducted.

5.6 Conclusion

Movements of infected individuals is a reality and introduced Zaire ebolavirus strain in Liberia and Sierra Leone in 2014 [166]. We formulated and analysed in this work, a model of EVD dynamics in which EVD2 is introduced in a country where EVD1 is endemic.

First, we considered that the immigration of individuals infected by EVD2 is continuous. The mathematical analysis of the model indicated the existence of a locally stable disease free equilibrium and an endemic equilibrium. It showed that when the invasion reproduction number of EVD2 is greater than one, EVD2 invades the country. The two strains coexist at an endemic state when the reproduction number of EVD1 is greater than the one of EVD2. Numerical simulations indicated a rapid and abrupt increase of the number of individuals infected by EVD2 which allows less time for control

measures' implementation. A fast decrease of the number of individuals infected by EVD1 was noticed as well and this can be the ideal solution if clearing EDV1 from the population is the objective.

Second, immigration of individuals infected by EVD2 was considered to be impulsive and we proved that the reproduction number of EVD2 must be less than the ratio $\mu/(\Lambda+\pi)$ in order to limit the number of individuals infected by EVD2. We also found that a fixed period of impulse is better for EVD2 control since it helps to evaluate with precision the number of impulses that minimizes the number of individuals infected by EVD2. Numerical simulations' results indicated that the smaller the immigration rate of individuals infected by EVD2, the larger the number of individuals infected by EVD1. This sheds the light on the competition between the two ebolavirus strains for the susceptible population.

In summary, we state that the impulsive type of migration of individuals infected by the less infectious EVD strain would be a better scenario. We argue that this type of migration of infectives is manageable because it allows more time for control measures to be implemented, increasing the chances of stopping EVD irrespective of the strain. An unknown outbreak started in Guinea in December 2013 and was only declared as an EVD outbreak later in March 2014 by the WHO [166]. In case of co-infection by different strains of EVD, such delay will lead to a death toll far larger than the 11000 recorded in 2016. An impulsive movement of infectives even in such situation, is preferable to a continuous movement of infectives as it delays the increase in the number of infected migrants. The study presented in this work considers two of the five existing strains of Ebola virus and describes well the scenario of a multi-strain epidemic of Ebola. Considering more strains is what we endeavour to do in the future as it will give a bigger picture of a potential co-infection situation.

Chapter 6

Modelling the potential influence of economic migration on Ebola virus disease dynamics

6.1 Introduction

Poverty is a multidimensional phenomenon characterized by weak consumption of goods, malnutrition, bad living conditions and difficult access to public and social services [167]. In the monetary approach of poverty, low income countries are those whose per capita gross national income (GNI) per year is $\$995$ or less [2]. The GNI is defined as the sum of value added by all resident producers plus any product taxes not included in the valuation of output, plus net receipts of primary income from abroad [168]. West African countries affected by the $2013-2016$ Ebola virus disease (EVD) outbreak are classified as low income countries and are among the poorest in the world [2]. In Guinea, Liberia and Sierra Leone, the economic activities practised by the majority of the population are agriculture, mining, trade, fishery, manufacturing and services whereas waged and qualified jobs are practised by a very low proportion of the West African population [169, 170, 171].

The global burden of infectious diseases is higher in low income countries [172]. Poverty or monetary poverty is thus a predisposition to the spread of infectious diseases and data collected by the World Health Organisation (WHO) indicate that poor areas were the most vulnerable during EVD out-

break of 2013 – 2016 [46, 173]. EVD reached high income countries like USA or Spain, but the good economic status of these countries helped to rapidly stop its spread [46].

"A mathematical model that links health and economic development may have its limitations, but its consequences are too serious to ignore" [174]. Mathematical modelling is an important tool that can be used to evaluate the impact of economic poverty on a disease dynamics. Poverty and infectious diseases spread have already been linked in mathematical modelling. Rich and poor communities or classes are mostly used to model poverty and health [47, 96, 97]. Bhunu *et al.* [47] used a $SEIR$ model to assess the effects of poverty in tuberculosis transmission dynamics. Two main groups constituted their model: individuals living in poverty and those not living in poverty. The authors considered that the number of contacts made by poor individuals is larger than the one made by rich individuals since poor individuals live in overcrowded condition. Assuming heterogeneous interactions, they concluded that homogeneous mixing of the rich and the poor will improve the eradication of tuberculosis whereas heterogeneous mixing, will make it worse. However, they encouraged the rich to contribute to tuberculosis eradication within the poor communities. More than two socio-economic classes can also be used to analyse infectious diseases models. Collins *et al.* [48] analysed a SIR model of a water-borne disease with n socio-economic classes $\big(\text{SEC}\big)$, with $n \geq 1$. They only considered indirect transmission of the pathogen and assumed that n-SEC becomes more rich as n increases. The authors first determined the effects of a 2-SEC model on cholera transmission dynamics and extended their results to a n-SEC model. They concluded that a model without SEC may underestimate the reproduction number of the system and lead to a failure in the disease control. A n-SEC model with data was also used in statistical modelling to study the role of socio-economic status in longitudinal trends of cholera [49].

Economic migration within the African continent is a reality and is more intensive in West Africa in particular, because free movements of persons and goods is facilitated well through the Economic Community of West African States (ECOWAS) [152]. Among the West African countries affected by EVD in 2013 – 2016, those with a higher GNI, as represented in Figure 6.1, are assumed to be economically more attractive. Meliandou is a village

in Guinea considered as ground zero of EVD outbreak of 2013 – 2016. It is a triangular-shaped forested area where the borders of Guinea, Liberia and Sierra Leone converge [175]. The quest of many unemployed people to find work contributes to fluid population movements across borders, which fuels the spread of a highly contagious virus like Ebola [175]. The WHO investigation revealed that a very rapid movement of people from villages across the border was a feature that later became a major driving force as EVD outbreak evolved [175]. Besides, viruses can be carried for long distances and researchers claim that population movements were a challenge in controlling EVD in West Africa [90, 154]. So, we assume that populations' movements due to poverty during EVD outbreak contributed to the disease spread.

Understanding the drivers of population mobility and building more formal boundaries, especially in local communities is more efficient in case a disaster emerges [152]. It is then important to understand the drivers of population mobility during the 2013 – 2016 EVD outbreak, and especially the economic drivers. 80% of the total employment in Liberia and Sierra Leone were informal during EVD outbreak of 2013 – 2016 and many people lost their jobs due to EVD outbreak especially in the agricultural, mining and transport sectors. As a consequence, a large number of individuals were more predisposed to spread or contract the disease because they couldn't afford treatment in good hospitals, necessary protective or preventive materials like bleach, clean toilets or even transport to the nearest Ebola treatment center.

Several mathematical models of EVD dynamics evaluate the impact of interventions on the disease dynamics or the spatial spread of the disease [32, 57, 125, 152]. Currently, there is no mathematical model linking EVD dynamics and economic migration of populations, to the best of our knowledge. Countries affected by the outbreak of 2013 – 2016 are among the poorest in Africa as their per capita GNI are very low when compared to the average on the continent [176]. Among the different tools used to measure the health of the economy of a country, such as the GDP (the Gross Domestic Product) and the GNI, we choose to use the GNI because it relates more to the income per individual in the country. It is also is used to evaluate the impact of limited economy on infectious diseases spread [98, 99, 167]. We

observe in Figure 6.1 that the GNI in 2012 was increasing before the rise of EVD outbreak in the West African countries affected by EVD and started to decline after EVD hit these countries. Although it was not the first decline of GNI ever seen in West Africa, EVD slowed economic growth and aggravated an already bad situation [22]. We assume that the increasing number of EVD cases highly affected the economies of these countries and contributed to a decrease of income in general, see also [169]. So, we choose to focus on the interaction between income and EVD and we study how they have impacted each other through human mobility. Data used to draw the graphs in Figure 6.1 were taken from [2] and data missing in the source are represented by empty spaces.

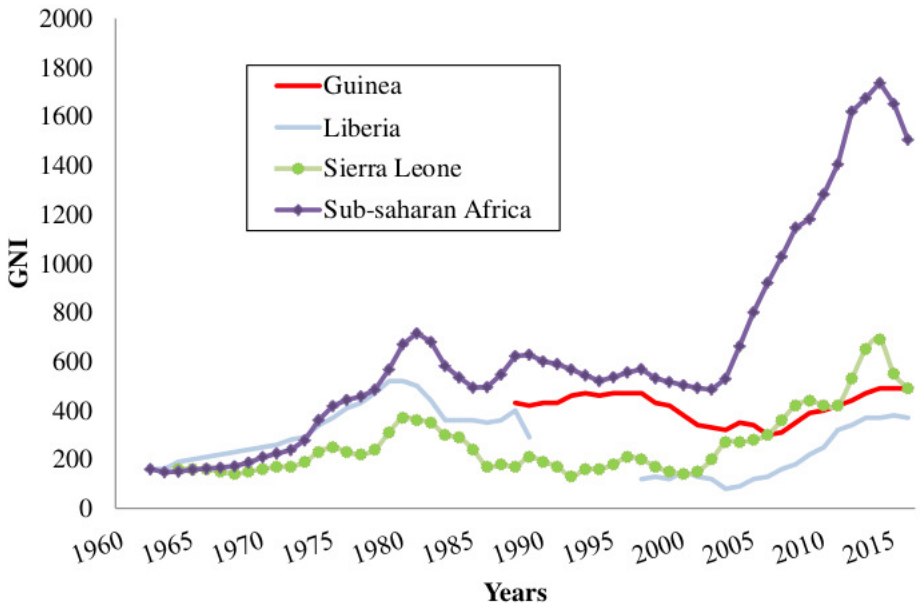

Figure 6.1: Annual Per capita GNI in Africa, source [2].

Movements between different socio-economic classes can result in the spread of an infectious disease such as EVD and the spatial spread of the disease is the immediate consequence of the population mobility. Kiskowski and Chowell [11] modelled household and community transmission of EVD by employing a stochastic individual-level model. Location of infectious individuals was done through a network and the spatial spread of the epidemic was implemented in the network with a household-community structure. They assumed that control measures or behaviour change could

explain sub-exponential growth of EVD and concluded that greater epidemic control plus limited community mixing decrease the size of an infectious wave [11]. Upadhyay and Roy [125] modelled the spatio-temporal dynamics of EVD with populations moving in the x and y directions with diffusion terms that represent random and uniform movements. They associated control measures such as contact tracing or patients' isolation and concluded that the spatio-temporal structure of the system can be reduced by diffusion terms [125]. However, none of these models associated the economic status of the affected countries to the spatial spread of EVD and our work is uniquely posed to address such an important observation.

Many economic migrants never return to their country of departure (or origin) but some do [177]. We first focus on a model for one way economic migration and then we consider a two way migration where migrants return to their country of origin for non economic reasons. We model the effect of low income on EVD dynamics through a one way economic migration of populations, by assuming that the increasing number of EVD cases contributes to a decrease of the GNI of the affected countries. We also model a two way migration model to evaluate the effects of the different scenarios on EVD dynamics in the two patches.

The word income refers to the per capita GNI in this work. We consider that movements of individuals between two patches, from patch 2 to patch 1, are due to a lower income in patch 2 and a higher income in patch 1. We consider that when the income is close to zero in at least one patch, there is no movement of individuals. In fact, if the income in patch 2 is zero, people cannot afford migrating since migration has a minimum cost, related to transport for example. If the income in patch 1 is zero, then the patch is not attractive economically. So, assuming that income decreases when the number of EVD infected individuals increases and based on the equation in [98] that links disease and income, we model the rate of change of income as

$$\frac{\mathrm{d}M_i}{\mathrm{d}t} = r_i M_i \left(\pi_i \left(1 - \frac{I_i}{\epsilon_i + I_i} \right) - M_i \right) \quad \text{for} \quad i = 1, 2$$

where M_i is the per capita income in patch i, π_i is the maximum income earned in the absence of EVD and ϵ_i is the half saturation constant in patch i. We define $r_i (r_i > 0)$ as the income growth rate per unit currency invested.

We assume that the unit currency is $ in this work. The work presented in this chapter is arranged as follows: we first analyse the one way migration model for which is presented in Section 6.2 the model formulation, in Section 6.3 and Section 6.4 respectively the analysis of the disease free equilibrium and the endemic equilibrium and in Section 6.5 the bifurcation analysis. The two way migration model is presented and analysed in Section 6.6. Numerical simulations are presented in Section 6.7 and we end with concluding remarks in Section 6.8.

6.2 One way migration model

The $SEIRD$ (Susceptible-Exposed-Infected-Recovered-Deceased) model framework is used to model the economic migration of populations from a low income country represented by patch 2 to a higher income country represented by patch 1 and vice versa. Let $i \in \{1,2\}$ be the index of each considered patch. Susceptible individuals in patch i (S_i), recruited at a rate Λ_i, get in contact with individuals infected by EVD (I_i) in the same patch and become exposed individuals (E_i). EVD transmission rate in patch i is β_i which is the product of the number of contacts an individual in patch i can have multiplied by the probability for the contact to be infectious. After the incubation period in patch i, exposed individuals progress at a rate δ_i to become infected and are assumed not to recover or die from EVD at this stage. Infected individuals can either recover at a rate α_i and join the recovered class R_i or may die because of the disease at a rate ϕ_i and join the compartment of the deceased D_i. Bodies of the deceased are assumed to be infectious and buried at a rate ρ_i. Assuming that the income in patch 1 is higher than the one in patch 2, we assume that susceptible and recovered individuals move from patch 2 to patch 1 at a rate θ_{12} in order to earn more income and improve their living standards. Exposed individuals move from patch 2 to patch 1 at a rate σ_{12} which is different from θ_{12} with $\sigma_{12} \leq \theta_{12}$. The difference is due to the disease status of the exposed that influences their probability of migrating. We also assume that visitors from patch 2 do not leave patch 1 during the modelling time. We also assume that in the total absence of income ($M_2 = M_1 = 0$), there is no movement of individuals between the patches ($\theta_{12} = \sigma_{12} = 0$). In this case the model in each patch is similar to the model developed and analysed in [137]. In this work, the

force of infection in patch i is given by

$$\lambda_i = \beta_i \Big(I_i + \eta_i D_i \Big).$$

The income-ratio m or GNI-ratio is the ratio of the income in patch 2 to the income in patch 1 (M_2/M_1). During EVD outbreak of $2013-2016$, which corresponds to the modelling time in this chapter, Sierra Leone and Guinea had the highest GNI among the three West African countries affected and represented then the most attractive countries economically.

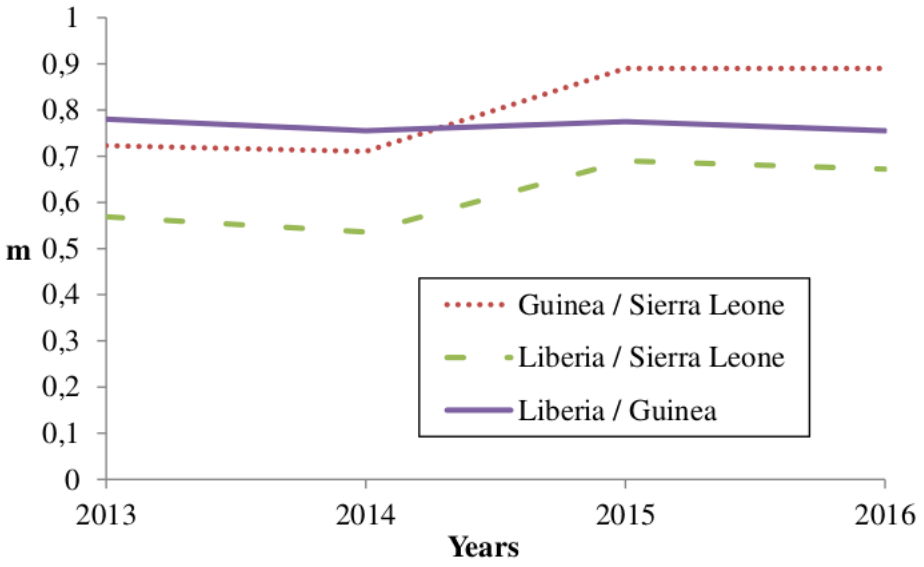

Figure 6.2: GNI-ratio of the countries affected by EVD in $2013-2016$.

We noted that the GNI-ratio did not vary that much during EVD outbreak of $2013-2016$ as shown in Figure 6.2, plotted with data from [2]. So, we consider m as a constant during the modelling time with, $0 < m \leq 1$, since the income in patch 1 is assumed to be higher than the income in patch 2. The constant m may be viewed as the economic gap between the considered economies. Low values of m (close to zero) indicate two distant economies while higher values (close to one) indicate very close economies in terms of their GNI. Diseases or natural catastrophes that tend to impact the economy of a country affect the value of m. All the parameters used in the model and their descriptions are given in Table 6.1.

Parameter	Description	Unit
Λ_1	Recruitment rate in patch 1	individual.day^{-1}
Λ_2	Recruitment rate in patch 2	individual.day^{-1}
β_1	EVD transmission rate in patch 1	individual^{-1}.day^{-1}
β_2	EVD transmission rate in patch 2	individual^{-1}.day^{-1}
$1/\delta_1$	EVD incubation period in patch 1	day
$1/\delta_2$	EVD incubation period in patch 2	day
α_1	Recovery rate of EVD infected in patch 1	day^{-1}
α_2	Recovery rate of EVD infected in patch 2	day^{-1}
ϕ_1	EVD related death rate in patch 1	day^{-1}
ϕ_2	EVD related death rate in patch 2	day^{-1}
μ	Natural death rate	day^{-1}
ρ_1	Burial rate of EVD deceased in patch 1	day^{-1}
ρ_2	Burial rate of EVD deceased in patch 2	day^{-1}
θ_{ji}	Migration rate of susceptible and recovered individuals from patch i to patch j	day^{-1}
σ_{ji}	Migration rate of exposed individuals from patch i to patch j	day^{-1}
π_1	Maximum income in the absence of EVD in patch 1	\$.individual^{-1}
π_2	Maximum income in the absence of EVD in patch 2	\$.individual^{-1}
η_1	Infectivity of the deceased in patch 1	
η_2	Infectivity of the deceased in patch 2	
r_1	Income growth rate in patch 1	\$$^{-1}$.day^{-1}
r_2	Income growth rate in patch 2	\$$^{-1}$.day^{-1}
ϵ_1	Half saturation constant in patch 1	individuals
ϵ_2	Half saturation constant in patch 2	individuals

Table 6.1: Parameters' description for EVD economic migration model.

The one way flow of individuals in the model is represented by Figure 6.3 and by the system of differential equations (6.2.1)-(6.2.10). Since the recovered individuals do not contribute to EVD transmission, their dynamics is decoupled from other variables in the closed system and their equation omitted.

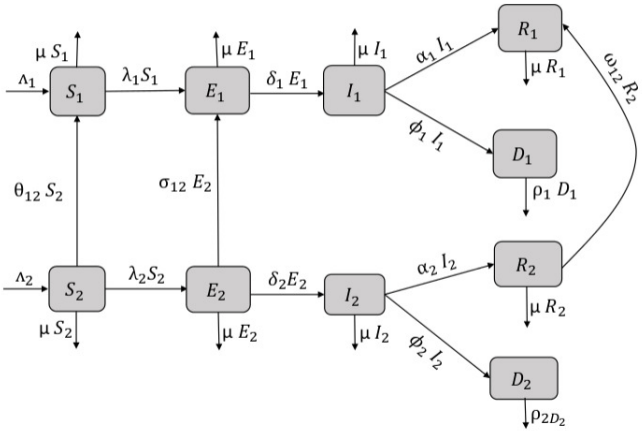

Figure 6.3: Flow chart diagram of EVD economic migration model.

$$\frac{dS_1}{dt} = \Lambda_1 - \left(\lambda_1 + \mu\right) S_1 + (1-m)\,\theta_{12}\,S_2, \tag{6.2.1}$$

$$\frac{dS_2}{dt} = \Lambda_2 - \left(\lambda_2 + \mu + (1-m)\,\theta_{12}\right) S_2, \tag{6.2.2}$$

$$\frac{dE_1}{dt} = \lambda_1\,S_1 - Q_1\,E_1 + (1-m)\,\sigma_{12}E_2, \tag{6.2.3}$$

$$\frac{dE_2}{dt} = \lambda_2\,S_2 - Q_2\,E_2 - (1-m)\,\sigma_{12}E_2, \tag{6.2.4}$$

$$\frac{dI_1}{dt} = \delta_1\,E_1 - Q_3\,I_1, \tag{6.2.5}$$

$$\frac{dI_2}{dt} = \delta_2\,E_2 - Q_4\,I_2, \tag{6.2.6}$$

$$\frac{dD_1}{dt} = \phi_1\,I_1 - \rho_1\,D_1, \tag{6.2.7}$$

$$\frac{dD_2}{dt} = \phi_2\,I_2 - \rho_2\,D_2, \tag{6.2.8}$$

$$\frac{dM_1}{dt} = r_1\,M_1\left(\pi_1\left(1 - \frac{I_1}{\epsilon_1 + I_1}\right) - M_1\right), \tag{6.2.9}$$

$$\frac{dM_2}{dt} = r_2\,M_2\left(\pi_2\left(1 - \frac{I_2}{\epsilon_2 + I_2}\right) - M_2\right), \tag{6.2.10}$$

where $Q_1 = \mu + \delta_1, Q_2 = \mu + \delta_2, Q_3 = \mu + \alpha_1 + \phi_1$ and $Q_4 = \mu + \alpha_2 + \phi_2$. The initial conditions are

$$S_1(0) > 0, E_1(0) \geq 0, I_1(0) \geq 0, D_1(0) \geq 0, M_1(0) > 0,$$

$$S_2(0) > 0, E_2(0) \geq 0, I_2(0) \geq 0, D_2(0) \geq 0, M_2(0) > 0.$$

6.2.1 Existence and positivity of solutions

Theorem 6.2.1. *The invariant region is given by*

$$\Theta = \left\{\Pi \in \mathbb{R}^{10}_{+} : S + E + I \leq \frac{\Lambda}{\mu}, D_1 \leq \frac{\Lambda\,\phi_1}{\mu\,\rho_1}, D_2 \leq \frac{\Lambda\,\phi_2}{\mu\,\rho_2}, M_1 \leq \hat{M}_1, M_2 \leq \hat{M}_2\right\}$$

where $\Pi = \left(S_1, S_2, E_1, E_2, I_1, I_2, D_1, D_2, M_1, M_2\right)$, $S = S_1 + S_2$, $E = E_1 + E_2$,

$I = I_1 + I_2$, $\Lambda = \Lambda_1 + \Lambda_2$, $\hat{M}_i = \pi_i\left[1 - \left(1 - \frac{\pi_i}{M_i(0)}\right)\exp\left(-r_i\pi_i t\right)\right]^{-1}$,

$i = 1, 2$.

Proof. We set $H(t) = S(t) + E(t) + I(t)$. Adding equations (6.2.1)-(6.2.6) yields $\frac{dH(t)}{dt} \leq \Lambda - \mu H(t)$. We solve the corresponding differential equation and use Gronwall inequality to obtain $H(t) \leq \frac{\Lambda}{\mu}$. Since $I_i(t) < H(t) \leq \frac{\Lambda}{\mu}$ for $i \in \{1,2\}$, we obtain respectively from equations (6.2.7) and (6.2.8)

$$\frac{dD_1}{dt} \leq \phi_1 \frac{\Lambda}{\mu} - \rho_1 D_1, \tag{6.2.11}$$

$$\frac{dD_2}{dt} \leq \phi_2 \frac{\Lambda}{\mu} - \rho_2 D_2, \tag{6.2.12}$$

resulting in the solutions $D_1 \leq \frac{\Lambda \phi_1}{\mu \rho_1}$ and $D_2 \leq \frac{\Lambda \phi_2}{\mu \rho_2}$.

Since

$$1 - \frac{I_i}{1 + I_i} \leq 1, \quad \text{for} \quad i = 1,2 \tag{6.2.13}$$

from equations (6.2.9) and (6.2.10) we have

$$\frac{dM_1}{dt} \leq -r_1 M_1 \Big(M_1 - \pi_1 \Big), \tag{6.2.14}$$

$$\frac{dM_2}{dt} \leq -r_2 M_2 \Big(M_2 - \pi_2 \Big). \tag{6.2.15}$$

Solving the differential equations corresponding to equations (6.2.14) and (6.2.15) and applying Gronwall inequality yields

$$M_1 \leq \pi_1 \left[1 - \left(1 - \frac{\pi_1}{M_1(0)} \right) \exp\left(- r_1 \pi_1 t \right) \right]^{-1},$$

$$M_2 \leq \pi_2 \left[1 - \left(1 - \frac{\pi_2}{M_2(0)} \right) \exp\left(- r_2 \pi_2 t \right) \right]^{-1}.$$

□

Theorem 6.2.2. *All the solutions of the system* (6.2.1)-(6.2.10) *are non-negative for non-negative initial conditions.*

Proof. Using equation (6.2.1) and setting $A_1(t) = \lambda_1 + \mu$, we obtain

$$\dot{S_1} \geq \Lambda_1 - A_1(t)\, S_1. \tag{6.2.16}$$

Solving equation (6.2.16) for all $t \geq 0$ yields

$$S_1(t) \geq \exp\left(-\int_0^t A_1(u)du\right)\left(S_1(0) + \int_0^t \Lambda_1 \exp\left(\int_0^s A_1(u)du\right)ds\right).$$

So, $S_1(t) > 0$ since $S_1(0) > 0$. Similarly, we set $A_2(t) = \lambda_2 + \mu + \theta_{12}(1-m)$ and from equation (6.2.2) we obtain

$$S_2(t) \geq \exp\left(-\int_0^t A_2(u)du\right)\left(S_2(0) + \int_0^t \Lambda_2 \exp\left(\int_0^s A_2(u)du\right)ds\right) > 0.$$

Equations (6.2.9) and (6.2.10) imply

$$\frac{dM_1}{dt} \geq -r_1 M_1^2, \tag{6.2.17}$$

$$\frac{dM_2}{dt} \geq -r_2 M_2^2, \tag{6.2.18}$$

since $\pi_i\left(1 - \frac{I_i}{1+I_i}\right) > 0$ for $i = 1, 2$.

Applying Gronwall inequality to equations (6.2.17) and (6.2.18) yields $M_1(t) \geq r_1 t + \frac{1}{M_1(0)} > 0$ and $M_2(t) \geq r_2 t + \frac{1}{M_2(0)} > 0$. So, M_1 and M_2 are positive provided $M_1(0)$ and $M_2(0)$ are positive.

System (6.2.3)-(6.2.8) can be rewritten as $\frac{dG(t)}{dt} = T\,G(t)$ where

$$G(t) = \left[E_1(t), E_2(t), I_1(t), I_2(t), D_1(t), D_2(t)\right]'$$

with

$$T = \begin{bmatrix} -Q_1 & (1-m)\sigma_{12} & \beta_1 S_1 & 0 & \beta_1 \eta_1 S_1 & 0 \\ 0 & -(1-m)\sigma_{12} - Q_2 & 0 & \beta_2 S_2 & 0 & \beta_2 \eta_2 S_2 \\ \delta_1 & 0 & -Q_3 & 0 & 0 & 0 \\ 0 & \delta_2 & 0 & -Q_4 & 0 & 0 \\ 0 & 0 & \phi_1 & 0 & -\rho_1 & 0 \\ 0 & 0 & 0 & \phi_2 & 0 & -\rho_2 \end{bmatrix}.$$

Since all the off diagonal elements of T are non-negative, T is a Metzler matrix and G is monotone and positive, see [163]. So, $\mathbb{R}^6_+$ is invariant under $\frac{dG(t)}{dt}$ and $G(t)$ is non-negative.
Finally, $E_1, E_2, I_1, I_2, D_1, D_2$ are non-negative and we can conclude that all the solutions of the system (6.2.1)-(6.2.10) are non-negative. □

6.3 Disease free equilibrium

The disease free equilibrium (DFE) is given by $E^0 = \left(S_1^0, S_2^0, 0, 0, 0, 0, 0, 0, \pi_1, \pi_2\right)$ where

$$S_1^0 = \frac{\Lambda_1}{\mu} + \frac{\Lambda_2\,\theta_{12}\,(1-m)}{\mu\left(\mu+\theta_{12}\,(1-m)\right)} \quad \text{and} \quad S_2^0 = \frac{\Lambda_2}{\left(\mu+\theta_{12}\,(1-m)\right)}.$$

At equilibrium the DFE, all the differential equations of the system (6.2.1)-(6.2.10) are equal to zero with $I_1 = I_2 = D_1 = D_2 = 0$. We solve equation (6.2.1) for S_1 to get S_1^0 and equation (6.2.2) for S_2 to get S_2^0.
At the DFE,

$$\begin{aligned}(6.2.1) &\Longleftrightarrow \frac{\mathrm{d}S_1}{\mathrm{d}t} = 0,\\ &\Longrightarrow S_1 = S_1^0,\\ (6.2.2) &\Longleftrightarrow \frac{\mathrm{d}S_2}{\mathrm{d}t} = 0,\\ &\Longrightarrow S_2 = S_2^0.\end{aligned}$$

By using the next generation matrix method to compute the reproduction number R_0 of the system (6.2.1)-(6.2.10), we obtain

the renewal matrix F_e and the transfert matrix V_e as

$$F_e = \begin{bmatrix} 0 & 0 & \beta_1 S_1 & 0 & \beta_1\eta_1 S_1 & 0\\ 0 & 0 & 0 & \beta_2 S_2 & 0 & \beta_2\eta_2 S_2\\ 0 & 0 & 0 & 0 & 0 & 0\\ 0 & 0 & 0 & 0 & 0 & 0\\ 0 & 0 & 0 & 0 & 0 & 0\\ 0 & 0 & 0 & 0 & 0 & 0 \end{bmatrix}$$

$$V_e = \begin{bmatrix} Q_1 & (-1+m)\sigma_{12} & 0 & 0 & 0 & 0\\ 0 & (1-m)\sigma_{12}+Q_2 & 0 & 0 & 0 & 0\\ -\delta_1 & 0 & Q_3 & 0 & 0 & 0\\ 0 & -\delta_2 & 0 & Q_4 & 0 & 0\\ 0 & 0 & -\phi_1 & 0 & \rho_1 & 0\\ 0 & 0 & 0 & -\phi_2 & 0 & \rho_2 \end{bmatrix}.$$

The spectral radius of the matrix $F_e.V_e^{-1}$ gives

$$R_0 = \max\left\{R_1, R_2\right\}$$

where

$$R_1 = \frac{S_1^0\,\beta_1\,\delta_1}{Q_1\,Q_3\,\rho_1}\left(\rho_1+\eta_1\,\phi_1\right) \quad \text{and} \quad R_2 = \frac{S_2^0\,\beta_2\,\delta_2\,(\rho_2+\eta_2\,\phi_2)}{Q_4\,\rho_2\left(Q_2+(1-m)\,\sigma_{12}\right)}.$$

R_1 is the reproduction number in patch 1 and R_2 is the reproduction number in patch 2. The stability of the DFE for a multi-city compartmental model is extensively discussed by Van Den Driessche and Arino in [92], so that we have the following result

Theorem 6.3.1. *The DFE of system* (6.2.1)-(6.2.10) *is locally asymptotically stable whenever* $R_0 < 1$ *and unstable otherwise.*

6.4 Endemic equilibrium

The endemic equilibrium is given by:

$$E^* = \left(S_1^*, S_2^*, E_1^*, E_2^*, I_1^*, I_2^*, D_1^*, D_2^*, M_1^*, M_2^*\right)$$

where

$$\begin{aligned}
S_1^* &= \frac{\rho_1\left((1-m)\,\theta_{12}\,(\Lambda_1+\Lambda_2)\,\rho_2 + I_2^*\,\rho_1\,\beta_2\,\Lambda_1\,(\rho_2+\eta_2\,\phi_2)\right)}{\rho_2\left(\mu+(1-m)\,\theta_{12}\right)\left(\mu\,\rho_1+\beta_1\,I_1^*\,(\rho_1+\eta_1\,\phi_1)\right)},\\
S_2^* &= \frac{\Lambda_2\,\rho_2\,S_2^0}{\left(\Lambda_2+S_2^0\,I_2^*\,\beta_2\,(\rho_2+\eta_2\,\phi_2)\right)}, E_1^* = \frac{Q_3}{\delta_1}\,I_1^*, E_2^* = \frac{Q_4}{\delta_2}\,I_2^*, \qquad (6.4.1)\\
I_2^* &= \left(R_2-1\right)\frac{\beta_2\,(\rho_2+\eta_2\,\phi_2)}{\rho_2\left(\mu+(1-m)\,\theta_{12}\right)}, D_1^* = \frac{\phi_1}{\rho_1}\,I_1^*, D_2^* = \frac{\phi_2}{\rho_2}\,I_2^*,\\
M_1^* &= \frac{\epsilon_1\,\pi_1}{\epsilon_1+I_1^*}, M_2^* = \frac{\epsilon_2\,\pi_2}{\epsilon_2+I_2^*}.
\end{aligned}$$

To obtain the endemic equilibrium points, we solve equation (6.2.10) for M_2 to obtain M_2^*, we solve equation (6.2.9) for M_1 to obtain M_1^*. We solve equation (6.2.7) for D_1 to obtain D_1^* and equation (6.2.8) for D_2 to get D_2^*. We solve equation (6.2.5) for E_1 to obtain E_1^* and equation (6.2.6) for E_2 to get E_2^*. We solve equation (6.2.3) for S_1 to obtain S_1^* and equation (6.2.4) for S_2 to get S_2^*. We solve equation (6.2.2) for I_2 to obtain I_2^*.
At the endemic equilibrium,

$$
\begin{aligned}
(6.2.10) &\iff \frac{\mathrm{d}S_1}{\mathrm{d}t} = 0, \\
&\implies M_2 = M_2^*, \\
(6.2.9) &\iff \frac{\mathrm{d}M_1}{\mathrm{d}t} = 0, \\
&\implies M_1 = M_1^*, \\
(6.2.7) &\iff \frac{\mathrm{d}D_1}{\mathrm{d}t} = 0, \\
&\implies D_1 = D_1^*, \\
(6.2.8) &\iff \frac{\mathrm{d}D_2}{\mathrm{d}t} = 0, \\
&\implies D_2 = D_2^*, \\
(6.2.5) &\iff \frac{\mathrm{d}I_1}{\mathrm{d}t} = 0, \\
&\implies E_1 = E_1^*, \\
(6.2.6) &\iff \frac{\mathrm{d}I_2}{\mathrm{d}t} = 0, \\
&\implies E_2 = E_2^*, \\
(6.2.3) &\iff \frac{\mathrm{d}E_1}{\mathrm{d}t} = 0, \\
&\implies S_1 = S_1^*, \\
(6.2.4) &\iff \frac{\mathrm{d}E_2}{\mathrm{d}t} = 0, \\
&\implies S_2 = S_2^*, \\
(6.2.2) &\iff \frac{\mathrm{d}S_2}{\mathrm{d}t} = 0, \\
&\implies I_2 = I_2^*.
\end{aligned}
$$

I_1^* is a positive solution of the polynomial (6.4.2). By replacing all the state variables in equation (6.2.1) by their expressions at equilibrium from system (6.4.1), we obtain,

$$P(I_1^*) = a_0 I_1^{*2} + a_1 I_1^* + a_2 \tag{6.4.2}$$

where

$$a_0 = \frac{R_1 R_2}{S_1^0 S_2^0 \delta_1} \rho_1 \rho_2 Q_1^2 Q_3^2 Q_4 \Big(Q_2 + (1-m)\sigma_{12}\Big)^2,$$
$$a_1 = \Big(R_a - 1\Big) \psi_2 \Big(\psi_3 \mu Q_1 Q_3 \rho_1 + (1-m)\sigma_{12} \Lambda_2 \psi_1\Big),$$
$$a_2 = \psi_0 \Big(1 - R_2\Big),$$

where $\psi_1 = \beta_1 \delta_1 \Big(\rho_1 + \phi_1 \eta_1\Big), \psi_2 = \beta_2 \delta_2 \Big(\rho_2 + \phi_2 \eta_2\Big),$ $\psi_3 = \Big(Q_2 + (1-m)\sigma_{12}\Big)$, $\psi_0 = \mu \rho_1 \delta_1 \rho_2 Q_4 (1-m)\sigma_{12} \Big(\mu + (1-m)\theta_{12}\Big) \psi_3$,

$$R_a = \frac{\psi_3 \psi_1 Q_4 \rho_2 \psi_2 \Lambda_1 + (1-m)(\theta_{12} + \mu\sigma_{12})}{\psi_2 \Big(\psi_3 \mu Q_1 Q_3 \rho_1 + (1-m)\sigma_{12} \Lambda_2 \psi_1\Big)}.$$

Theorem 6.4.1. *Polynomial* (6.4.2) *admits:*

(i) one positive root if $R_2 > 1$,

(ii) zero or two positive roots if $R_2 < 1$.

Proof. Descartes' Law of signs helps to determine the number of positive roots of polynomial (6.4.2). We count the number of sign changes of the coefficients of the polynomial and the value obtained is the maximum number of positive roots of the polynomial. The coefficient a_0 is always positive. The coefficient a_2 is positive when $R_2 < 1$ and negative when $R_2 > 1$. The maximum number of sign changes of the coefficients of the polynomial (6.4.2) is 2 if $a_1 < 0$ and zero if $a_1 > 0$ when $R_2 < 1$. When $R_2 > 1$, the maximum number of sign changes of the polynomial (6.4.2) is one. □

From equations in (6.4.1), we can say that $R_2 > 1$ guarantees the existence of a unique endemic equilibrium point in patch 2 so that I_1^* and I_2^* co-exist in this case. When $R_2 < 1$ there is no endemic equilibrium point in patch 2 whereas up to two positive values of I_1^* can exist. In this case, controlling EVD in patch 1 is then more complex as multiple endemic equilibria could exist. So, the existence of positive values of I_1^* relies more on values of R_2 and not on values of R_1 as we could have expected. In fact, movements of exposed individuals from patch 2 to patch 1 continuously feed patch 1 with exposed individuals that later become infectious, so that irrespective of the value of R_1, the number of infected individuals in patch 1 is positive.

So, whether there are secondary infections in patch 1 or not, movements of exposed individuals into this patch guarantees always the existence of an endemic equilibrium. EVD control in patch 1 should then first target immigration's control and its consequences We notice that in the absence of movements of exposed individuals ($\sigma_{12} = 0$), polynomial (6.4.2) becomes

$$P(I_1^*) = \left(b_0\, I_1^* + b_1\right) I_1^*$$

and admits a unique positive root with

$$\begin{aligned} b_0 &= \frac{R_1\, R_2}{S_1^0\, S_2^0}\, \rho_1\, \rho_2\, Q_1^2\, Q_2^2\, Q_3^2\, Q_4, \\ b_1 &= \psi_2\, Q_1\, Q_2\, Q_3\, \mu\, \rho_1 \left(R_b - 1\right), \\ R_b &= \frac{Q_2\, \psi_1\, Q_4\, \rho_2\, \psi_2\, \Lambda_1 + (1-m)\, \theta_{12}}{\psi_2\, Q_1\, Q_2\, Q_3\, \mu\, \rho_1}. \end{aligned}$$

In fact, movements of exposed individuals from patch 2 to patch 1 continuously feed patch 1 with exposed individuals that later become infectious, so that irrespective of the value of R_1, the number of infected individuals in patch 1 is positive. So, whether there are secondary infections in patch 1 or not, movements of exposed individuals into this patch guarantees always the existence of an endemic equilibrium. EVD control in patch 1 should then first target immigration's control and its consequences.

Theorem 6.4.2. *The endemic equilibrium E^* exists when $R_2 > 1$ and is locally asymptotically stable.*

Proof. The jacobian matrix J_{E^*} of system (6.2.1)-(6.2.10) at the endemic equilibrium is given by

$$J_{E^*} = \left[\begin{array}{c|c|c} U & V & 0_{6\times 2} \\ \hline 0_{4\times 4} & W & A \end{array}\right]$$

where

$$U = \begin{bmatrix} \psi_4 & (1-m)\theta_{12} & 0 & 0 \\ 0 & \psi_5 & 0 & 0 \\ \beta_1(I_1^* + \eta_1 D_1^*) & 0 & -Q_1 & (1-m)\sigma_{12} \\ 0 & \beta_2(I_2^* + \eta_2 D_2^*) & 0 & -(1-m)\sigma_{12} - Q_2 \\ 0 & 0 & \delta_1 & 0 \\ 0 & 0 & 0 & \delta_2 \end{bmatrix},$$

$$V = \begin{bmatrix} -S_1^*\beta_1 & 0 & -S_1^*\beta_1\eta_1 & 0 \\ 0 & -S_2^*\beta_2 & 0 & -S_2^*\beta_2\eta_2 \\ S_1^*\beta_1 & 0 & S_1^*\beta_1\eta_1 & 0 \\ 0 & S_2^*\beta_2 & 0 & S_2^*\beta_2\eta_2 \\ -Q_3 & 0 & 0 & 0 \\ 0 & -Q_4 & 0 & 0 \end{bmatrix}, W = \begin{bmatrix} \phi_1 & 0 & -\rho_1 & 0 \\ 0 & \phi_2 & 0 & -\rho_2 \\ \psi_6 & 0 & 0 & 0 \\ 0 & \psi_8 & 0 & 0 \end{bmatrix},$$

$$A = \begin{bmatrix} 0 & 0 \\ 0 & 0 \\ \psi_7 & 0 \\ 0 & \psi_9 \end{bmatrix},$$

$0_{i\times j}$ is the zero matrix of order i, j with

$$\begin{aligned}
\psi_4 &= -\mu - \beta_1\left(I_1^* + \eta_1 D_1^*\right), \\
\psi_5 &= -\mu - \beta_2\left(I_2^* + \eta_2 D_2^*\right) - (1-m)\,\theta_{21}, \\
\psi_6 &= -\frac{\epsilon_1\, r_1 \pi_1 M_1^*}{\left(1 + I_1^*\right)^2}, \\
\psi_7 &= -r_1 M_1^* - r_1\left(M_1^* - \frac{\epsilon_1\,\pi_1}{\epsilon_1 + I_1^*}\right), \\
\psi_8 &= -\frac{\epsilon_2\, r_2 \pi_2 M_2^*}{\left(1 + I_2^*\right)^2}, \\
\psi_9 &= -r_2 M_2^* - r_2\left(M_2^* - \frac{\epsilon_2\,\pi_2}{\epsilon_2 + I_2^*}\right).
\end{aligned}$$

From equations (6.2.9) and (6.2.10), we obtain at equilibrium

$$M_1^* = \pi_1\left(1 - \frac{I_1^*}{\epsilon_1 + I_1^*}\right), \tag{6.4.3}$$

$$M_2^* = \pi_2\left(1 - \frac{I_2^*}{\epsilon_2 + I_2^*}\right). \tag{6.4.4}$$

Using equations (6.4.3) and (6.4.4) to simplify ψ_7 and ψ_9 yields
$\psi_7 = -r_1 M_1^* < 0$ and $\psi_9 = -r_2 M_2^* < 0$.
Since J_{E^*} is a block triangular matrix, its diagonal entries are its eigenvalues. Since all the diagonal entries of the matrix J_{E^*} are negative, we can conclude that all the eigenvalues of J_{E^*} are negative and the endemic equilibrium E^* is locally asymptotically stable. □

6.5 Bifurcation analysis

A change of the topological structure of a system is called bifurcation [126]. A bifurcation driven by R_2 is illustrated in Figure 6.4.

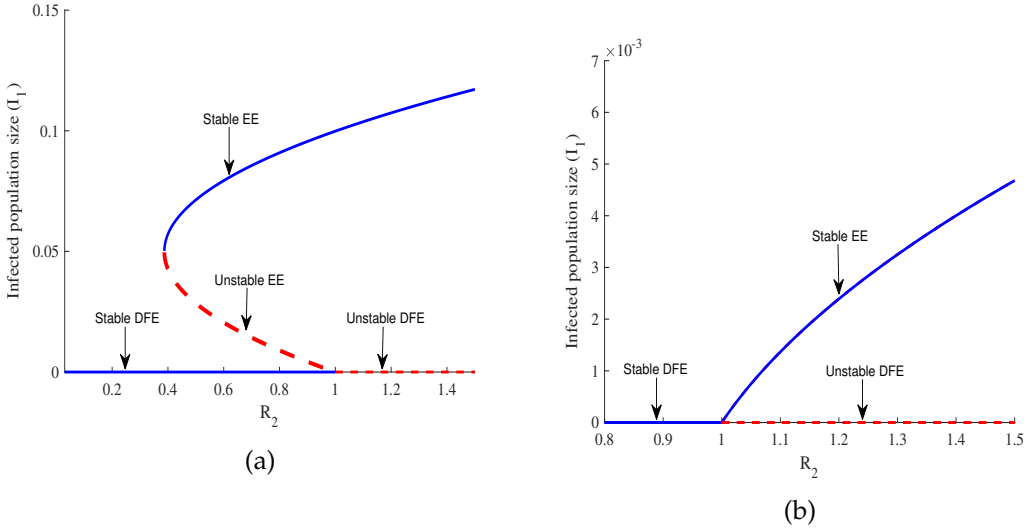

Figure 6.4: Backward bifurcation in (a) for $\Lambda_1 = 6270$, $\Lambda_2 = 5370$, $\beta_1 = 0.525$, $\beta_2 = 0.385$, $\alpha_1 = 0.283$, $\alpha_2 = 0.394$, $\phi_1 = 0.304$, $\phi_2 = 0.373$, $\rho_1 = 0.738$, $\rho_2 = 0.637$, $\eta_1 = 2.78$, $\eta_2 = 2.81$, $\delta_1 = 10^{-6}$, $\delta_2 = 10^{-6}$, $\mu = 0.048$, $\theta_{12} = 0.277$, $\sigma_{12} = 0.637$, $m = 0.7$. Forward bifurcation in (b) for $m = 0.982$.

Figures 6.4(a) and 6.4(b) illustrate the possible number of positive roots of the polynomial (6.4.2) when R_2 is varied. A backward bifurcation is observed in Figure 6.4(a) when $R_2 < 1$ and a forward bifurcation is observed in Figure 6.4(b) when $R_2 > 1$. The complexity of the system of equations (6.2.1)-(6.2.10) makes it difficult to prove the existence of The backward bifurcation but we can observe it thanks to numerical simulations.
The backward bifurcation shows a locally stable DFE and an unstable EE. In any disease control, reaching a globally stable DFE is the main target, but

this is more difficult to realise in the case of a backward bifurcation since the DFE is globally stable only below a threshold $R_t = 1 - \frac{a_1^2}{4\,a_0\,\psi_0}$, whose value might be far from 1. The expression of R_t is obtained by setting to zero the discriminant of the polynomial (6.4.2). The forward bifurcation represented in Figure 6.4(b) offers an easier possibility because reducing R_2 to values less than one is enough in this case to reach a globally stable DFE and is then the preferable scenario for EVD control.

The income-ratio describes the gap between two economies and this gap is considered as the main driving factor of migration in this work. We observe in Figure 6.4 that a backward bifurcation is changed into a forward bifurcation for the chosen parameter values when the value of m is increased. Increasing the value of m corresponds to bringing closer the two economies considered and this can be done by increasing the per capita income in patch 2 for example. This increase of income certainly improves the living condition of people in this patch and reduces their chances of migrating. EVD control becomes easier in this case as exposed individuals can be easily tracked and isolated in both patches. Improving the economy of poor countries exposed to EVD in order to stop or limit the migration of individuals exposed to the disease is a useful measure to be implemented by all governments, especially governments of rich countries because migration of infected individuals might cause an EVD outbreak on their sol.

6.6 Two way migration

Some economic migrants return for short or long stay to their home countries. These returns are sometimes due to one of the following reasons: the migrants couldn't find a job in the host country, they have simply realised that the reality of the host country do not meet their initial expectations or they return to visit their families. Migrants transfer savings, education and skills to their home country when they return after a stay in a more developed country [177]. We assume in this case a two way migration of populations for which susceptible migrants from patch 1 return to patch 2 at the rate θ_{21} and exposed migrants return at a rate σ_{21} after a stay in patch 1. The flow chart diagram representing the two ways migration is given in Figure 6.5.

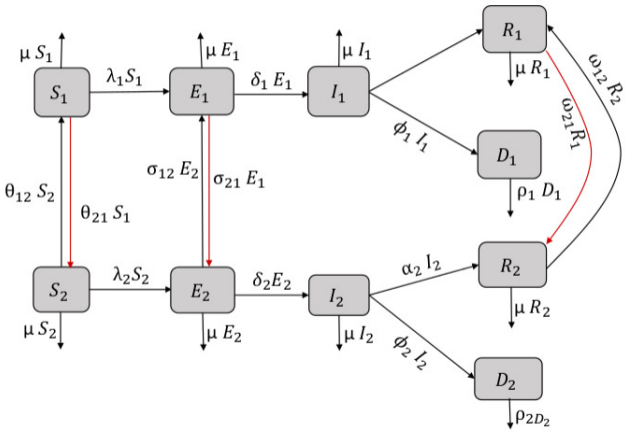

Figure 6.5: Flow chart diagram of the two way migration model

$$\frac{dS_1}{dt} = \Lambda_1 - \left(\lambda_1 + \mu + \theta_{21}\right) S_1 + (1-m)\,\theta_{12}\,S_2, \tag{6.6.1}$$

$$\frac{dS_2}{dt} = \Lambda_2 - \left(\lambda_2 + \mu + (1-m)\,\theta_{12}\right) S_2 + \theta_{21}\,S_1, \tag{6.6.2}$$

$$\frac{dE_1}{dt} = \lambda_1\,S_1 - \left(Q_1 + \sigma_{21}\right) E_1 + (1-m)\,\sigma_{12}E_2, \tag{6.6.3}$$

$$\frac{dE_2}{dt} = \lambda_2\,S_2 - Q_2\,E_2 - (1-m)\,\sigma_{12}E_2 + \sigma_{21}\,E_1, \tag{6.6.4}$$

$$\frac{dI_1}{dt} = \delta_1\,E_1 - Q_3\,I_1, \tag{6.6.5}$$

$$\frac{dI_2}{dt} = \delta_2\,E_2 - Q_4\,I_2, \tag{6.6.6}$$

$$\frac{dD_1}{dt} = \phi_1\,I_1 - \rho_1\,D_1, \tag{6.6.7}$$

$$\frac{dD_2}{dt} = \phi_2\,I_2 - \rho_2\,D_2, \tag{6.6.8}$$

$$\frac{dM_1}{dt} = r_1\,M_1\left(\pi_1\left(1 - \frac{I_1}{\epsilon_1 + I_1}\right) - M_1\right), \tag{6.6.9}$$

$$\frac{dM_2}{dt} = r_2\,M_2\left(\pi_2\left(1 - \frac{I_2}{\epsilon_2 + I_2}\right) - M_2\right). \tag{6.6.10}$$

Solutions of the system (6.6.1)-(6.6.10) exist and are positive and the proof follows the proof of Theorem 6.2.1.

At DFE, $E_g^0 = \left(S_1^g, S_2^g, 0, 0, 0, 0, 0, 0, \pi_1, \pi_2\right)$ where

$$S_1^g = \frac{(1+\Lambda_2)(1-m)\,\theta_{21} + \mu}{\mu\left(\mu + \theta_{12} + (1-m)\,\theta_{21}\right)} \quad \text{and} \quad S_2^g = \frac{(\mu+\theta_{12})\,\Lambda_2 + \theta_{12}\,\Lambda_1}{\mu\left(\mu + \theta_{12} + (1-m)\,\theta_{21}\right)}.$$

We first set $E_1 = E_2 = I_1 = I_2 = D_1 = D_2 = 0$. Then, we solve equation (6.6.1) for S_1 to get S_1^g and we solve equation (6.6.2) for S_2 to obtain S_2^g. We solve equation (6.6.9) for M_1 to obtain π_1 and equation (6.6.10) for M_2 to obtain π_2.

The next generation matrix method [115] is used to compute the reproduction number which is the largest eigenvalue of the product $F_g.(V_g)^{-1}$ where F_g is the renewal matrix and V_g is the transfer matrix.

We set $\left(F_g.(V_g)^{-1}\right) = \left(a_{ij}\right)_{i,j\in\{1,\ldots,6\}}$ where $a_{ij} = 0 \quad \forall\, i,j \in \{1,\ldots,6\}$, except

$$a_{11} = \frac{Q_1}{\chi_1} S_1^g\,\delta_1\,\psi_3, \qquad a_{21} = \frac{\delta_2}{\chi_2} S_2^g\,\sigma_{21},$$
$$a_{12} = \frac{S_1^g\,\delta_1}{\chi_1}(1-m)\,\sigma_{12}, \qquad a_{22} = \frac{\delta_2}{\chi_2} S_2^g\left(Q_1 + \sigma_{21}\right),$$
$$a_{13} = \frac{S_1^g\,\delta_1}{Q_3\,\rho_1}, \qquad a_{24} = \frac{S_2^g\,\delta_2}{Q_4\,\rho_2\,Q_2},$$
$$a_{15} = \frac{S_1^g\,\beta_1\,\eta_1}{\rho_1}, \qquad a_{26} = \frac{S_2^g\,\beta_2\,\eta_2}{\rho_2},$$

where $\chi_1 = Q_3\,\rho_1\left((1-m)\,\sigma_{12}\,Q_1 + (\sigma_{21}+Q_1)\,Q_2\right)$ and

$\chi_2 = Q_4\,\rho_2\left(\sigma_{21}\,Q_2 + Q_1\,\psi_3\right)$.

The reproduction number R_0^g in this case is

$$R_0^g = \max\left\{R_1^g, R_2^g\right\}$$

where $R_1^g = \frac{1}{2}\left[a_{11} + a_{22} + \sqrt{\Delta_g}\right]$, $R_2^g = \frac{1}{2}\left[a_{11} + a_{22} - \sqrt{\Delta_g}\right]$ with $\Delta_g = 4\,a_{12}\,a_{21} + (a_{11} - a_{22})^2$.

Since $a_{ij} \geq 0 \quad \forall\, i,j$, $R_1^g \geq R_2^g$ and the reproduction number is $R_0^g = R_1^g$.

The endemic equilibrium is given by

$E^{**} = \left(S_1^{**}, S_2^{**}, E_1^{**}, E_2^{**}, I_1^{**}, I_2^{**}, D_1^{**}, D_2^{**}, M_1^{**}, M_2^{**}\right)$ where

$$S_1^{**} = \frac{\rho_1 \left(I_1^{**}\, Q_3\, Q_2\, (Q_1 + \sigma_{21}) - \left(1 - m\, I_2^{**}\, Q_4\, Q_1\, \sigma_{21}\right)\right)}{I_1^{**}\, \beta_1\, Q_1\, Q_2\, (\rho_1 + \delta_1\, \eta_1)}, \; E_1^{**} = \frac{Q_3}{\delta_1}\, I_1^{**},$$
$$S_2^{**} = \frac{\rho_2 \left(-I_1^{**}\, Q_3\, \sigma_{21} + I_2^{**}\, Q_4\, Q_1 \left((1-m)\, \sigma_{21} + Q_2\right)\right)}{I_2^{**}\, \beta_2\, Q_1\, Q_2\, (\rho_2 + \delta_2\, \eta_2)}, \; E_2^{**} = \frac{Q_4}{\delta_2}\, I_2^{**}, \tag{6.6.11}$$
$$D_1^{**} = \frac{\phi_1}{\rho_1}\, I_1^{**}, \; D_2^{**} = \frac{\phi_2}{\rho_2}\, I_2^{**}, \; M_1^{**} = \frac{\epsilon_1\, \pi_1}{\epsilon_1 + I_1^{**}}, \; M_2^{**} = \frac{\epsilon_2\, \pi_2}{\epsilon_2 + I_2^{**}}.$$

At the endemic equilibrium, the number of infected individuals is positive. To obtain the endemic equilibrium points, we solve equation (6.6.10) for M_2 to obtain M_2^{**}, we solve equation (6.6.9) for M_1 to obtain M_1^{**}. We solve equation (6.6.7) for D_1 to obtain D_1^{**} and equation (6.6.8) for D_2 to get D_2^{**}. We solve equation (6.6.5) for E_1 to obtain E_1^{**} and equation (6.6.6) for E_2 to get E_2^{**}. We solve equation (6.6.3) for S_1 to obtain S_1^{**} and equation (6.6.4) for S_2 to get S_2^{**}.
I_1^{**} and I_2^{**} are the positive solutions of the system of equations (6.6.12) obtained by substituting the values of the state variables from system (6.6.11) in equations (6.6.1) and (6.6.2).

$$(I_2^{**})^2\, \xi_1 + I_1^{**}\, \xi_2 + I_2^{**} \left(\xi_3 + \delta_2 \left(I_1^{**} Q_3\, \sigma_{21} + \Lambda_2\, Q_1\right)\right) = 0, \tag{6.6.12}$$
$$(I_2^{**})^2\, \xi_4 + (I_1^{**})^2\, \xi_5 + (I_1^{**})^2\, I_2^{**}\, \xi_6 - I_1^{**}\, I_2^{**} \delta_1\, \Lambda_1\, \frac{\delta_2}{Q_2}\, \rho_1\, \sigma_{21} = 0,$$

where

$$\xi_1 = Q_4\, \frac{\delta_2}{Q_2}\, (m-1)\, \sigma_{21}, \xi_2 = Q_3\, (\mu + (1-m)\, \theta_{12} - \theta_{21})\, \rho_2\, Q_2\, \sigma_{21},$$
$$\xi_3 = Q_4 \left(\mu + (1-m)\, \theta_{12} - \theta_{21}\right) \rho_1\, \rho_2 \left((m-1)\, \sigma_{21} - Q_2\right),$$
$$\xi_4 = (m-1)\, Q_4\, \frac{\delta_2}{Q_2}\, (\mu + \theta_{21})\, \rho_1 \sigma_{21},$$
$$\xi_5 = \delta_1\, \theta_{12}\, \rho_2 \left((1-m)\, \sigma_{21}\, (Q_3\, Q_2^2 + 1) + Q_2\right),$$
$$\xi_6 = \delta_1\, \frac{\delta_2}{Q_2} \left(Q_3\, Q_2^2\, (\rho_1 + \sigma_{21}) + \sigma_{21}\right).$$

The complexity of the resolution of system (6.6.12) does not enable us to give explicit expressions for I_1^{**} and I_2^{**} and this does not facilitate the study

of the stability of equilibria. However, the use of the next generation matrix method to compute the reproduction number guarantees at least the local stability of E_g^0. We now resort to numerical simulations to study the system further.

6.7 Numerical simulations

We simulate a scenario where susceptible and exposed individuals from a given community in Liberia move to Sierra Leone, based on the fact that since 1990, the GNI of Sierra Leone has always been larger than that of Liberia. The value of the parameters we use are either from the literature or estimated and are given in Tables 6.2 and 6.3.

Parameter	Λ_1	β_1	δ_1	α_1	ϕ_1	ρ_1	θ_{12}	σ_{12}	η_1	π_1	r_1	ϵ_1
Value	3000.2	9×10^{-5}	0.08	0.1751	0.75	0.2	0.7	0.5	1.01	50	0.5	100
Source	Est.	Est.	[137]	[125]	[125]	[32]	Est.	Est.	Est.	Est.	Est.	Est.

Table 6.2: Parameters with index 1 are for Sierra Leone. Est. stands for estimated.

Parameter	Λ_2	β_2	δ_2	α_2	ϕ_2	μ	ρ_2	η_2	π_2	r_2	m	ϵ_2
Value	2000.2	8×10^{-5}	0.12	0.1751	0.5	0.1	0.49	1.25	50	0.5	0.56	100
Source	Est.	Est.	[137]	[125]	[125]	Est.	[32]	Est.	Est.	Est.	[2]	Est.

Table 6.3: Parameters with index 2 are for Liberia. Est. stands for estimated.

6.7.1 Sensitivity analysis

Some parameters are more influential than others and can be estimated through sensitivity analysis. Among all the existing techniques of sensitivity analysis, the LHS/PRCC sensitivity analysis presents the advantage of sampling the parameters independently of one another [122]. The objective of the LHS/PRCC sensitivity analysis is to determine and rank important parameters whose uncertainties increase prediction imprecision. For a

given parameter, the LHS procedure consists of dividing the parameter values range into equally probable intervals and assigning a probability distribution to each parameter [122]. The PRCC that describes the linear relationship between the LHS parameters and the outcome measure is a statistical technique used to measure the strength of the relationship between the outcome measures and the parameters in a model [122].
EVD dynamics is well described by the variation in the number of infected individuals. But, since some of the parameter values used are estimated, there is some uncertainty in the results obtained and we use LHS/PRCC sensitivity analysis to identify key parameters that increase imprecision in the results obtained from system (6.2.1)-(6.2.10).

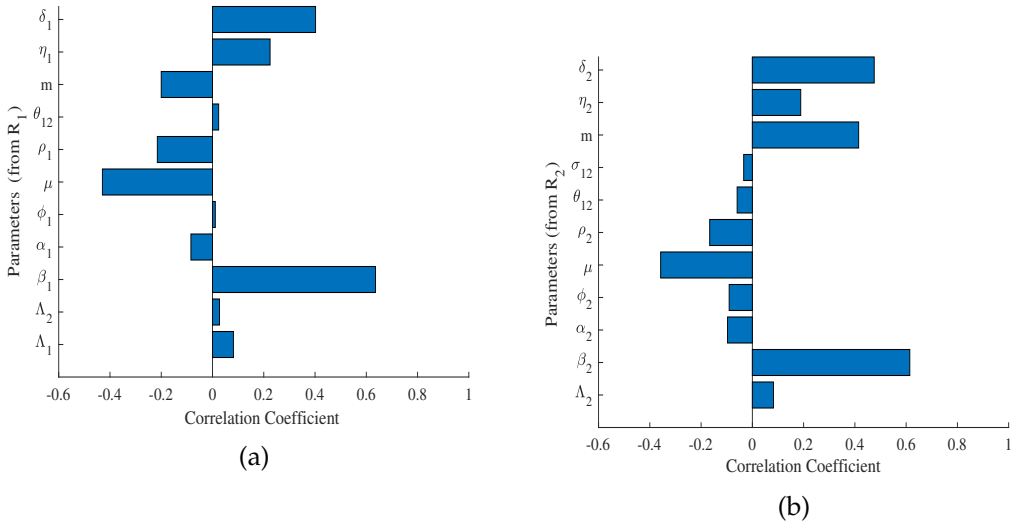

Figure 6.6: Sensitivity plots of the reproduction number in patch 1 in (a) and in patch 2 in (b) for the one way migration model.

The reproduction number of system (6.2.1)-(6.2.10) is the largest of the two reproduction numbers in the two patches. Figure 6.6 represents the type and importance of the correlation between each reproduction number and the parameters of the model. We observe in Figure 6.6(a) that β_1, ϕ_1, η_1 and σ_{12} have a positive correlation to R_1 whereas α_1, μ, ρ_1 and m have a negative correlation to R_1. β_1, ϕ_1, η_1 are the components of EVD force of infection in patch 1. Therefore, they drive EVD spread in patch 1 and then have a positive correlation with R_1. σ_{12} describes movements of exposed individuals into patch 1 who become later infectious, increasing then the

number of infected individuals into the patch and this explains the positive correlation with R_1. Natural death rate, recovery rate and safe burials rate (considered as dead bodies disposal rate) respectively represented by α_1, μ, ρ_1 in patch 1, reduce the number of individuals susceptible to EVD and therefore reduce R_1. This explains the negative correlation between these parameters and R_1. Increasing the value of m corresponds to reducing the economy of patch 1. In the case of a poor economy in patch 1, less people will move to patch 1, limiting then the number of people susceptible to EVD in patch 1 and this will then decrease R_1. This explains the negative correlation between m and R_1. Similarly, the results observed in Figure 6.6(b) represent the sensitivity analysis in patch 2, with the difference being that m has a positive correlation to R_2 and σ_{12} has a negative correlation to R_2. In fact, movements of infected individuals from patch 2 reduces the infected population size and as a consequence, the reproduction number R_2 is reduced as well. m has a positive correlation to R_2 because increasing the value of m in patch 2 corresponds to improving the economy in this patch which results in fewer people leaving the patch. This increases the size of the population susceptible to contract EVD in patch 2 and as a consequence, the reproduction number R_2 is increased. Key parameters whose uncertainty in the estimation of their values, might lead to imprecision in the results of the model analysis are then identified and represent a very important reserve of information for EVD control in this case. The estimation of these parameter values must then be carefully done during the formulation and implementation of control measures against EVD spread.

6.7.2 Dynamics of the infected individuals

The evolution of the number of infected individuals is represented in Figure 6.7.

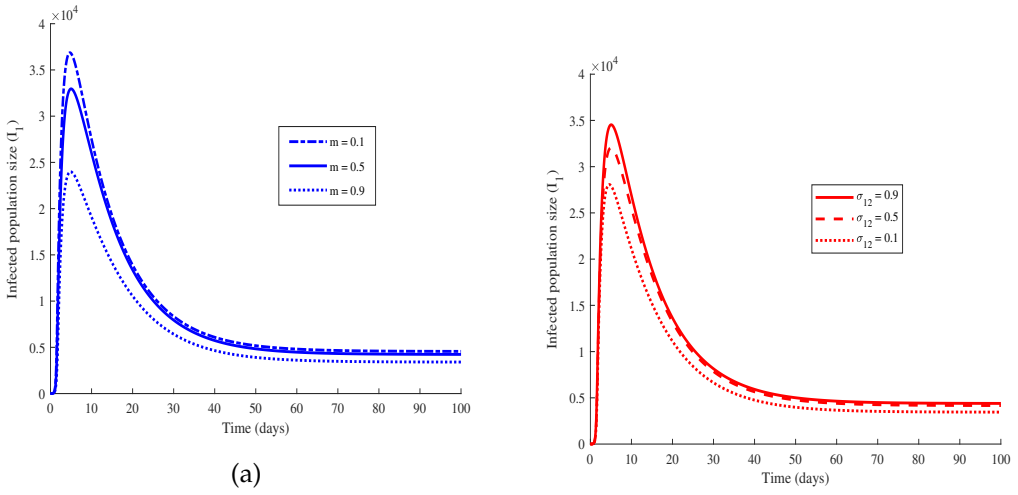

Figure 6.7: Effect of migration of infected individuals on EVD dynamics for the one way migration model. The value of the parameters used are in Tables 6.2 and 6.3.

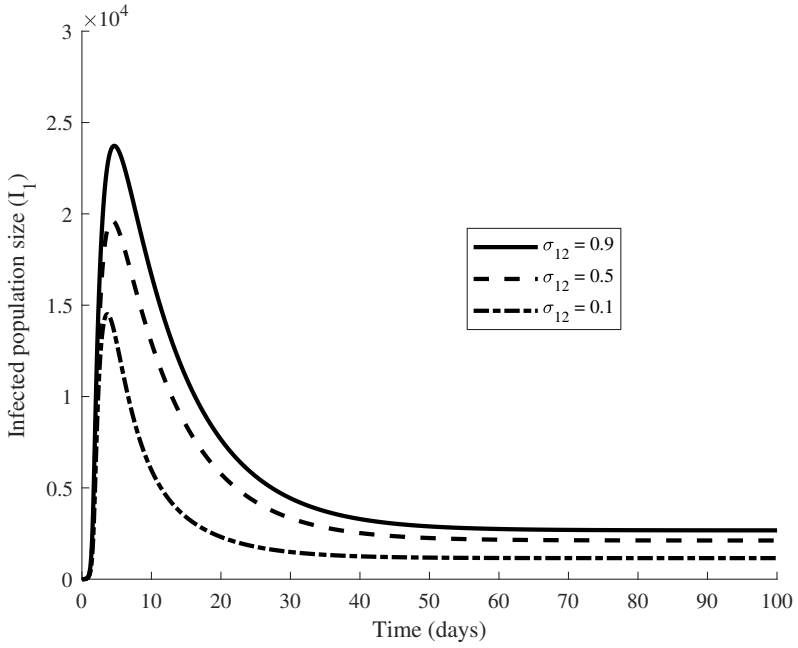

Figure 6.8: Effect of migration of infected individuals on EVD dynamics in the case of a two way migration. The value of the parameters used are in Tables 6.2 and 6.3 with $\theta_{21} = 0.7$ and $\sigma_{21} = 0.5$

Figure 6.7(a) shows an increase of the number of infected individuals in patch 1 when the value of m is decreased. A reduction of the income-ratio

m corresponds to an increase of the gap between the economies of the two considered patches or communities. This decrease can either be due to an increase of the GNI in patch 1 or a decrease of the GNI in patch 2. In both cases, the immediate consequence is that more individuals leave patch 2 for patch 1 either because the economy of their residing country is worse or because there are better opportunities elsewhere. Figure 6.7(b) confirms this hypothesis since we observe an increase in the number of infected individuals in patch 1 when the value of σ_{12} is increased. The economies of countries that can be potentially affected by EVD must then be very close in order to avoid movements of individuals towards the rich countries. This economic migration in fact can import Ebola virus into a country and can potentially cause an outbreak.

In the case of a two way migration, we notice in Figure 6.8 that the size of the infected population is smaller when compare to Figure 6.7(b) where migration is only one way. Migration of populations from rich countries returning to their country of origin helps in EVD control in the rich country as it limits the number of EVD infected individuals. Although these returns are not motivated by the improvement of the economic situation of the country of origin, it represents a better scenario for the rich country. It affirms the necessity for rich countries to facilitate more returning residents by providing those who want to return with entrepreneurial skills and funds to start their own businesses as they arrive at their country of origin for example. It might also be viewed as a call to facilitate the flow between countries through easy visa procedures for example.

6.8 Conclusion

Economic migration has always been a way of improving some people's living conditions. Migration from Africa to Europe is the most advertised route for economic migrants, who sometimes illegally enter Europe through Italy [178]. Intra-African economic migration is less advertised, although free movements of persons and goods that facilitates such type of migration is a reality in some regions of the continent [152]. The health status of migrants is often unknown or not well documented and they can therefore, possibly transport a virus to different geographical locations [179]. We formulated in this chapter, a model of EVD with two patches, that first con-

siders economic migration of individuals from patch 2 to patch 1, whose economy is assumed to be better and second we also consider returning of migrants to patch 2. We chose the GNI to represent the economy in each patch and we used the income-ratio, which is the ratio of the lowest economy to the highest economy, to represent the gap between two economies.

First, we proved that the one way migration model makes biological sense in an invariant set. We found that the reproduction number of the system is the largest reproduction number of the two patches and the disease free equilibrium of the system is locally stable when the reproduction number is less than one. We found that there exists a unique endemic equilibrium point in patch 2 when $R_2 > 1$ and there is a possibility of having multiple endemic equilibria in patch 1. The multiplicity of equilibrium points characterises a bifurcation which, in this case, is backward when $R_2 < 1$ and forward when $R_2 > 1$. We found from the bifurcation analysis that improving the economy in patch 2 limits movements of infected individuals and facilitates EVD control

Second, we considered that migrants also return to their countries of departure and this changed the first model into a two way migration model which presented a locally stable disease free equilibrium.

We simulated a scenario where individuals from a community in Liberia move to Sierra Leone whose economy is better as an example for the one way migration model. We found the most sensitive parameters of the model by using LHS/PRCC sensitivity analysis and results from the numerical simulations show that limiting the migration of infected individuals into patch 1 by improving the economy of patch 2 contributes to a reduction of the number of EVD cases in patch 1. Rich countries are then not completely in the shadow of EVD since the good health of their economy attracts individuals from poorer countries, who might bring with them Ebola virus. Since scenario of all migrants at the borders of a country is very difficult to achieve, we suggest that poor countries improve the living conditions of their populations, for example by abolishing corruption that deprives its population from their wealth. We also suggest that developed countries contribute to the development of the poorest countries in order to avoid an invasion of EVD on their soils through economic migration. Simulations

of the two way model showed that less individuals are infected in the rich patch when some move to the poorer patch.

The work presented in this chapter describes a scenario where EVD spread through economic migration, but it is not without shortcomings since other factors, other than economic conditions, motivate the migration of people. In fact, in the 21*st* century, political instability is a major cause of migration. People fleeing from conflict areas, which may be affected by infectious diseases, enter new areas of the terrestrial globe with a chance of spreading infectious diseases on their arrival. It will then be of great interest to assess the impact of such movements on the health of countries receiving refugees so as to raise awareness against war and other forms of conflict that are often the drivers of migration.

Chapter 7

Conclusion and discussion

The main objective of this thesis was to build mathematical models to examine the impact of socio-economic factors on EVD dynamics. We focused on four factors, namely limited hospital beds, human behaviour, migration and economy which were measured using hospitalisation rate, incidence rate, migration rate and GNI respectively.

First, we formulated a deterministic compartmental model with a time dependent number of beds available. The analysis of the model showed the existence of an unstable disease free equilibrium E_1^0, when there are no hospital beds, for values of the reproduction number less than 1 or the existence of a globally stable disease free equilibrium E_2^0 for values of the reproduction number less than a threshold R_h^c when at equilibrium the maximum beds capacity of ETUs is reached. Further, we proved that the number of beds available in ETUs is a determining factor in the disease control. We showed that when there are no beds or a limited number of available beds, controlling EVD is difficult because of the presence of a backward bifurcation. We proved that when the maximum capacity of ETUs is increased, a forward bifurcation appears and reducing the reproduction number to values less than 1 hence stops the spread of EVD. As part of the model validation, the model was fitted to Ebola case data from Liberia and Sierra Leone. We recommend a timely supply of beds into ETUs and the need for upgraded infrastructures in countries affected by the last EVD outbreak.

Second, the global stability analysis of the steady states of a model of EVD with a non linear incidence function was presented. The non linear incidence function was chosen to represent the influence of human behaviour

on EVD evolution. The proof of the global stability of equilibria was done with suitably chosen Lyapunov functions. Data from Liberia and Sierra Leone were used in the fitting process whose results showed how closely the model describes the evolution of EVD with human behaviour. Parameter values obtained in the fitting process support the assumptions made in the development of the model that behaviour change was motivated by disease prevalence.

Third, we formulated and analysed a model of EVD dynamics with two different strains of Ebola virus: EVD1 and EVD2. We considered that EVD2 is introduced in a country where EVD1 is endemic by a continuous or an impulsive immigration of infectives or by a strain mutation. In the case of a continuous immigration of infectives, the mathematical analysis of the model indicated the existence of a locally stable disease free equilibrium and an endemic equilibrium. It showed that when the invasion reproduction number of EVD2 is greater than one, EVD2 invades the country. The analysis also indicated that the two strains coexist at an endemic state when the reproduction number of EVD1 is greater than that of EVD2. Numerical simulations indicated a rapid and abrupt increase of the number of individuals infected by EVD2 which allows less time for control measures' implementation. A fast decrease of the number of individuals infected by EVD1 was noticed as well and this can be the ideal solution if clearing EDV1 from the population is the objective. In the case of an impulsive immigration of infectives, we proved that the reproduction number of EVD2 must be less than the ratio $\mu/(\Lambda+\pi)$ in order to limit the number of individuals infected by EVD2. We also found that a fixed period of impulse is better for EVD2 control since it helps to evaluate with precision the number of impulses that minimizes the number of individuals infected by EVD2. Numerical simulations indicated that the smaller the immigration rate of individuals infected by EVD2, the larger the number of individuals infected by EVD1. This shed the light on the competition between the two ebolavirus strains for the susceptible population. We found that the impulsive type of migration of individuals infected by the less infectious EVD strain would be a better scenario. We argued that the impulsive type of migration of infectives is manageable because it allows more time for control measures to be implemented, increasing the chances of stopping EVD irrespective of the strain.

Finally, we formulated a model of EVD with two patches, that considers migration of individuals between the two patches. The economy of patch 1 is assumed better than that of patch 2. We chose the GNI to represent the economy in each patch and we used the income-ratio, which is the ratio of the lowest economy to the highest economy, to represent the gap between two economies. We started with a one way migration model, where people move from patch 2 to patch 1. We proved that the model makes biological sense in an invariant set. We found that the reproduction number of the system obtained in this case is the largest reproduction number of the two patches and the disease free equilibrium of the system is locally stable when the reproduction number is less than one. We proved the existence of a unique endemic equilibrium point in patch 2 when its reproduction number is greater than 1 and also proved that there is a possibility of having multiple endemic equilibria in patch 1, which characterises a backward bifurcation in this case when $R_2 < 1$ and a forward bifurcation when $R_2 > 1$. We deduced from the bifurcation analysis that improving the economy in patch 2 limits movements of infected individuals and facilitates EVD control. The analysis of the two way migration model also showed that the disease free equilibrium in this case is locally stable. We simulated a scenario where individuals from a community in Liberia move to Sierra Leone whose economy is better as an example. We found the most sensitive parameters of the model by using LHS/PRCC sensitivity analysis and results from the numerical simulations showed that limiting the migration of exposed individuals into patch 1 by improving the economy of patch 2 contributes to a reduction of the number of EVD cases in patch 1. Rich countries are then not completely in the shadow of EVD since the good health of their economy attracts individuals from poorer countries, who might bring with them Ebola virus. Since the scenario of all migrants at the borders of a country is very difficult to achieve, we suggested that poor countries improve the living conditions of their populations, for example by abolishing corruption that deprives its population from their wealth. We also suggested that developed countries contribute to the development of the poorest countries in order to avoid an invasion of EVD on their soils through economic migration.

7.1 Limitations and future work

The models formulated in this thesis describe scenarios where limited hospital beds, human behaviour, migration and poverty increase EVD spread. The various fittings show that these models are consistent with the dynamics of EVD in West Africa, but the overall work done is not without shortcomings.

In Chapter 3, the lack of sufficient data on the number of beds supplied into ETUs in the affected countries limited the numerical analysis and interpretation. Obtaining the complete dataset would have given a more realistic picture of beds capacity in ETUs during the outbreak of $2013-2016$ and would have helped to obtain more accurate results. The only health resource considered in this chapter was the number of beds, but other equipments like personal protective equipments and laboratory materials were used for EVD patients' management and care. Considering also such equipments in a future model could help to have a global view of the potential impact of health resources on EVD dynamics.

In Chapter 4, we used a deterministic approach to model human behaviour which is complex and unpredictable. A stochastic version of the incidence function could be worth looking at as an alternative albeit the challenges associated with its formulation and the mathematical analysis. The use of individual based models or network models could have potentially solved the inadequacies of dealing with deterministic models. However this model presents interesting mathematical results on the global stability of an EVD model with human behaviour and a non-linear incidence rate.

In Chapter 5, we formulated a model that considers two of the five existing strains of Ebola virus and that describes well the scenario of a multi-strain epidemic of EVD. Considering more strains could have given a bigger picture of a potential co-infection scenario.

In Chapter 6, a scenario where migration of populations was only due to poverty in their residing countries was considered. But in the $21st$ century, political instability is also a major cause of populations' migration. People fleeing from conflict areas, which may be affected by infectious diseases, enter new areas of the terrestrial globe with a chance of spreading or con-

tracting infectious diseases. It will then be of great interest to assess the impact of such movements on the health of countries receiving refugees so as to raise awareness against war and other forms of conflict that are often the drivers of migration.

While several models were fitted to data in this thesis and it is well documented that the goodness of fit measures the discrepancy between observed data and values expected from the model. In this work, no goodness of fit tests were done but we relied on the least squares method for the model fitting. These tests would have given a better estimation of the discrepancy between observed data and values expected from the model, and then helped to adjust our parameter values. Considering these tests in the future will be a useful step in connecting data to a model.

Appendix A

Appendix

A.1 Local stability of the endemic equilibrium

To prove the stability of the endemic equilibrium, the theorem, remark and corollary in [121] which are based on the centre manifold theory were used in this thesis.

Theorem A.1.1. *Consider a general system of ordinary differential equations with a parameter ϕ:*

$$\frac{\mathrm{d}x}{\mathrm{d}t} = f(x,\phi), \qquad f : \mathbb{R}^n \times \mathbb{R} \longrightarrow \mathbb{R}^n \quad \text{and} \quad f \in \mathbb{C}^2(\mathbb{R}^n \times \mathbb{R}). \tag{A.1.1}$$

Without loss of generality, it is assumed that 0 is an equilibrium for system (A.1.1) for all values of the parameter ϕ, that is $f(0,\phi) \equiv 0$ for all ϕ.

Assume

$A1 : A = D_x f(0,0) = \left(\frac{\partial f_i}{\partial x_j}(0,0)\right)$ *is the linearisation matrix of System (A.1.1) around the equilibrium 0 with ϕ evaluated at 0. Zero is a simple eigenvalue of A and all other eigenvalues of A have negative real parts;*

A2: Matrix A has a non negative right eigenvector w and a left eigenvector v corresponding to the zero eigenvalue. Let f_k be the kth component of f and

$$a = \sum_{k,i,j=1}^{n} v_k w_i w_j \frac{\partial^2 f_k}{\partial x_i \partial x_j}(0,0), \quad b = \sum_{k,i=1}^{n} v_k w_i \frac{\partial^2 f_k}{\partial x_i \partial \phi}(0,0).$$

The local dynamics of (A.1.1) around 0 are totally determined by a and b.

1. *$a > 0, b > 0$. When $\phi < 0$ with $\mid \phi \mid \ll 1$, 0 is locally asymptotically stable, and there exists a positive unstable equilibrium; when $0 < \phi \ll 1$,*

0 *is unstable and there exists a negative and locally asymptotically stable equilibrium;*

2. $a < 0, b < 0$. *When* $\phi < 0$ *with* $\mid \phi \mid \ll 1$, 0 *is unstable; when* $0 < \phi \ll 1$, 0 *is locally asymptotically stable, and there exists a positive unstable equilibrium;*

3. $a > 0, b < 0$. *When* $\phi < 0$ *with* $\mid \phi \mid \ll 1$, 0 *is unstable, and there exists a locally asymptotically stable negative equilibrium; when* $0 < \phi \ll 1$, 0 *is stable, and a positive unstable equilibrium appears;*

4. $a < 0, b > 0$. *When* ϕ *changes from negative to positive,* 0 *changes its stability from stable to unstable. Correspondingly a negative unstable equilibrium becomes positive and locally asymptotically stable.*

Corollary A.1.2. *When* $a > 0$ *and* $b > 0$, *the bifurcation at* $\phi = 0$ *is subcritical or backward.*

Remark A.1.3. *According to Remark* 1 *in [121], if the equilibrium of interest in Theorem* (A.1.1) *is a non-negative equilibrium* x_0, *then the requirement that* w *is non negative in Theorem* (A.1.1) *is not necessary. When some components in* w *are negative, one can still apply Theorem* (A.1.1) *on condition that:*

$$\begin{cases} w(j) > 0 & \text{if} \quad x_0(j) = 0, \\ \text{if} \quad x_0(j) > 0, & w(j) \text{ does not need to be positive,} \end{cases}$$

where $w(j)$ *and* $x_0(j)$ *denote the* j*th component of* w *and* x_0 *respectively.*

A.2 Descartes' law of signs

Theorem A.2.1. *Let* $P = a_p X^p + a_{p-1} X^{p-1} + \ldots + a_0$ *be a univariate polynomial in* $\mathbb{R}[X]$. *We write Var* (P) *for the number of sign variations in* $a_0, \ldots, a_p$ *and* $pos(P)$ *for the number of positive real roots of* P, *counted with multiplicity.*

* $Var(P) \geq pos(P)$,

* $Var(P) - pos(P)$ *is even.*

A.3 Matlab codes used for the numerical simulations

The followings codes were run using using Matlab 2017a.

A.3.1 Bifurcation

The following code is used to plot Figure 3.3. It represents the real and positive roots of a polynomial of order 3. Other bifurcation graphs are obtained by editing the order and the coefficients of the polynomial and by using the indicated parameter values.

```
%This code is used for both backward and forward bifurcation.
% The values corresponding to each case is given as a comment.
% To plot the backward bifurcation, the user must comment
%the forward bifurcation parameters and
%uncomment the backward bifurcation ones.

lambda = 1866;
delta1 = 0.309;
delta2= 0.251;
rho= 0.457;
alpha = 0.177;
mu = 194;
omega = 0.256;
eta1 = 0.341;
eta2= 3.78;
beta = 0.569;
c = 15.5;
mu0 = 0.087;
mu1 = 0.172;
%bmax = 1.8; % backward bifurcation
bmax = 10.8 % forward bifurcation
rend=100000;
rlst=linspace(0,2,rend);
mylist1=zeros(1,length(rlst));
mylist2=zeros(1,length(rlst));
mylist3=zeros(1,length(rlst));

Q1=  mu + alpha + delta1;
Q2= delta2 + mu + omega;

for i=1:1:rend
```

```
r=rlst(i);
% Ao, A1, A2, A3 are the coefficients of the polynomial obtained t the
% endemic equilibrium point E*
Ao = beta*c*(mu0 + Q1)*(mu0*(delta2*eta2 + eta1*rho) + Q2*(delta1*eta2
+rho));
A1 = beta*c*(delta2*eta2 + eta1*rho)*(mu0*(2*bmax*mu1 + bmax*Q1 + ...
lambda) + bmax*mu1*Q1) + Q2*(beta*c*delta1*eta2*(bmax*(mu0 + mu1) - .
lambda) + beta*c*rho*(bmax*mu1 - lambda) + mu0*rho*(beta*bmax*c + mu
Q1*(2*beta*bmax*c*delta1*eta2 + rho*(2*beta*bmax*c + mu)));
A2= bmax*(Q2*(beta*c*delta1*eta2*(bmax*mu1- 2*lambda )+ ...
rho*(mu1*(beta*bmax*c + mu ) - 2*beta*c*lambda + mu*mu0) + ...
Q1*(beta*bmax*c*delta1*eta2 + beta*bmax*c*rho + 2*mu *rho)) + ...
beta*c*(delta2*eta2 + eta1*rho)*(mu1*(bmax*(mu1 + Q1) + lambda) + ...
lambda*mu0));
A3= bmax^2*rho*Q2*mu*(Q1 + mu1)*(1-r);
mypoly=[Ao,A1,A2,A3];
sol=roots(mypoly); % we plot the roots (sol) of the polynomial mypoly
mylist1(i)=sol(1);
mylist2(i)=sol(2);
mylist3(i)=sol(3);
% we replace negative roots by zero and only store the real positive
% roots into mylist
if imag(mylist1(i))~=0
mylist1(i)=0;
else
mylist1(i)=max(0, mylist1(i));
end
if imag(mylist2(i))~=0
mylist2(i)=0;
else
mylist2(i)=max(0, mylist2(i));
end
if imag(mylist3(i))~=0
mylist3(i)=0;
else
mylist3(i) = max(0, mylist3(i));
```

```
end
end
% we determine the number i from the rlist for each function mylist
% where the root of the polynomial is real and positive.

lstpos=find(mylist1~=0);
index1=min(lstpos);
index2=max(lstpos);
mlstpos=find(mylist2~=0);
index3=min(mlstpos);
index4=max(mlstpos);
vlstpos=find(mylist3~=0);
index5=min(vlstpos);
index6=max(vlstpos);
% we formulate the disease free equilibrium lines on the x-axis
s= linspace(0,1,rend);
z= linspace(1,1.5,rend);
y1=  + 0*s;
y2= + 0*z;
%axis([0.3,1.5,0,5])% backward bifurcation
axis([0.7,1.5,0,4])% forward bifurcation
hold on
%we plot the positive roots of the polynomial
%plot(rlst(index1:index2),mylist1(index1:index2),'b-',
%rlst(index3:index4),mylist2(index3:index4),'b-',rlst(index5:index6),
%mylist3(index5:index6),'r--','linewidth',2)%bacward bifurcation
plot(rlst(index1:index2),mylist1(index1:index2),'b-', ...
rlst(index3:index4),mylist2(index3:index4),'b-',...
rlst(index5:index6),mylist3(index5:index6),'b-','linewidth',2)% forwa
plot(s, y1,'b-','linewidth',2)
plot(z, y2,'r--','linewidth',2)
%xlimit([0.2, 1.8])
xlabel('Reproduction number Rh')
ylabel('Infected population size I(t)')
hold off
```

A.3.2 Sensitivity analysis

The code for the sensitivity analysis initially developed by Gomero [122] is used as a template. We have edited the code as indicated by the author. The procedure is the following:
parapdfs.txt (enter the data ranges), $R_C - LHS.m$ (enter your $R0$, parameters in the same order as parapdfs.txt, as many outputs as you need), calculation.m (enter your $R0$ and parameters, same as $R_C - LHS$) Run prcc2.m to get prccs (and runs LHS within it). Then run $R_C - LHS.m$ to get the sensitivity graphs. Note that R_C represent the reproduction number R_0 of our model. All the following codes must be saved in the same folder and then run from there.

A.3.2.1 apply-constraints

```
%This code must be saved  as apply_constraints.m
 % Fills in arrays for the parameters that
% are constrained in some way (type > 1)

function [para] = apply_constraints(max_val, min_val, ...
constraints, paraval, num, starts, ends, para, N)

for i=1:num
if (constraints(i)~=0) % means is constrained in some way
found=0;
j=1;

% looking for other parameter it's constrained to
while ((found==0)&&(j<=num))
diff=0;

if (diff==0)  % meaning found match bet.
%for para to be constrained to
found=1;
else
j=j+1;
end
```

```
end
if ((constraints(i)~=5)&&(constraints(i)~=6)&&(constraints(i)~=9))
starts(i)=starts(j);
ends(i)=ends(j);
end

if (constraints(i)==2)     % same as another parameter
for k=1:N
para(k,i)=para(k,j);
end
end
if (constraints(i)==3) % less than another parameter
starts(i)=0.0;
for k=1:N
yes=0;
while (yes==0)
cho=  1 + round((N-1)*rand);
if (cho<=N)
yes=1;
end
end
choice=(cho)/(N);

para(k,i)=choice*para(k,j);
end
end
if (constraints(i)==4)
ends(i)=mults(i)*ends(j);
for k=1:N
yes=0;
while (yes==0)
cho =  1 + round((N-1)*rand);
if (cho<=N)
yes=1;
end
end
```

```
choice=(1.0+(mults(i)-1.0)*(cho)/(N));
end
end
if (constraints(i)==5)
if (constraints(j)~=0)
make_paraval(j);
end
for z=1:N
fprintf('%lf\n',paraval(j,z));
end
for z=1:N
[q]=determine_rank(z,j);
rnk = q;
para(z,i)=paraval(i,rnk);
end
end
if (constraints(i)==6)
starts(i)=min_val(i);
ends(i)=ends(j);
if (constraints(j)~=0)
make_paraval(j);
end
for k=1:N
yes=0;
while (yes==0)
cho = 1 + round((N-1)*rand);
if (cho<=N)
yes=1;
end
end
choice=(cho)/(N);
para(k,i)=min_val(i)+choice*(para(k,j)-min_val(i));
end
end
if (constraints(i)==7)
ends(i)=(1.0/min_val(i));
```

```
for k=1:N
yes=0;
while (yes==0)
cho = 1 + round((N-1)*rand);
if (cho<=N)
yes=1;
end
end
choice=(cho)/(N);
para(k,i)=(para(k,j)+choice*((1.0/min_val(i))-para(k,j)));
end
end
if (constraints(i)==8)
starts(i)=starts(j);
ends(i)=max_val(i);
if (constraints(j)~=0)
make_paraval(j);
for k=1:N
yes=0;
while (yes==0)

cho = 1 + round((N-1)*rand);
if (cho<=N)
yes=1;
end
end
choice=(cho)/(N);
para(k,i)=para(k,j)+choice*(max_val(i)-para(k,j));
end
end
if (constraints(i)==9)
starts(i)=min_val(i);
ends(i)=1/starts(j);
if (constraints(j)~=0)
make_paraval(j);
end
```

```
for k=1:N

yes=0;
while (yes==0)
cho = 1 + round((N-1)*rand);
if (cho<=N)
yes=1;
end
end
choice=(cho)/(N);

para(k,i)=min_val(i)+choice*(1/para(k,j)-min_val(i));

end
end
end
end
end
```

A.3.2.2 calculation

This code must be saved as calculation.m

```
function [R_C] = calculation(para)

for i=1:1000;

delta1(i)=para(i,1);
delta2(i)=para(i,2);
beta(i)=para(i,3);
mu(i)=para(i,4);
cn(i)=para(i,5);
mu1(i) = para(i,6);
alpha(i) = para(i,7);
rho(i) = para(i,8);
eta1(i) = para(i,9);
eta2(i) = para(i,10);
omega(i) = para(i,11);
```

```
Lambda(i) = para(i,12);
Q1(i) = mu(i) + delta1(i )+ omega(i) ...
+ alpha(i); Q2(i) = mu(i) + delta2(i);
R_C = (Lambda./mu).*beta.*cn.*((1./(Q1+ mu1)) + ...
(1./rho.*(Q1+ mu1)).*(eta2.*delta1)+ (mu1.*(delta2.*eta2 ...
+ rho.*eta1)./(Q2)));

end
```

A.3.2.3 Checking data distribution

```
%This code must be saved as check_para_dist.m
      content.. % to create plotpara.txt file and check the
      % distribution of sampling data for parameters

      function check_para_dist(N, num, ends, starts, para)

      bins = zeros(2,150);

      fnumbins=N/50.0;
      numbins=round(fnumbins);

      plot=fopen('plotpara.txt','w');
      for i=1:num

      for k=1:numbins
      bins(1,k)=0;
      bins(2,k)=0;
      end

      binsize=(ends(i)-starts(i))/numbins;
      for k=1:numbins
      bins(1,k)=starts(i)+(k-1)*binsize;
      end
      for k=1:N
      j=1;
```

```
found=0;
while ((found==0) && (j<=numbins))
if (binsize>0)
if (para(k,i)<bins(1,j))
found=1;
else
j = j + 1;
end
else
if (para(k,i)>bins(1,j))
found=1;
else
j = j + 1;
end
end
end
bins(1,j)=bins(1,j)+1;
end


% write to file of plot
fprintf(plot,'parameter %s:\n',names(i));
fprintf(plot,'start_of_bin\tmidpt_of_bin\tnum_in_bin\n');
for k=1:numbins
fprintf(plot,'%12.8f\t%5.4f\t%4.3f\n', bins(0,k),...
(bins(0,k)+binsize/2.0),bins(1,k));
end
fprintf(plot,'\n');

end
fclose(plot);
```

A.3.2.4 Ranking

```
% This code must be saved as create_outcome_rank.m
```

```
% ranks variable from matrix "outcome";
% creates an array: rank_outcome[sim#] for each tslot (time)

function [rank_outcome] = create_outcome_rank(N, num, outcome)

%       for i = 1:N
%           rank_outcome(i)=0;
%       end
%       clear i;
%
%       for i = (N-1):-1:1
%
%               max=0;
%
%               for j = 1:N
%               for k = 1:num
%
%           if ((outcome(j,k)>max)&&(rank_outcome(j)==0))
%                           max=outcome(j,k);
%                           marker=j;
%                       end
%               end
%           end
%       rank_outcome(marker)=i;
%       end


[sorted, order] = sort(outcome(:,num));
c = 1;

for i = 1:N

j = order(i);
rank(j) = c;
c = c + 1;
end
```

```
rank_outcome = rank;
```

A.3.2.5 Matrix of the ranks

```
% This code should be saved as create_rank_matrix.m

% creates a matrix: rank[num_of_sims][num_of_paras]
% of the ranks of each parameter for each simulation

function [rank, ranks] = create_rank_matrix(N, num, ...
parameters, rank, rank_outcome)

for i = 1:N

for j = 1:num

rank(i,j)=0;

end
end

% creating rank matrix

for i = 1:num

for j = (N-1):-1:1

max=0.0;

for k = 1:N

if ((parameters(k,i)>max)&&(rank(k,i)==0))
max=parameters(k,i);
marker=k;
end
```

```
end
rank(marker,i)=j;
end
end

for i = 1:N

rank(i,num)=rank_outcome(i);

end


ranks = rank(1:N, 1:num);
```

A.3.2.6 Rank determination

```
    %This code must be saved as determine_rank.m
 % for constraint choice #5, need match ranks, this procedure
% determines the rank of the already sampled parameters to which
% the new parameter is to be constrained by equal rank

function [q] = determine_rank(simnum,paranum)

got=0;
q=1;
while (got==0)
if (para(simnum,paranum)==paraval(paranum,q))
got=1;
else
q=q+1;
end
end
```

A.3.2.7 Find PRCC

```
% This code must be saved as find_prcc.m
% calculates prcc (gamma) for the given variable and parameters
% to test the significance of a given PRCC (gamma) value, the t-
```

```
% Student's T test with N-2 degrees of freedom, a t-value is calc
% eeach PRCC here--using p. 242 of LHS technique paper

function find_prcc(double BB[20][20])


for i = 1:num

gamma=(-BB(i,num))/(sqrt(BB(i,i)*BB(num,num)));
tt=gamma*sqrt((N-2.0)/(1.0-gamma));

end
```

A.3.2.8 parameters and data

```
% This code must be saved as gendata.m

function [paraval, constraints, starts, ends] = gendata(N, num,.
mults, constraints, starts, ends, paraval, max_val, min_val, ...
kind, start, finish, peak)


for j=1:num

mults(j)=0;
constraints(j) = 0;
end

for i=1:num

oldkind=0;


if (kind(i)==5)
oldkind=5;
end
```

```
if (kind(i)==0)

if (oldkind==5)
kind(i)=5;
end

starts(i)=start(i);

ends(i)=finish(i);
paraval(i,1)=start(i) + (finish(i)-start(i))/(2*N);

for j=2:N
paraval(i,j)=paraval(i,j-1)+(finish(i)-start(i))/N;
end
elseif (kind(i)==1)

if (oldkind==5)
kind(i)=5;
end

starts(i)=start(i);

ends(i)=finish(i);

ht(i)=2.0/(finish(i)-start(i));

if (peak(i)~=start(i))
slope(i)=ht(i)/(peak(i)-start(i));
done(i)=0;
else
done(i)=1;
end
x_l(i)=start(i);
y_old(i)=0.0;
j=1;
```

```
while (done(i)==0)
x_r(i)=(-y_old(i)+sqrt(y_old(i)*y_old(i)+ ...
2.0*slope(i)/N))/slope(i) + x_l(i);
if (x_r(i)<=peak(i))
paraval(i,j)=(x_l(i)+(x_r(i)-x_l(i))/2.0);
j=j+1;
y_old(i)= y_old(i) + slope(i)*(x_r(i)-x_l(i));
x_l(i)=x_r(i);
else
done(i)=1;
end
end
amt_prepeak(i)=((peak(i)-x_l(i))*y_old(i) + ...
(slope(i)*(peak(i)-x_l(i)))*(peak(i)-x_l(i))/2.0);
slope(i)=-ht(i)/(finish(i)-peak(i));
x_r(i)=(((-ht(i)+sqrt(ht(i)*ht(i)+ ...
2.0*slope(i)*((1.0/N)-amt_prepeak(i))))/slope(i))+peak(i));
paraval(i,j)=(x_l(i)+(x_r(i)-x_l(i))/2.0);
j=j+1;
x_l(i)=x_r(i);
y_old(i)=ht(i)+slope(i)*(x_r(i)-peak(i));

done(i)=0;
while (done(i)==0)
disc(i)= (y_old(i)*y_old(i)+2.0*slope(i)/N);
if (disc(i)>=0.0)
x_r(i)=(((-y_old(i)+sqrt(y_old(i)*y_old(i) + ...
2.0*slope(i)/N))/slope(i))+x_l(i));
else
if (j==N)
x_r(i)=finish(i);
else
x_r(i)=finish(i)+1;
end
done(i)=1;
end
```

```
if (x_r(i)<=finish(i))
paraval(i,j)=(x_l(i)+(x_r(i)-x_l(i))/2.0);
j=j+1;
y_old(i) = y_old(i) + slope(i)*(x_r(i)-x_l(i));
x_l(i)=x_r(i);
else
done(i)=1;
end
end
else if ((kind(i)==2)||(kind(i)==3)||(kind(i)==4)||(kind(i)==5 .
)||(kind(i)==6)||(kind(i)==7)||(kind(i)==8)||(kind(i)==9))
constraints(i)=kind(i);

end
if (kind(i)==4)

mults(i)=mult;
end
if ((kind(i)==6)||(kind(i)==7)||(kind(i)==9))

min_val(i)=fmult;
end
if (kind(i)==8)

max_val(i)=fmult;
end
end
end
ReturnValue=1;
end
```

A.3.2.9 LHS routine

```
% This code must be saved as LHS.m

% Calling program for LHS routine; feed in file
%called parapdfs.txt which
```

```
% contains the name of each parameter,
% min/max/peak value and distribution
% type; the file format is a n x (n+1) matrix

% After file is read in, initial values
% are declared for the program and
% the number of simulations desired,
%denoted by N, is assigned by the user

% The program is set-up to %
%to read the number of parameters, denoted
%by num,  from the table
% in parapdfs.txt

% The output of the program is a
%N x num matrix containing the sample for
% each parameter in the parapdfs.txt

% read in values from input file
%to create arrays for each parameter
% distribution type, lower/upper limit,
%start, end and peak are read in

[name, kind, start, finish, peak] = ...
textread('parapdfs.txt', ...
'%s %d %f %f %f','headerlines',1);
%         [name, kind, start, finish, peak] = t...
%extread('parapdfs_erad.txt',...
%'%s %d %f %f %f','headerlines',1);

%  Declaration of parameters

constraints = zeros(100,1);
mults = zeros(100,1);
paraval = zeros(100,1500);
para = zeros(1500,100);
```

```
starts = zeros(100,1);
ends = zeros(100,1);
min_val = zeros(100,1);
max_val = zeros(100,1);



N = 1000; % number of simulations desired
a = size(name);  % number of parameters in table
num = a(1);

% Below is where different functions
%are called to run the LHS routine;

% gendata takes the values from parapdfs.txt and
%creates an array which to
% sample values from based on
%the pdf of each parameter

% samples: begins to build samples
% based on array created on gendata
% the reamaining programs apply
%any constraints to the parameter values and
% generates the LHS

[paraval, constraints, starts, ends] = gendata(N, num, mults, ...
constraints, starts, ends, paraval, max_val, min_val, kind, start,.
finish, peak);
[para] = samples(N,num, constraints, paraval);
[para] = apply_constraints(max_val, min_val, constraints,...
paraval, num, starts, ends, para, N);
[paraval] = make_paraval(num, para, paraval, N);
[lhstable] = output_para(N, num, para);
[R_C] = calculation(para);
latin_output = zeros(N, num + 1);
latin_output(1:N, 1:num) = para; latin_output(:, num+1) = R_C';
```

```
%check_para_dist(N, num, ends, starts, para);
```

A.3.2.10 Create matric C

```
% This code must be saved as make_c_matrix.m
% creates matrix C (bottom p. 241 of LHS technique paper,
% Blower and Dowlatabadi)

function [CC] = make_c_matrix(N, num, rank)

m_u = (1.0+N)/2.0;

for r = 1:num  % changed num + 1 to num

for c = 1:num % changed num + 1 to num

numer=0.0;
denomr=0.0;
denomc=0.0;

for i = 1:N

numer = numer + (rank(i,r)-m_u)*(rank(i,c)-m_u);
denomr = denomr + (rank(i,r)-m_u)*(rank(i,r)-m_u);
denomc = denomc + (rank(i,c)-m_u)*(rank(i,c)-m_u);

end
denom=sqrt(denomr*denomc);
CC(r,c)=numer/denom;

end
end
```

A.3.2.11 Matching parameter rank

```
% This code must be saved as make_paraval.m
  % if a parameter's constraint is type #5, need to match
% its rank to another para.
```

```
% if the para to which it is to be matched has been created
% by constraint to another para, there is no array storing
% its values in rank-order.
% this file creates such an array: paraval(para_#_ranking)(number_o

function [paraval] = make_paraval(num, para, paraval, N)

use = zeros(1500,1);

for q=1:N
use(q)=0;
end
for q=1:N
low=100000.0;
for r=1:N

if ((para(r,num)<=low)&&(use(r)==0))

% fprintf("q= %i r= %i\n",q,r);
low=para(r,num);
lowmark=r;
end
end
use(lowmark)=1;
paraval(num,q)=para(lowmark,num);
end
```

A.3.2.12 Create LHS table

```
% This code must be saved as output_para.m
 % Creates lhs table


function [lhstable] = output_para(N, num, para)

lhstable=fopen('lhstable.txt','w');
```

```
fprintf(lhstable,'%d\t%d\n',N,num);
fprintf(lhstable,'sim');


for j=1:N
fprintf(lhstable,'%d',j);
for i=1:num
fprintf(lhstable,'\t%lf',para(j,i));
end
fprintf(lhstable,'\n');
end

fclose(lhstable);
```

A.3.2.13 Calling program to generate PRCC

```
% This code must be saved as prcc2.m
clear;
% Calling program to generated PRCC for LHS; call the LHS program wh
% generates the sample; all input variables are included in the LHS
% and output of the program is the matrix CC from Blower's technique

LHS; % call the LHS program
b = size(latin_output);
c = length(latin_output);


%      test1 = 1./latin_output(:,7);
%      test2 = 1./latin_output(:,8);
%      test3 = 1./latin_output(:,9);
%
%  latin_output(:,7) = test1;
%  latin_output(:,8) = test2;
%  latin_output(:,9) = test3;
num = b(2);

% delcare initial parameters
```

```
rank_outcome = zeros(1000,1);
rank = zeros(1000,10);
outcome = zeros(1000,100);
parameters = zeros(1000,10);
CC = zeros(10, 10);
lengthofmatrix = b(2);
% read in data from LHS; program creates matrices outcome and
% parameters that are used to calculate the PRCCs
% variables are then ranked and results are put into rank_outcome
% matrix which is fed into create_rank_matrix which creates
%a matrix of the ranks of each
% parameter for each simulation; the CC matrix then created in the la
% program

[parameters, outcome] = read_in_data(N, num, latin_output);
[rank_outcome] = create_outcome_rank(N, num, outcome);
[rank, ranks] = create_rank_matrix(N, num, parameters, rank, rank_out
[CC] = make_c_matrix(N, num, rank);



set(0,'defaulttextinterpreter','tex');
fig11 = figure(11);
barh(CC(1:length(CC)-1,length(CC)))
set(gca,'YTick',1:12)
set(gca,'YTickLabel',{'\delta_1','\delta_2','\beta',...
'\mu','c','\mu_1', '\alpha','\rho','\eta_1','\eta_2','\omega','\Lamb
%%%%%%%%%%%%%%%%%%
% set(0,'defaulttextinterpreter','tex');
% fig11 = figure(11);
% barh(CC(1:length(CC)-1,length(CC)))
% set(gca,'YTick',1:16)
%set(gca,'YTickLabel',{'\delta_1','\delta_2','\beta',
%'\alpha','\mu','cn','\mu_0','\mu_1','k','b_0','bmax','\nu','\rho','
% legend2latex(fig11);
```

```
% laprint( 1, 'figure9');
%



% boxplot(R_C)
% axis([0.5 1.5 0 1])
```

A.3.2.14 Tornado plot

```
% This code must be saved as R_C_LHS.m
% I have to run LHS first, then define a new matrix C to be para.
% run prcc2.m to have the tornado plot

for i=1:1000;
delta1(i)=para(i,1);
delta2(i)=para(i,2);
beta(i)=para(i,3);
mu(i)=para(i,4);
cn(i)=para(i,5);
mu1(i) = para(i,6);
alpha= para(i,7);
rho(i) = para(i,8);
eta1(i) = para(i,9);
eta2(i) = para(i,10);
omega(i) = para(i,11);
Lambda(i) = para(i,12);
Q1(i) = mu(i) + delta1(i ) + alpha(i); ...
Q2(i) = mu(i) + delta2(i) + omega(i);

R_C = (Lambda./mu).*beta.*cn.*((1./(Q1+ ...
mu1)) + (1./rho.*(Q1+ mu1)).*(eta2.*delta1)+...
(mu1.*(delta2.*eta2 + rho.*eta1)./(Q2)));


end

v=0;
```

```
figure(1)
plot(delta1, log(R_C), '.', delta1, v)
xlabel(' \delta1 ')
ylabel('log(R_{0UD})')

figure(2)
plot(delta2, log(R_C), '.', delta2, v)
xlabel('\delta_2')
ylabel('log({R}_{0})')

figure(3)
plot(beta, log(R_C), '.', beta, v)
xlabel('\beta','fontsize',14,'fontweight','b','color','k')
ylabel('log(R_{0UD})','fontsize',14,'fontweight','b','color','k')

figure(4)
plot(mu, log(R_C), '.', mu, v)
xlabel('\mu','fontsize',14,'fontweight','b','color','k')
ylabel('log(R_0)','fontsize',14,'fontweight','b','color','k')
%

figure(5)
plot(cn, log(R_C), '.',cn, v)
xlabel('c','fontsize',14,'fontweight','b','color','k')
ylabel('log(R_0)','fontsize',14,'fontweight','b','color','k')
xlim([0.8 1.1])


figure(6)
plot(mu1, log(R_C), '.', mu1, v)
xlabel('\mu_1')
ylabel('log(R_0)')



figure(7)
```

```
plot(alpha, log(R_C), '.', alpha, v)
xlabel('\alpha')
ylabel('log(R_0)')


figure(8)
plot(rho, log(R_C), '.', rho, v)
xlabel('\rho')
ylabel('log(R_0)')

figure(9)
plot(eta1, log(R_C), '.', eta1, v)
xlabel('\eta_1')
ylabel('log(R_0)')

figure(10)
plot(eta2, log(R_C), '.', eta2, v)
xlabel('\eta_2')
ylabel('log(R_0)')

figure(11)
plot(omega, log(R_C), '.', omega, v)
xlabel('\omega')
ylabel('log(R_0)')

figure(12)
plot(omega, log(R_C), '.', Lambda, v)
xlabel('\Lambda')
ylabel('log(R_0)')
```

A.3.2.15 Create matrices

```
% This code must be saved as read_in_data.m
%   creates matrices: outcome[sim#][time] from input variable file
%   and parameters[sim#][paramter] from inpt parameter file
```

```
function [parameters, outcome] = read_in_data(N, num, latin_output)


for i = 1:N  % N is sim number
for j = 1:num % num is "time"

%Eof=fscanf(vfile,"%f",&temp);
outcome(i,j) = latin_output(i,j);
% see c file...outcome and parameters are set to the same thing
end
end

%reading in parameter data

for i = 1:N
for j = 1:num
%Eof=fscanf(pfile,"%f",&temp);
parameters(i,j)= latin_output(i,j);
end
end
```

A.3.2.16 Contacts

```
%This code must be saved as repnumberAndContacts.m~
% parameters
Pi =
rho = 0.2;
omega = 8.12*10^-3;
beta = 1;
K = 10^7;
mu = 5.48*10^-5;
delta1 = 0.012;
delta2 = 0;
gamma1 = 0.02;
gamma2 = 0.2;
Kp = 10^8;
```

```
alpha1 = 0.5;
alpha2 = 50;
r = 0.7;
mup= 0.02;
Q1 = (mu+delta1+gamma1); Q2 = (mu +delta2+gamma2); Q4= (mup-r);
Beta = linspace(0,0.2,100);
c = linspace(0,0.2,100);
[beta,C] = meshgrid(Beta,c);
R = rho*Pi./(mu*Q1.*Q4).*(beta*alpha1/K +C.*Q4) + ...
(1-rho)*Pi./(mu*Q2.*Q4).*(beta*alpha2/K +C.*Q4);
%surf(beta,C,R)
meshc(C,beta,R)
%, 'FaceColor', 'magenta','EdgeColor','blue')
xlabel('C');
ylabel('\beta');
zlabel('R_0(C,\beta)');
grid on
```

A.3.2.17 Constraints and samples

```
%This code must be saved as samples.m

function [para] = samples(N,num, constraints, paraval)

used = zeros(100,1500);

for i=1:num
for j=1:N
used(i,j)=0;
end
end

for j=1:N
for i=1:num
if constraints(i)==0
found=0;
```

```
while found==0
choice= 1 + round((N-1)*rand);

if (choice<=N)

if (used(i,choice)==0)
used(i,choice)=1;
para(j,i)=paraval(i,choice);
found=1;
end

end
end
end
end
end
```

A.3.2.18 Parameters definition

This code must created and saved as parapdfs.txt in Microsoft office Excel for example. It indicates the range and peak of each parameter value used. Besides, a text document must be created to save the LHS values and this document must be saved as lhstable.txt

```
name   kind    start      finish    peak

delta1 0    0.000066     0.9       0.37
delta2 0    0.00031      0.7       0.001
beta   0    0.15         0.8       0.48
mu     0    0.040        5         2.1
cn     0    1            10        4.3
mu1    0    0.008        0.9       0.4
alpha  0    0.0002       0.5       0.5
rho    0    0.01         0.9       0.7
eta1   0    0            1         0.16
eta2   0    1            5         1.7
```

omega	0	0.02	0.5	0.2
Lambda	0	0.040	5	2.1

A.3.3 Data fitting

The Following code was used to produce Figure 4.2. The other fitting graphs are obtained by changing the system of differential equations, the parameters values and range contained in this code.

```
% This function must be saved as ebolafitbehaviour.m
 function ebolafitbehaviour(do_estimation)
 warning off;
 P_Data(:,1)=[1:19]; %Sierra Leone
 %P_Data(:,1)=[1:21]; %Liberia
 % cumulative number of Ebola cases, data from 2014
to 2015, monthly
 %P_Data(:,2)=[ 12 13 51 249 1082 3280 4665 7168...
 % 7862 8478 9238 9602 10212 10666 10666 10673 ...
 %10672 10672 10672 10675 10675 ]./ 100; % Liberia
 P_Data(:,2)=[ 158 525 907 1813 3706 6599...
 9004 10340 11301 11841 12362 12701 13093 ...
 13264 13541 13846 14052 14122 14122 ]./ 700; % SierraLeone

 Lambda = 60000; % sierra Leone
 %Lambda = 30000; % Liberia
 p = 0.8;
 rho= 0.62;
 mu = 0.012;
 eta = 2.1;
 beta = 0.00000001;
 alpha = 0.01;
 delta = 0.6;
 k=0.0044;
 Q1= alpha + mu + delta;
 %S0=4600000; I0= 1; D0=0; %Liberia
```

```
S0=7396000; I0= 1; D0=0; % Sierra Leone
INITIAL=[S0, I0, D0];
Istart= 1;    %month to start the model simulation
%Iend= Istart + 19; %Sierra Leone
Iend= Istart + 21;  % Liberia

OPTIONS=odeset('AbsTol',0.001,'RelTol',0.001,'MaxStep',1/12);

%Estimate parameters
%by minimizing the sum of squares
%when fitting modeled to real prevalence data
do_estimation=1;
if(do_estimation)
xdata=P_Data(:,1)';
ydata=P_Data(:,2)';
x0(1,1)= 30000;
x0(1,2)=0.8;
x0(1,3)= 0.62;
x0(1,4)=0.012;
x0(1,5)=2.1;
x0(1,6)= 0.00000001;
x0(1,7)= 0.01;
x0(1,8)= 0.0044;
x0(1,9)= 0.6;
% Parameters range, LB = upper bound, LB = lower bound
LB=[0.1001  0.1 0.6 0.010 2 0.0000001 0.0100
0.001 0.5];%both
UB=[ 60000  0.9 0.9 0.8 5 0.000005 0.9 0.5 0.9]; % Sierra Leone
%UB=[ 30000  0.9 0.9 0.8 5 0.000005 0.9 0.5 0.9]; % Liberia
x=lsqcurvefit(@Model_Inc,x0,xdata,ydata,LB,UB,optimset);

'estimated parameters'
Lambda =x(1)
p =x(2)
rho  =x(3)
mu =x(4)
```

```
eta =x(5)
beta =x(6)
alpha=x(7)
k=x(8)
delta=x(9)
end
[t y] = ode45(@ebolafitbehaviour,[0:1/12:(Iend-Istart)], INITIAL);
S=y(:,1);
I=y(:,2);
D=y(:,3);
incidence = y(:,2);
close all;
figure(1);
hold on
h_l=plot(Istart+t,y(:,2),'r-');
set(h_l,'linewidth',2);
h_l=plot(P_Data(:,1),P_Data(:,2),'bo','Markersize',8);
set(h_l,'linewidth',2);
box off
axis([Istart Iend 0 10]);
% The ylimit is corrected on the final i.e multiplied by ...
%100 for Liberia
% and by 700 for Sierra Leone since the initial data ...
%where divided by those numbers.
ylim([0 25]) % Sierra Leone
%ylim([0 150]) % Liberia
%title('Ebola Prevalence(%)');
% xticks([ 1 2 3 4 5 6 7 8 9 10 11 12 13 14 15 16 17 18...
% 19 20 21]) % Liberia
%      xticklabels({'April_{2014}','May','Jun','Jul',...
%'Aug','Sept','Oct','Nov','Dec','Jan_{2015}','Feb',...
%'Mar','Apr','May','Jun','Jul','aug',...
%'Sept','Oct','Nov','Dec'})

xticks([ 1 2 3 4 5 6 7 8 9 10 11 12 13 1...
%4 15 16 17 18 19]) % Sierra Leone
```

```
xticklabels({'Jun_{2014}','Jul','Aug','Sept',...
'Oct','Nov','Dec','Jan_{2015}','Feb','Mar',...
'Apr','May','Jun','Jul','aug',...
'Sept','Oct','Nov','Dec'})

xlabel('Months','fontsize',12)
ylabel('Cumulative number of Ebola cases','fontsize', 12)
xtickangle(-45)
hold off

function [ydot]=ebolafitbehaviour(t,y)
S=y(1);
I=y(2);
D=y(3);

ydot(1) = Lambda - (beta*(1-p)*(y(2) + eta*y(3))*exp(-((y(2)+ ...
eta*y(3))*k)))*y(1)- mu*y(1);
ydot(2) = (beta*(1-p)*(y(2) + eta*y(3))*exp(-((y(2)+ ...
eta*y(3))*k)))*y(1) - Q1*y(2);
ydot(3) = delta*y(2) - rho*y(3);
ydot=ydot';

end % function


function Inc=Model_Inc(x0,xdata)

Inc=0;      %intialization of this not to have an empty array
Lambda =x0(1);
p=x0(2);
rho=x0(3);
mu =x0(4);
eta =x0(5);
beta=x0(6);
alpha=x0(7);
k=x0(8);
```

```
delta=x0(9);
%S0=4600000; I0=1;    D0=0; %Liberia
S0=7396000; I0= 1; D0=0;  % Sierra Leone
INITIAL=[S0, I0, D0];
OPTIONS=odeset('AbsTol',0.001,'RelTol',0.001,'MaxStep',1/12);
tdur=50;
[t y] = ode45(@ebolafitbehaviour, [0:1/12:Iend-Istart], INITIAL);
S=y(:,1);
I=y(:,2);
D=y(:,3);
incidence= y(:,2);
for j=1:length(xdata)
ind=find(xdata(j)-Istart==t);
S=y(ind,1);
I=y(ind,2);
D=y(ind,3);
Inc(j)= I;
end

end      % end of Model_prev

end      %end of ebola_fit
```

A.3.4 Impusive differential equations

The following code was developed from a template for coding impulsive differential equations, initially formulated by Robert Smith ? [180]. It is used to plot Figure 5.5.

A.3.5 system of ordinary differential equations

```
% This code must be saved as impulse_strain_ode.m
function yp=impulse_strain_ode(t,y)

%we define the parameters of the system

global Lambda beta1 beta2 mu eta1 eta2 varphi1 ...
```

```
varphi2 alpha1 alpha2 pi rho1 rho2

% varphi1 and varphi2 represent the ...
%disease induced death rates of the infected,
% S= y(1), I1= y(2), D1 = y(3), I2 = y(4),...
% D2 = y(5), y(6) represents
% the maximal solution of the the differential equation with ...
% impule
yp(1,:)=Lambda - (beta1.*(y(2)+ eta1.*y(3)) + beta2.*(y(4)+ ...
eta2.*y(5))).*y(1)- mu*y(1);
yp(2,:)=beta1.*(y(2)+ eta1.*y(3)).*y(1) - (mu + alpha1 +...
varphi1).*y(2);
yp(3,:)=  varphi1.*y(2) - rho1.*y(3);
yp(4,:)= beta2.*(y(4)+ eta2.*y(5)).*y(1) - (mu + alpha2 +...
varphi2).*y(4);
yp(5,:)= varphi2.*y(4) - rho1.*y(5);
yp(6,:)= (((Lambda.*(Lambda + pi).*beta2.*(rho2 + ...
eta2.*varphi2))./((mu^2.*rho2).*(mu + alpha2 + varphi2))) ...
- 1).*(mu + alpha2 + varphi2).*y(6);
```

A.3.6 Plotting command

```
% This code must be saved as impulse_strain.m
clear all
global Lambda beta1 beta2 mu eta1 ...
eta2 varphi1 varphi2 alpha1 alpha2 pi  rho1 rho2
Lambda = 8.37;
varphi1 = 0.5;
rho1= 0.9;
mu = 0.1;
eta1 = 2.5;
beta1 = 0.00009;
alpha1 = 0.012;
varphi2 = 0.5;
rho2 = 0.9;
eta2 = 2.5;
beta2 = 0.00009;
```

```
alpha2 = 0.012;
pi = 500; % we change the value of \pi ...
when needed and run the code several times
t0=0;
tq=[];
yq=[];
tfinal=20;
x0=[16000 2 0 2 0 2]; % ODE initial conditions
tq=[];
xq=[];
mq=[];
t0=0;
reps = 5; % number of impulses (n)
tau=4; %timespan between two impulses
%tau = sort(t0 + (tfinal - t0)*rand(1,reps), 'ascend');
%tau = sort(t0 + (tfinal - t0)*rand(1,reps), 'descend');


for i=1:reps
tspan =[t0 tau+t0]; %ascend
%tspan=[t0+tau t0]; %descend
%tspan=[t0 12];
[t,x] = ode45(@impulse_strain_ode,tspan,x0);
n=length(x);
x0=x(n,:);
x0(4)=x(n,4) + pi;
x0(6)= x(n,6) + pi;
tf=t(n);
tq=[tq;t(1:n)];
xq=[xq;x((1:n),:)];
mq=[mq;mean(x)];
t0=tf;
end
hold on
plot(tq,xq(:,2),'b--',tq,xq(:,4),'g-', 'linewidth', 2)
%plot(tq,xq(:,1),tq,xq(:,2),tq,xq(:,3),tq,xq(:,4),tq,xq(:,5))
```

```
%axis ([ 0 40 0 400])
 xlabel('Time(months)')
 ylabel('Infected population size')
```

A.3.7 Dynamics of the population

The following code was used to plot Figures 6.7 and 6.8. The other population dynamics graphs can be obtained by changing the ODE system and the parameters value.

A.3.7.1 System of ODE

```
% This code must be saved as economic_ode.m
function [ydot] = economic_ode(t,y)
%%
%%
% List all parameters below
global  Lambda1 Lambda2 m sigma21 sigma12 alpha_1 alpha_2 beta_1 ...
pi_1 pi_2 r_1 r_2 eta_1 beta_2  eta_2  mu
epsilon1 theta21 ...
theta12 phi_1 rho_1 phi_2 rho_2 delta1 delta2 epsilon2;

% Define all variables
% S_1 = y(1), E_1 = y(2), I_1 = y(3), D_1 = y(4),
%M_1 = y(5), S_2 = y(6),
%E_2 = y(7),I_2 = y(8), D_2 = y(9),M_2 = y(10)

% Assign Model parameter Values

Lambda1 = 3000.2;
Lambda2 = 2000.2;
beta_1 = 0.001;
eta_1 = 1.01;
beta_2 = 0.0008;
eta_2 = 1.25;
mu = 0.01;
```

```
alpha_1= 0.1751;
alpha_2 = 0.1751;
rho_1 = 0.2;
rho_2 = 0.49;
pi_1 = 50;
pi_2= 50;
r_1 = 0.5;
r_2= 0.5;
phi_1 = 0.750;
phi_2 = 0.5;
epsilon1=100;
epsilon2=100;
sigma12 = 0.5;
theta12= 0.7;
sigma21 = 0; % We set this value to zero in the case of a one way.
theta21= 0; % We set this value to zero in the case of a one way.
m=0.9;
delta1 = 0.08;
delta2 = 0.12;
Q_1 =  mu + alpha_1 + phi_1;
Q_2  = mu + alpha_2 + phi_2;
P1 = mu + delta1;
P2 = mu + delta2;
ydot(1) = Lambda1 - (beta_1*(y(3)+ eta_1*y(5)) + mu)*y(1) +...
theta12*(1 - m)*y(6) - theta21*(1 - m)*y(1);
ydot(2) = (beta_1*(y(3)+ eta_1*y(5)))*y(1)
- P1*y(2) +...
sigma12*(1 - m)*y(7) - sigma21*(1 - m)*y(2);
ydot(3) = delta1*y(2)  - Q_1*y(3);
ydot(4) = -r_1*y(4)*(y(4) - pi_1*(1 - (y(3)/(y(3) + epsilon1))));
ydot(5) = phi_1*y(3) - rho_1*y(5);
ydot(6) = Lambda2 - (beta_2*(y(8)+ eta_2*y(10)) + mu)*y(6)- ...
theta12*(1 - m)*y(6) + theta21*(1 - m)*y(1);
ydot(7) = (beta_2*(y(8)+ eta_2*y(10)))*y(6)
- P2*y(7) - ...
sigma12*(1 - m)*y(7) + sigma21*(1 - m)*y(2);
```

```
ydot(8) = delta2*y(7) - Q_2*y(8);
ydot(9) = -r_2*y(9)*(y(9) - pi_2*(1 - (y(8)/(y(8) + epsilon2))));
ydot(10) = phi_2*y(8) - rho_2*y(10);
ydot = ydot';

end
```

A.3.7.2 Plotting the solutions of the ODE

```
% This code must be saved as economic_plot.m
%[t,y] = ode45('sylvie_work',[0 100],[2000,10,0,0,0]);
% initial conditions for the variables
[t,y] = ode45('economic_ode',[0 150],[300000,3,3,10,0 ...
,300000,3,3,0,10]);
figure(6)
plot(t,y(:,3),'b-*','linewidth',2)
axis([0 100 0 40000]);
xlabel('Time (days)');
%title('All classes');
ylabel('Infected population size (I_1)');
% use the appropriate legend when changing the parameter
legend('m = 0.1', 'm = 0.5', 'm = 0.9')
%legend('\sigma_{12} = 0.9', '\sigma_{12} = 0.5', ...
'\sigma_{12} = 0.1')
legend('location','northeast')
box off
hold on
```

A.3.8 Region of existence of endemic equilibrium point

The following code was used to produce Figure 5.2.

```
x = [0; 1; 2; 3];
y = [0;  1; 2; 0];
y(1,1)=0;
y(1,2)=-260;
fig = figure
area(x,y)
```

```
axis([0 2 0 2])
box off
```

A.4 Excel sheets

A.4.1 Number of EVD cases and beds

The following tables were typed in an Excel sheet and used to plot respectively Figures 3.7 and 3.8.

Liberia

Year-Month	New Ebola cases	Number of beds
14-Mar	0	
Apr	0	
May	1	
Jun	157	
Jul	367	
Aug	382	
Sept	906	481
Oct	1893	862
Nov	2893	843
Dec	2405	918
15-Jan	1336	645
Feb	961	577
Mar	537	577
Apr	521	349

Sierra Leone

Year-Month	New Ebola cases	Number of beds
14-Mar	0	
Apr	0	
May	1	
Jun	157	
Jul	367	
Aug	382	
Sept	906	318
Oct	1893	315
Nov	2893	328
Dec	2405	783
15-Jan	1336	1,180
Feb	961	1,177
Mar	537	1,038
Apr	521	580

A.4.2 Gross national income data

The following data were used to draw Figure 6.1 from an Excel sheet.

Years	Guinea	Liberia	Sierra Leone	Sub-saharan Africa
1962		160		160
1963		160		147,6373644
1964		190	160	150,2969815
1965		200	160	157,9041895
1966		210	160	162,4116511
1967		220	150	166,0408403
1968		230	140	172,2087119
1969		240	150	186,7842627
1970		250	160	208,996667
1971		260	170	223,8934766
1972		280	170	238,0997922
1973		290	190	277,5369547
1974		340	230	361,0017663
1975		370	250	417,6644148
1976		410	230	443,4075798
1977		430	220	457,1672474
1978		470	240	483,9758955
1979		520	310	567,7277137
1980		520	370	669,7637963
1981		500	360	715,0953278
1982		440	350	679,4290896
1983		360	300	581,7775042
1984		360	290	534,2830876
1985		360	240	493,5675282
1986		350	170	495,3457129
1987		360	180	546,8874235
1988	430	400	170	621,5122053
1989	420	290	210	627,4459111
1990	430		190	599,83
1991	430		170	589,182
1992	460		130	566,998
1993	470		160	543,106
1994	460		160	520,391
1995	470		180	535,194
1996	470		210	555,062
1997	470	120	200	568,4427512
1998	430	130	170	531,2909949
1999	420	120	150	515,9731428
2000	380	150	140	503,4447344
2001	340	130	150	491,7505485
2002	330	120	200	485,1201613
2003	320	80	270	529,62365
2004	350	90	270	662,1553338
2005	340	120	280	801,3033129
2006	300	130	300	921,5501229

Years	Guinea	Liberia	Sierra Leone	Sub-saharan Africa
2007	310	160	360	1027.898718
2008	350	180	420	1145.890079
2009	390	220	440	1181.795843
2010	400	250	420	1283.196049
2011	420	320	420	1405.434704
2012	440	340	530	1620.453916
2013	470	370	650	1674.959721
2014	490	370	690	1737.641724
2015	490	380	550	1651.550407
2016	490	370	490	1505.387001

List of references

[1] WHO. Ebola maps, 2016. http://www.who.int/csr/disease/ebola/global_ebolaoutbreakrisk_20140818-1.png?ua=1, (accessed on May 30, 2016).

[2] World Bank. Data-low countries, 2015. https://datahelpdesk.worldbank.org/knowledgebase/articles/906519-world-bank-country-and-lending-groups, (accessed on January 18, 2017).

[3] JJ Muyembe et al. Ebola virus outbreaks in Africa: past and present. *Onderstepoort Journal of Veterinary Research*, 79:1–8, 2012.

[4] WHO. Ebola data and statistics, 2017. http://apps.who.int/gho/data/node.ebola-sitrep.ebola-country-GIN-20141112?lang=en, (accessed on February 27, 2017).

[5] CDC. Ebola virus disease distribution map, 2017. https://www.cdc.gov/vhf/ebola/outbreaks/history/distribution-map.html, (accessed on May 12, 2017).

[6] WE Diehl et al. Ebola virus glycoprotein with increased infectivity dominated the 2013–2016 epidemic. *Cell*, 167:1088–1098.e6, 2016.

[7] KA Alexander et al. What factors might have led to the emergence of Ebola in West Africa ? *Plos Neglected Tropical Diseases*, 9:e0003652, 2015.

[8] H Feldmann, TW Geisberg. Ebola haemorrhagic fever. *Lancet*, 387:849–862, 2011.

[9] EM Leroy et al. Human asymptomatic Ebola infection and strong inflammatory response. *Lancet*, 355:2210–2215, 2000.

[10] WHO. Ebola and Marburg disease epidemics: preparedness, alert, control and evaluation, 2014. http://www.who.int/csr/disease/ebola/manual_EVD/en/, (accessed on May 26, 2016).

[11] M Kishowski, G Chowell. Modeling household and community transmission of Ebola virus disease: Epidemic growth, spatial dynamics and insights for epidemic control. *Virulence*, 7:163–173, 2015.

[12] S Baize et al. Emergence of Zaire Ebola virus disease in Guinea. *The New England Journal of Medicine*, 371:1418–1425, 2014.

[13] MG Dixon, IJ Schafer. Ebola virus disease outbreak-West Africa. *Morbity and Mortality Weekly Report*, 63:548–551, 2014.

[14] M Awumbila et al. Across artificial borders: an assessment of labour migration in the ECOWAS region. Technical report, ACP Observatory on Migration, International Organization for Migration, 2014. http://publications.iom.int/system/files/pdf/ecowas_region.pdf, (accessed on May 29, 2016).

[15] ECOWAS-SWAC/OECD. *Atlas on regional integration in West Africa*. OECD, 2006. https://www.oecd.org/migration/38409521.pdf, (accessed on May 29, 2016).

[16] R Maconachie et al. Temporary labour migration and sustainable post-conflict return in Sierra Leone. *GeoJournal*, 67:223–240, 2006.

[17] Government of the Republic of Liberia. 2008 population and housing census final results. Monrovia, Liberia. Technical report, Liberia Institute of Statistics and Geo-Information Services, 2009. http://www.google.com/url?sa=t&rct=j&q=&esrc=s&source=web&cd=1&ved=0ahUKEwig2tDDrv_MAhXJKcAKHfCADzUQFggdMAA&url=http%3A%2F%2Funstats.un.org%2Funsd%2Fdnss%2FdocViewer.aspx%3FdocID%3D2075&usg=AFQjCNFt_Y4r2kn4GqP4oflURWH2aA_KfQ&sig2=Flj6GzP6XXIknxVmW9kHKg, (accessed on May 29, 2016).

[18] V Piana. Gross Domestic Product, 2001. http://www.economicswebinstitute.org/glossary/gdp.htm, (accessed on June 1, 2016).

[19] United Nations. UNdata, statistics, per capita GDP at current prices-US dollars. 2016. http://data.un.org/Data.aspx?d=SNAAMA&f=grID%3A101%3BcurrID%3AUSD%3BpcFlag%3A1, (accessed on June 1, 2016).

[20] World Bank. Economic conditions and prospect of Zaire, 1997. http://www-wds.worldbank.org/external/default/WDSContentServer/WDSP/IB/2002/\10/18/000178830_98101911450677/Rendered/PDF/multi0page.pdf, (accessed on June 1, 2016).

[21] African Development Bank Group. West Africa monitor. Technical report, African Development Bank Group, 2013. https://www.afdb.org/fileadmin/uploads/afdb/Documents/Publications/West_Africa_Monitor_2013.pdf, (accessed on January 15, 2016).

[22] The World Bank Group. The economic impact of the 2014 Ebola epidemic: short and medium term estimates for West Africa. Technical report, The World Bank Group, 2014. http://documents.worldbank.org/curated/en/194681468119639844/pdf/929950PUB0Box30UBLIC009781464804380.pdf, (accessed on May 28, 2017).

[23] CDC. Cost of the Ebola epidemic. Technical report, Centers for Disease Control and Prevention, 2016. https://www.cdc.gov/vhf/ebola/pdf/impact-ebola-economy.pdf, (accessed on June 15, 2017).

[24] A Zafar et al. 2014–2015 West Africa Ebola crisis: impact update. Technical report, World Bank, 2016. http://pubdocs.worldbank.org/en/297531463677588074/Ebola-Economic-Impact-and-Lessons-Paper-short-version.pdf, (accessed on June 12, 2017).

[25] WHO. *Monitoring the building blocks of health systems: a handbook of indicators and their measurements strategies*. WHO, 2010.

[26] United Nations, Economic mission for Africa. Socio-economic impacts of the Ebola virus disease on Africa. Technical report, United Nations, 2014.

[27] United Nations, World Bank, European Commission, African Development Bank. Recovering from the Ebola crisis. Technical report, United Nations, 2015.

[28] CDC. 2014 Ebola outbreak in West Africa-case counts, 2014. http://www.cdc.gov/vhf/ebola/outbreaks/2014-west-africa/case-counts.html, (accessed on July 30, 2016).

[29] W Collins, E Berscheid. The relationship context of human behaviour and development. *Psychological Bulletin*, 126:844–872, 2000.

[30] J Lambo et al. Communication for behavioural impact. Technical report, WHO, 2012. http://apps.who.int/iris/bitstream/handle/10665/75170/WHO_HSE_GCR_2012.13_eng.pdf;jsessionid=BF1C5141AF2E27ECA07834E96A975138?sequence=1, (accessed on July 11, 2017).

[31] S Funk, M Gwenan. Ebola: the power of behaviour change. *Nature*, 515:492, 2014.

[32] CM Rivers et al. Modeling the impact of interventions on an epidemic of Ebola in Sierra Leone and Liberia. *Plos Current Outbreaks*, 6:1–14, 2014.

[33] WHO. Ebola and Marburg virus disease epidemics: preparedness, alert, control, and evaluation, 2014. http://apps.who.int/iris/bitstream/10665/130160/1/WHO_HSE_PED_CED_2014.05_eng.pdf?ua=1&ua=1, (accessed on July 30, 2016).

[34] MC Auld. Ebola-local beliefs and behaviour change. Technical report, Health and Education Advice and Research team, 2014. http://www.heart-resources.org/wp-content/uploads/2014/11/Final-Ebola-Helpdesk-Report.pdf, (accessed on July 30, 2016).

[35] AJ Kucharski et al. Measuring the impact of Ebola control measures in Sierra Leone. In *Proceedings of the National Academy of Sciences of the United States of America*, volume 112, pages 14366–14371, 2015.

[36] A Pandey et al. Strategies for containg Ebola in West Africa. *Sciencexpress*, 346:991–995, 2014.

[37] MI Meltzer et al. Estimating the fututre number of cases in the Ebola epidemic - Liberia and Sierra Leone, 2014-2015. *Morbidity and Mortality Weekly Report*, 63:1–14, 2014.

[38] CL Althaus. Estimating the reproduction number of Ebola virus (EBOV) during the 2014 outbreak in West Africa. *Plos Current Outbreaks*, 6:ecurrents.outbreaks.91afb5e0f279e7f29e7056095255b288, 2014.

[39] G Chowell, H Nishiura. Transmission dynamics and control of Ebola virus disease (EVD): a review. *BMC Medicine*, 12:196, 2014.

[40] D Fisman, E Khoo, A Tuite. Early epidemics of the West African 2014 Ebola outbreak: estimates derived with a simple two-parameter model. *Plos Currents Outbreaks*, 6:ecurrents.outbreaks.89c0d3783f36958d96ebbae97348d571, 2014.

[41] S Towers, O Patterson-Lomba, C Castillo-Chavez. Temporal variations in the effective reproduction number of the 2014 West Africa Ebola outbreak. *Plos Current Outbreaks*, 6:ecurrents.outbreaks.9e4c4294ec8ce1adad283172b16bc908, 2014.

[42] SE Bellan et al. Ebola control: effect of asymptomatic infection and acquired immunity. *The Lancet*, 384:1499–1500, 2014.

[43] AG Baxter. Symptomless infection with Ebola virus . *The Lancet*, 355:2178–2179, 2014.

[44] A Rachab, DFM Torres. Mathematical modelling, simulation and optimal control of the 2014 Ebola outbreak in West Africa. *Discrete Dynamics in Nature and Society*, 2015.

[45] SD Djiomba, F Nyabadza. Modelling the potential role of media campaigns in Ebola transmission dynamics. *International Journal of Differential Equations*, 2017, 2017.

[46] United Nations Development Group. Socio-economic impact of Ebola virus disease in West African countries. A call for national and regional containment, recovery and prevention. Technical report, United Nations, 2015. http://reliefweb.int/sites/reliefweb.

int/files/resources/ebola-west-africa.pdf, (accessed on May 26, 2016).

[47] CP Bhunu, S Mushayabasa, RJ Smith ? Assessing the effects of poverty in tuberculosis transmission dynamics. *Applied Mathematical Modelling*, 36:4173–4185, 2012.

[48] OC Collins, SL Robertson, KS Govinder. Analysis of a water-borne disease model with socio-economic classes. *Mathematical Biosciences*, 269:86–93, 2015.

[49] AM Plucinski et al. The role of socio-economic status in longitudinal trends of cholera in Matlab, Bangladesh, 1993–2007. *Plos Neglected Tropical Diseases*, 7:e1997, 2013.

[50] A Camacho et al. Potential for large outbreaks of Ebola virus disease. *Epidemics*, 9:70–78, 2014.

[51] KVLN Ramacharyulu, NC Pattabhi Ramacharyulu. On the stability of an Ammensal-enemy harvested species pair with limited resources. *International Journal of Open Problems in Computer Science*, 4:1–16, 2010.

[52] L Zhou, M Fan. Dynamics of an SIR model with limited medical ressouces revisited. *Non Linear Analysis: Real World Applications*, 13:312–324, 2012.

[53] A Abdelrazec et al. Modelling the spread and control of dengue with limited public resources. *Mathematical Biosciences*, 271:136–145, 2016.

[54] P Nouvellet et al. The role of rapid diagnostics in managing Ebola epidemics. *Nature*, 528:109–116, 2015.

[55] JA Lewnard et al. Dynamics and control of Ebola virus transmission in Montserrado, Liberia: a mathematical modeling analysis. *Lancet Infectious Diseases*, 14:1189–1195, 2014.

[56] PK Drain. Ebola: between mathematics and reality. *Correspondance*, 15:147, 2015.

[57] SD Djiomba Njankou, F Nyabadza. An optimal control model for Ebola virus disease. *Journal of Biological Systems*, 24:29–49, 2016.

[58] E Bonyah, K Badu, SK Asiedu-Addo. An optimal control application to an Ebola model. *Asian Pacific Journal of Tropical Biomedecine*, 4:283–289, 2016.

[59] E Hansen, T Day. Optimal control of epidemics with limited resources. *Journal of Mathematical Biology*, 62:423–451, 2011.

[60] WH McNeill. *Plagues and people*. Garden City, Anchor press, 1976.

[61] S Funk, M Salathé, VAA Jansen. Modelling the influence of human behaviour on the spread of infectious diseases: a review. *Journal of the Royal Society*, 5:1247–1256, 2010.

[62] S Funk et al. Nine challenges in incorporating the dynamics of behaviour in infectious diseases models. *Epidemics*, 10:21–25, 2015.

[63] M Salathé, M Bonhoeffer. The effect of opinion clustering on disease dynamics. *Journal of the Royal Society*, 5:1505–1508, 2008.

[64] JM Epstein et al. Coupled contagion dynamics of fear and disease: mathematical and computational explorations. *Plos One*, 3:e3955, 2008.

[65] WHO. *Ebola Response, annexes: key considerations for implementing a community care center (CCC)*. WHO, 2014. http://apps.who.int/iris/bitstream/handle/10665/146469/WHO_EVD_Guidance_Strategy_14.3_eng.pdf?sequence=1, (accessed on July 14, 2017).

[66] N Ferguson. Capturing human behaviour. *Nature*, 446:733, 2007.

[67] DH Zanette, S Risau-Gusmán. Infection spreading in a population with evolving contacts. *Jounal of Biology Physics*, 34:135–148, 2008.

[68] T Gros, CJ Dommar D'Lima, C Blasius. Epidemic dynamics on an adaptative network. *Physical Review Letters*, 96:208701, 2006.

[69] LB Shaw. Fluctuating epidemics on adaptative networks. *Physical Review EE*, 77:066101, 2008.

[70] CT Bauch. Imitation dynamics predict vaccinating behaviour. *Proceedings of the Royal Society*, 272:1669–1675, 2005.

[71] CT Bauch, DJD Earn. Vaccination and the theory of game. *Proceedings of the National Academy of Sciences*, 101:13391–13394, 2004.

[72] A Perisic, CT Bauch. Social contact network and disease eradicability under voluntary vaccination. *Plos Computational Biology*, 5:e1000280, 2009.

[73] KTD Eames. Networks of influence and infection: parental choices and childhood disease. *Journal of the Royal Society*, 6:811–814, 2009.

[74] MM Tanaka, J Kum, MW Feldman. Coevolution of pathogens and cultural practices: a new look at behavioural heterogeneity in epidemics. *Theoretical Population Biology*, 62:111–119, 2002.

[75] S Del Valle et al. Effects of behavioural changes in a Smallpox attack model. *Mathematical Biosciences*, 195:228–251, 2005.

[76] S Funk et al. The spread of awareness and its impact on epidemic dynamics. *Proceedings of the National Academy of Sciences*, 106:6872–6877, 2009.

[77] IZ Kiss et al. The impact of information transmission on epidemic outbreak. *Mathematical Biosciences*, 2009.

[78] X Wang, Z Dao, J Wang. Influence of human behaviour on cholera dynamics. *Mathematical Bioscience*, 267:361–377, 2015.

[79] MC Auld. Choices, beliefs and infectious disease dynamics. *Journal of Health Economics*, 22:991–995, 2003.

[80] JR Conrad et al. *Mathematical and statistical modeling for emerging and re-emerging infectious diseases*. Springer, 2016.

[81] NTJ Bailey. *Spatial models in the epidemiology of infectious diseases, Lecture notes in Biomathematics*, volume 38. Springer, 2016. Lecture Notes in Biomathematics.

[82] FG Ball, OD Lyne. *Epidemics among a population of households*, volume 126. Springer, 2002. The IMA Volumes in Mathematics and its Applications.

[83] F Arrigoni, A Pugliese. Limits of a multi-patch SIS epidemic model. *Journal of Mathematical Biosciences*, 45:419–440, 2002.

[84] NG Becker, K Dietz. The effect of household distribution on the transmission and control of highly infectious diseases. *Elsevier*, 1994.

[85] A Mesnard, P Seabright. Migration and the equilibrium prevalence of infectious diseases. *Journal of Demographic Economics*, 82:1–26, 2016.

[86] L Sattenspiel, K Dietz. A structured epidemic model incorporating geographic mobility among regions. *Mathematical Biosciences*, 128:71–91, 1995.

[87] W Wang, X Zhao. An epidemic model in a patchy environment. *Mathematical Biosciences*, 190:97–112, 2004.

[88] J Arino, P Van Den Driesche. A multi-city epidemic model. *Mathematical Populations Studies*, 10:175–193, 2010.

[89] JB Hatson Njangara, F Nyabadza. A metapopulation model for cholera transmission dynamics between communities linked by migration. *Applied Mathematics and Computation*, 241:317–331, 2014.

[90] R Roos. Migrations in West Africa seen as challenge to stopping Ebola. *CIDRAP News*, 2014. cidrap.umn.edu/news-perspective/2014/11/migrations-west-africa-seen-challenge-stopping-ebola, (accessed on December 15, 2016).

[91] EF Doungmo Goufo, R Maritz. A note on Ebola outbreak and human migration dynamic. *Journal of Human Ecology*, 51:257–263, 2015.

[92] J Arino, P Van Den Driesche. The basic reproduction number in a multi-city compartmental epidemic model. *Lecture Notes in Control and Information Science*, 294:135–142, 2003. In: L Benvenuti, A De Santis, L Farina (eds) Positive Systems.

[93] M Ajelli et al. Spatiotemporal dynamics of the Ebola epidemic in Guinea and implications for vaccination and disease elimination: a computational modeling analysis. *BMC Medicine*, 14:130, 2016.

[94] Merler et al. Spatiotemporal spread of the 2014 outbreak of Ebola virus disease in Liberia and the effectiveness of non-pharmaceutical interventions: a computational modelling analysis. *The Lancet Infectious Diseases*, 15:204–211, 2015.

[95] K Silverman et al. A potential role of anti-poverty programs in health promotion. *Preventive Medecine*, 92:58–61, 2016.

[96] S Mushayabasa et al. A mathematical model for assessing the impact of poverty on yaws eradication. *Applied Mathematical Modelling*, 36:1653–1667, 2012.

[97] SA Pedro, JM Tchuenche. HIV/AIDS dynamics: impact of economic classes with transmission from poor clinical settings. *Journal of Theoretical Biology*, 267:481–485, 2010.

[98] AM Plucinski et al. Health safety nets can break cycles of poverty and disease: a stochastic ecological model. *Journal of the Royal Society Interface*, 8:1796–1803, 2011.

[99] AM Plucinsky et al. Clusters of poverty and disease emerge from feedbacks on an epidemiological network. *Journal of the Royal Society Interface*, 2017. http://rsif.royalsocietypublishing.org/, (accessed on January 18, 2017).

[100] CN Ngonghala et al. Poverty, disease, and the ecology of complex systems. *Plos Biology*, 12:e1001827, 2014.

[101] MH Bonds et al. Poverty trap formed by the ecology of infectious diseases. *Proceedings of the Royal Society*, 277:1185–1192, 2009.

[102] MM Pluciński et al. Clusters of poverty and disease emerge from feedbacks on an epidemiological network. *Journal of the Royal Society Interface*, 2012.

[103] D Phong Do et al. Investigating the relationship between neighborhood poverty and mortality risk: A marginal structural modeling approach. *Social Science and Medecine*, 91:58–66, 2013.

[104] WHO. Ebola situation report, 2016. http://apps.who.int/ebola/current-situation/ebola-situation-report\-3-february-2016, (accessed on February 15, 2016).

[105] European CDC. Ebola outbreak in West Africa (2013-2016). http://ecdc.europa.eu/en/healthtopics/ebola_marburg_fevers/pages/ebola-outbreak-west-africa.aspx, (accessed on September 2, 2016).

[106] WHO. Media center, Ebola virus disease. http://www.who.int/mediacentre/factsheets/fs103/en/, (accessed on September 2, 2016).

[107] JP Townsend, LA Skrip, AP Galvani. Impact of bed capacity on spatiotemporal shifts in Ebola transmission. In *Proceedings of the National Academy of Sciences of the United States of America*, volume 112, pages 14125–14126, 2015.

[108] E Tambo, EC Ugwu, JY Ngongang. Need of surveillance response systems to combat Ebola outbreaks and other emerging infectious diseases in African countries. *Infectious Diseases of Poverty*, 3:29, 2014.

[109] B Gleason et al. Establishment of an Ebola treatment unit and laboratory-Bombali district, Sierra Leone, July 2014-January 2015. *Morbidity and Mortality Weekly Report*, 64:1108–1111, 2015.

[110] C Shan , H Zhu. Bifurcations and complex dynamics of an SIR model with the impact of the number of hospital beds. *ScienceDirect*, 257:1662–1688, 2014.

[111] Humanitarian Data Exchange. Ebola treatment centers or units. https://data.humdata.org/dataset/ebola-treatment-centers/resource/e8a9fa59-5068-4d2d-855e-788c63d061e8, (accessed on October 11, 2017).

[112] WHO. WHO statistics 2013, 2016. http://www.who.int/gho/publications/world_health_statistics/EN_WHS2013_Full.pdf?ua=1, (accessed on March 14, 2016).

[113] SG Lobanov, OG Smolyanov. *Ordinary differential equations in locally convex spaces*, volume 49. Russian Mathematical Survey, 1994.

[114] AA Coddington, N Levinson. *Theory of ordinary differential equations*. TATA McGRAW-HILL production, New Delhi, 1955.

[115] P Van Den Driessche, J Watmough. Reproduction numbers and subthreshold endemic equilibria for compartmental models of disease transmission. *Mathematical Biosciences*, 180:29–48, 2002.

[116] JP LaSalle, Z Artstein. *The stability of dynamical systems, appendix A limiting equations and stability of non autonomous ordinary differential equations*, volume 15. Society for Industrial and Applied Mathematics, 1876.

[117] H Guo, MY Li. Global stability of tuberculosis model with immigration and treatment. *Canadian Applied Mathematics Quaterly*, 3, 2006.

[118] F Nyabadza, Z Mukandavire, SD Hove-Musekwa. Modelling the HIV/AIDS epidemic trends in South Africa: insights from a simple mathematical model. *Non-linear Analysis, Real Word Applications*, 12:2091–2104, 2011.

[119] C Conell Mcclusky. Lyapunov functions for tuberculosis models with fast and slow progression. *Mathematical Biosciences and Engineering*, 3:603–614, 2006.

[120] E Bereta, V Capasso. On general strucrure of epidemic systems: global asymptotical stability. *Computers and Mathematics with Applications*, 12:677–694, 1986.

[121] C Castillo-Chavez, B Song. Dynamical models of tuberculosis and their applications. *Mathematical Bioscience and Engeneering*, 2:361–404, 2004.

[122] B Gomero. Latin Hypercube Sampling and Partial Rank Coefficient analysis applied to an optimal control problem. *Tenessee Research and Creative Exchange*, 2012. http://trace.tennessee.edu/cgi/viewcontent.cgi?article=2443&context=utk_gradthes, (accessed on May 23, 2016).

[123] SM Blower et al. Drugs, sex and HIV: A mathematical model for New York city. *Philosophical Transactions:Biological Sciences*, 331:171–187, 1991.

[124] R Taylor. Interpretation of the correlation coefficient. a basic review. *Journal of Diagnostic Medical Sonography*, 6:35–39, 1990.

[125] RK Upadhyay, P Roy. Deciphering dynamics of recent epidemic spread and outbreak in West Africa: the case of Ebola virus. *International Journal of Bifurcations and Chaos*, 26:1630024, 2016.

[126] Y kuznetsov. *Elements of applied bifurcation theory*, volume 112. Springer Verlag, 1998.

[127] KP Hadeler, P Van Den Driessche. Backward bifurcation in epidemic control. *Mathematical Biosciences*, 146:15–35, 1997.

[128] AB Gumel. Causes of backward bifurcations in some epidemiological models. *Journal of Mathematical Analysis and Applications*, 395:1355–365, 2012.

[129] CDC. 2014 Ebola outbreak in West Africa-case count, 2016. http://www.cdc.gov/vhf/ebola/outbreaks/2014-west-africa/case-counts.html, (accessed on May 21, 2016).

[130] Z Xia et al. Modelling the transmission dynamics of Ebola virus disease in Liberia. *Scientific Reports*, page 13857, 2015.

[131] M Dubois et al. The Ebola response in West Africa, exposing the politics and culture of international aid. *Humanitarian Policy Group*, 2016. https://www.odi.org/sites/odi.org.uk/files/odi-assets/publications-opinion-files/9903.pdf, (accessed on May 21, 2016).

[132] CDC. Ebola virus disease, previous case counts, 2016. http://www.cdc.gov/vhf/ebola/outbreaks/2014-west-africa/previous-case-counts.html, (accessed on May 21, 2016).

[133] WHO. Ebola situation reports, 2016. http://www.who.int/csr/disease/ebola/situation-reports/archive/en/, (accessed on May 21, 2016).

[134] N Verdière et al. Mathematical modelling of human behaviour during catastrophic events. *HAL*, 2014. https://hal-insu.archives-ouvertes.fr/hal-00992945/document, (accessed on May 3, 2017).

[135] A Rachab, DFM Torres. Predicting and controlling the Ebola infection. *Mathematical Methods in the Applied Sciences*, 40:6155–6164, 2015.

[136] G Chowell et al. The basic reproductive number of Ebola and the effects of public health measures: the cases of Congo and Uganda. *Journal of Theoretical Biology*, 229:119–126, 2004.

[137] JS Weitz, J Dushoff. Modeling post-death transmission of Ebola: challenges for inference and opportunities for control. *Scientific reports*, 5(8751), 2015.

[138] J Legrand et al. Understanding the dynamics of Ebola epidemics. *Epidemiology and Infection*, 135:610–621, 2007.

[139] Z Xia et al. Modelling the transmission dynamics of Ebola virus disease in Liberia. *Scientific Reports*, 5(13857), 2015.

[140] SY Delvalle, SM Mniszewisky, JM Hyman. Modeling the impact of behavior changes on the spread of pandemic influenza. In *Modeling the interplay between human behavior and the spread of infectious diseases*, pages 59–77. Springer New York, 2013.

[141] P Lio et al. Risk perception, heuristics and epidemic spread. In *Modeling the interplay between human behavior and the spread of infectious diseases*, pages 139–152. Springer New York, 2013.

[142] SM Fast et al. The role of social mobilization in controlling Ebola virus in Lofa, Liberia. *Plos Current Outbreaks*, 7:ecurrents.outbreaks.c3576278c66b22ab54a25e122fcdbec1, 2015.

[143] G Chowell et al. The Western Africa Ebola virus disease exhibits both global exponential and local polynomial growth rate. *Plos Currents Outbreaks*, 7:ecurrents.outbreaks.8b55f4bad99ac5c5db3663e916803261, 2015.

[144] MW McCoy et al. Predicting predation through prey ontogeny using size-dependent functional response models. *The American Society of Naturalist*, 177:752–766, 2011.

[145] B Tsanou et al. A simple mathematical model for Ebola in Africa. *Journal of Biological Dynamics*, 11:42–14, 2017.

[146] CDC. Ebola-prevention, 2014. https://www.cdc.gov/vhf/ebola/prevention/index.html, (accessed on April 28, 2017).

[147] C Siettos et al. Modelling the 2014 Ebola virus epidemic, agent-based simulations, temporal analysis and future predictions for Liberia and Sierra Leone. *Plos Currents Outbreaks*, 7:ecurrents.outbreaks.8d5984114855fc425e699e1a18cdc6c9, 2015.

[148] WHO. Ebola data and statistics, 2017. http://apps.who.int/gho/data/node.ebola-sitrep.ebola-country-GIN-20141112?lang=en, (accessed on February 27, 2017).

[149] News24. Infectious disease, 2014. www.health24.com, (accessed on May 12, 2017).

[150] X Pourrut et al. The natural history of Ebola virus in Africa. *Microbes and Infection*, 17:1005–1014, 2005.

[151] S Baize. Ebola virus disease in West Africa: new conquered territories and new risks-or how I learned to stop worrying and (not) love Ebola virus. *Current Opinion in Virology*, 15:70–76, 2015.

[152] L Campbell. *Learning from the Ebola Response in cities: Population movement*. ALNAP Working Paper, 2017.

[153] GB Nkamleu, L Fox. Taking stock of research on internal migration in sub-saharan Africa. *Munich Personal RePEc Archive*, 2009. http://mpra.ub.uni-muenchen.de/15112, (accessed on July 16, 2017).

[154] W Shaw. *Migration in Africa: A Review of the Economic Literature on International Migration in 10 Countries*. World Bank, 2007. http://siteresources.worldbank.org/INTPROSPECTS/Resources/334934-1110315015165/Migration_in_Africa_WilliamShaw.pdf, (accessed on August 20, 2017).

[155] Le conseil du café–cacao. Campagne principale 2017/2018, 2017. http://www.conseilcafecacao.ci/index.php?option=com_content&view=article&id=105&Itemid=183, (accessed on July 16, 2017).

[156] WHO. Uganda birding, seasonality and migration, 2014. http://birding-uganda.com/birding-in-uganda/seasonality.html, (accessed on July 16, 2017).

[157] LD Valdez et al. Predicting the extinction of Ebola spreading in Liberia due to mitigation strategies. *Scientific reports*, 2015(12172), 2015.

[158] AM Kramer et al. Spatial spread of the West African Ebola epidemic. *Royal Society Open Science*, 3:160–294, 2016.

[159] F Brauer, P Van Den Driessche. Models for transmission of disease with immigration of infectives. *Mathematical Biosciences*, 171:143–154, 2001.

[160] A Tripathi et al. Modelling the spread of HIV/AIDS with infective immigrants and time delay. *International Journal of Non Linear Science*, 16:313–322, 2013.

[161] Bakewell et al. *African Migrations: continuities, discontinuities and recent transformations*. African Alternatives. Leiden: Brill, 2007.

[162] A Devillard, A Bacchi, M Noack. *International Organisation for Migration (IOM). A survey on migration policies in West Africa*, volume Second edition. Druckerei DGS Wien, 2016.

[163] VS Bokharaie. *Stability analysis of positive systems with application to epidemiology*. PhD thesis, University of Ireland Maynooth, 2012.

[164] M Benchohra et al. *Impulsive differential equations and inclusions*, volume 2. Hindawi Publishing Corporation, 2006.

[165] R Mirion. *Impulsive differential equations with applications to infectious diseases*. PhD thesis, University of Ottawa, 2014.

[166] WHO. Origins of the 2014 Ebola epidemic, 2017. http://www.who.int/csr/disease/ebola/one-year-report/virus-origin/en/, (accessed on July 10, 2017).

[167] International Monetary Fund. Guinea: poverty reduction strategy paper. *International Monetary Fund Publication Services*, 2013. http://www.imf.org, (accessed on February 27, 2017).

[168] Unicef. Information by country. https://www.unicef.org/infobycountry/stats_popup7.html, (accessed on September 29, 2017).

[169] African Union. *The social impact of Ebola and in particular the nature of the social protection interventions required*, 2015. https://au.int/sites/default/files/newsevents/workingdocuments/28072-wd-the_social_impact_of_ebola_-english.pdf, (accessed on August 16, 2016).

[170] Statistics Sierra Leone. Sierra Leone 2014 labour force survey report. Technical report, International Labour Organisation, 2015. https://www.statistics.sl/wp-content/uploads/2016/06/sierra_leone_labour_force_survey_report_2014.pdf, (accessed on December 12, 2015).

[171] International Monetary Fund. Liberia: poverty reduction strategy paper-annual progress report. *International Monetary Fund Publication Services*, 2012. http://www.imf.org, (accessed on February 27, 2017).

[172] AD Lopez et al. Global burden of disease and risk factors. *Oxford University press and World Bank*, 2006.

[173] A Rico et al. Epidemiology of epidemic Ebola virus disease in Conakry and surrounding prefectures, Guinea, 2014–2015. *Emerging Infectious Diseases*, 22:178–183, 2016.

[174] P Ball. Poor trapped in poverty by disease. *Nature*, 2009. http://www.nature.com/news/2009/091209/full/news.2009.1130.html, (accessed on January 18, 2017).

[175] WHO. Emergencies preparedness, response, Ebola at six months. http://www.who.int/csr/disease/ebola/ebola-6-months/guinea/en/, (accessed on November 1, 2017).

[176] World Bank. Data, Sub-saharan Africa. http://data.worldbank.org/region/sub-saharan-africa, (accessed on August 23, 2017).

[177] J Wahba. Who benefits from return migration to developing countries ? *IZA World of Labor*, 2015.

[178] ML Flahaux, H De Haas. African migration: trends, patterns, drivers. *Comparative Migration Studies*, 4:1, 2016.

[179] B Rechel et al. *Migration and health in the European Union*. McGraw-Hill Education, Two Penn Plaza, New York, 2011.

[180] Robert Smith ? A mathematical model for the eradication og Guinea Worm.